

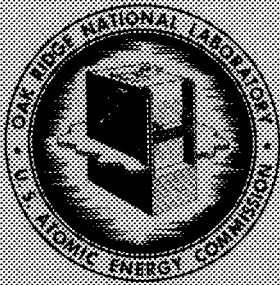
LOCKHEED MARTIN ENERGY RESEARCH LIBRARIES



SEARCH LIBRARY
COLLECTION

60

3 4456 0513357 5

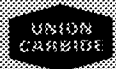


OAK

LABORATORY

operated by

UNION CARBIDE CORPORATION
NUCLEAR DIVISION



for the

U.S. ATOMIC ENERGY COMMISSION

ORNL - TM - 1903

HFIR FUEL ELEMENT STEADY STATE HEAT TRANSFER ANALYSIS

N. Hilvety

T. G. Chapman

OAK RIDGE NATIONAL LABORATORY
CENTRAL RESEARCH LIBRARY
DOCUMENT COLLECTION

LIBRARY LOAN COPY

DO NOT TRANSFER TO ANOTHER PERSON
If you wish someone else to see this
document, send its name with document
and the library will arrange a loan

LOCKHEED MARTIN ENERGY RESEARCH LIBRARIES

NOTICE This document contains information of a preliminary nature and was prepared primarily for internal use at the Oak Ridge National Laboratory. It is subject to revision or correction and therefore does not represent a final report.

LEGAL NOTICE

This report was prepared as an account of Government sponsored work. Neither the United States, nor the Commission, nor any person acting on behalf of the Commission:

- A. Makes any warranty or representation, expressed or implied, with respect to the accuracy, completeness, or usefulness of the information contained in this report, or that the use of any information, apparatus, method, or process disclosed in this report may not infringe privately owned rights; or
- B. Assumes any liabilities with respect to the use of, or for damages resulting from the use of any information, apparatus, method, or process disclosed in this report.

As used in the above, "person acting on behalf of the Commission" includes any employee or contractor of the Commission, or employee of such contractor, to the extent that such employee or contractor of the Commission, or employee of such contractor prepares, disseminates, or provides access to, any information pursuant to his employment or contract with the Commission, or his employment with such contractor.

ORNL-TM-1903

Contract No. W-7405-eng-26

Reactor Division

HFIR FUEL ELEMENT STEADY STATE
HEAT TRANSFER ANALYSIS

N. Hilvety and T. G. Chapman

DECEMBER 1967

OAK RIDGE NATIONAL LABORATORY
Oak Ridge, Tennessee
operated by
UNION CARBIDE CORPORATION
for the
U.S. ATOMIC ENERGY COMMISSION

LOCKHEED MARTIN ENERGY RESEARCH LIBRARIES



3 4456 0513357 5

FOREWORD

This report documents the early development of the HFIR heat transfer analysis and presents results which were judged adequate to provide reasonable assurance that the reactor could be operated at the design power level of 100 Mw for a typical fuel cycle duration of 15 days. During the middle of 1965 a critical review of this work indicated several areas in which it appeared that the analysis was not conservative and several areas in which the approach was overly conservative. In particular it was found that the assumptions regarding flow in a coolant channel which had sinusoidal buckling along its length were not conservative and a considerable flow reduction would actually occur for the channel variations predicted. On the other hand the assumed buckling mode was based on a preliminary analysis and was supported only by preliminary experimental data. Later tests which were carefully instrumented and which covered a wide range of operating conditions showed that the sinusoidal buckling previously assumed did not properly describe the situation. The review plus additional information from experimental programs led to the decision to rewrite the computer code in order to include the currently available information. The methods of analysis and the results of the later computations are presented in ORNL-TM-1904 which supersedes this report. The later analysis is based on a fuel cycle time of 25 days rather than 15 days as presented herein. The longer fuel cycle is representative of HFIR operating experience in which the typical fuel cycle has been found to be about 23 days.

T. E. Cole
Oak Ridge National Laboratory

CONTENTS

	<u>Page</u>
ABSTRACT	1
INTRODUCTION	2
METHOD OF ANALYSIS	7
A. Types of Factors Included in the Analysis	7
B. Variables to be Considered	8
C. Principal Assumptions	10
Fluid Flow	10
Hot Spot Size	11
Hot Streak Width	12
Fuel Plate Deflection	12
Operating Conditions	16
Flow of Heat Parallel to the Surface of the Fuel Plate	16
Hot Spot Location	18
D. General Computational Procedures	19
RESULTS AND CONCLUSIONS	20
A. Specific Results	20
B. General Conclusions	24
ACKNOWLEDGMENTS	26
BIBLIOGRAPHY	27
APPENDIX A -- DETAILS OF HEAT REMOVAL ANALYSIS PROCEDURE	53
I. HOT SPOT SUBROUTINE	54
Part A. Nominal Operating Conditions	54
Part B. Burnout Conditions	58
a. Zenkevich-Subbotin Burnout Correlation	58
b. Savannah River Correlation	60
II. HOT SPOT BURNOUT CALCULATION PROCEDURE	60
III. HOT SLOT INCIPIENT BOILING CALCULATION PROCEDURE	67
IV. INPUT DATA	70
V. OUTPUT DATA	71
NOMENCLATURE	73
SUBSCRIPTS	74
APPENDIX B -- HOMOGENEITY INSPECTION SPOT SIZE REQUIREMENTS	117

Contents (continued)

	<u>Page</u>
I. Introduction	117
II. Method of Analysis and Results	117
APPENDIX C - INFLUENCE OF FUEL SEGREGATION ON INCIPIENT BOILING POWER LEVEL	125
APPENDIX D - HFIR MODES OF OPERATION	127
APPENDIX E - FUEL ELEMENT DRAWINGS	131

LIST OF FIGURES

1. Dimensional Illustration of the Assembled High Flux Isotope Reactor Fuel Element.
2. Idealized Cross Sections for Experimental HFIR Fuel Plates (a) Inner Annulus, (b) Outer Annulus.
3. Heat Flux Peaking on Hot Side of Fuel Plate Due to Nonbonds.
4. Heat Flux Peaking on Cold Side of Fuel Plate Due to Nonbonds.
5. Model Employed for Calculation of Nonbond and Fuel Segregation Heat Flux Peaking Factors.
6. Alternate Arrangements of Adjacent Coolant Channels.
7. Computational Procedure - Simplified Block Diagram.
8. Effect of Fuel Element Flow Rate on Incipient Boiling Power Level and Allowable Local Heat Flux Peaking Factors for Incipient Boiling and Burnout at 100 Mw.
9. Minimum Calculated Coolant Gap Thickness After 15-Day Operation at 100 Mw.
10. Effect of Flow Rate and Operating Pressure on Incipient Boiling Power Level.
11. Effect of Alternative Assumptions on Fuel Plate Axial Thermal Buckling Calculated Incipient Boiling Power Level.
12. Effect of Hot Spot Elevation on Incipient Boiling Power Level.
13. Effect of Coolant Channel Tolerances on Incipient Boiling Power Level.

Appendix A

- A-1. Model Employed for Flow Calculations.
- A-2. Hot Slot Input Form-1.
- A-3. Hot Slot Input Form-2-1.
- A-4. Hot Slot Input Form-1.
- A-5. Hot Slot Input Form-2-1.
- A-6. Output Data from Sample Problems, Burnout Calculations.
- A-7. Output Data from Sample Problems, Incipient Boiling Calculations.
- A-8. Correlation of Burnout Output Data with Calculation Steps.
- A-9. Correlation of Incipient Boiling Output Data with Calculation Steps.

FIGURES (con't)

Appendix B

- B-3. Effect of Size of Segregation Spot on Local Heat Flux Peaking.

Appendix C

- C-1. Effect of Fuel Segregation Tolerances, System Pressure and Core Pressure Drop on Incipient Boiling Power Level.

Appendix E

- E-1. HFIR Inner Fuel Element Inner Side Plate.
E-2. HFIR Inner Fuel Element - Fuel Plate True Involute Curvature - Design Details.
E-3. HFIR Inner Fuel Element Fuel Plate Loading Details.
E-4. HFIR Inner Fuel Element Top Combs.
E-5. HFIR Inner Fuel Element Bottom Combs.
E-6. HFIR Inner Fuel Element - Outer Side Plate.
E-7. HFIR Inner Fuel Element - Assembly.
E-8. HFIR Fuel Elements - General Notes.
E-9. HFIR Outer Fuel Element - Inner Side Plate.
E-10. HFIR Outer Fuel Element - Fuel Plate True Involute Curvature - Design Details.
E-11. HFIR Outer Fuel Element Fuel Plate Loading Details.
E-12. HFIR Outer Fuel Element - Top Combs.
E-13. HFIR Outer Fuel Element - Bottom Combs.
E-14. HFIR Outer Fuel Element - Outer Side Plate.
E-15. HFIR Outer Fuel Element - Assembly.

HFIR FUEL ELEMENT STEADY STATE
HEAT TRANSFER ANALYSIS

N. Hilvety and T. G. Chapman

ABSTRACT

In order to achieve the desired high performance in the HFIR it was essential that the heat removal analysis be conducted in a manner that would minimize tendencies toward over-conservatism and that would take into consideration all items, such as control system requirements and fuel element fabrication tolerances, that have a significant effect on the practicality of the design. In addition to analytically demonstrating the operability of the HFIR at the design power level of 100 Mw from the standpoint of heat transfer, the results of this study have been useful in establishing permissible normal operating conditions for the various proposed modes of operation, in helping to fix the control and safety system set points, in providing a basis for analog studies of transient behavior during postulated nuclear excursions, and in helping to establish fuel element fabrication tolerances, especially those concerned with coolant gap thickness and fuel homogeneity.

The basic approach to this study has been to assign values to the individual hot-spot factors influencing the various aspects of the heat transfer. The calculational procedure was set up so that the individual factors could be considered simultaneously; furthermore, it was assumed that all factors actually would occur simultaneously where physically possible. The individual factors are considered in a rather detailed manner in respect to their interactions with each other and a number of considerations are included which are not normally a part of such an analysis (e.g., oxide buildup and fuel plate deflections). The calculations give information on reactor power level limitations as well as the more usual heat flux peaking limitations. Great care has been taken to insure that the results of these studies are conservative and at the same time to minimize the degree of conservatism. Thus, the results are believed to reflect quite reasonably the lower bounds of the onset of nucleate boiling or burnout, as the case may be. These bounds are based on the calculated power level for the onset of nucleate boiling or burnout at the hot spot. For all but the case of natural convection cooling the onset of nucleate boiling was used as a limiting condition rather than burnout because a suitable burnout correlation was not available for the very narrow HFIR coolant channels under high power, hot spot conditions.

These studies indicate that at the end of a 15 day, 100 Mw fuel cycle and with the anticipated reactor flow rate and operating pressure, (600 psi) the incipient boiling power level is 139 Mw, the corresponding average fuel plate temperature was calculated to be 212°F and the maximum hot spot fuel plate temperature was 480°F.

INTRODUCTION

The entire HFIR fuel loading, shown in Figure 1, consists of just two fuel elements. The assembled elements constitute two concentric annuli containing 50-mil-thick involute-shaped aluminum fuel plates with 50-mil coolant channels. The thickness of the fuel-bearing portions of the plates is varied radially, as shown in Figure 2, so as to flatten the power distribution. The elements are forced-convection cooled by water flowing downward through the coolant channels.

The basic design requirements placed on the HFIR were that the reactor operate at a power level of 100 Mw and produce ^{252}Cf as rapidly as feasible (i.e., the thermal neutron flux in the target should be as high as possible). The design data listed in Table 1 represent the combined results of the nuclear,¹ hydraulic, mechanical,² and heat transfer design studies.

That an extensive heat transfer analysis of the HFIR fuel element was required is evident when one considers the high power densities required to achieve the desired neutron fluxes. These power densities represent a significant extrapolation of current practice and experience. Specifically, there are two principal problems encountered: first, due to the limited headroom imposed by the requirements for a maximum available neutron flux, the degree of conservatism in the heat transfer analysis must be carefully limited, without being eliminated; and secondly, the analysis must be conducted in such a manner as to facilitate individual evaluation of each of those factors influencing heat transfer, such as mechanical design details and tolerances, fuel plate strength and buckling characteristics, nuclear characteristics, control system characteristics, reactor operating procedures, and changes which might occur during the fuel element lifetime such as oxide film buildup.

One method of reducing the degree of conservatism in this sort of analysis is that of applying statistical weighting factors to each of the individual variables which might influence the heat transfer characteristics. The magnitude of the weighting factor to be applied to an individual variable is determined by the probability of existence of that condition both individually and concurrently with the other variables

which influence heat transfer. In order to employ this method, it is necessary, of course, to have the appropriate statistical data for each of the variables involved and for combinations thereof. In the case of the HFIR many of the design concepts and fabrication techniques are sufficiently different from the usual that adequate statistical data are not available and will not be available until quite some time after the reactor commences operation. Thus the conservative approach of assuming that all detrimental uncertainties and deviations from the nominal occur simultaneously and at the same spot when physically possible has been employed. It has also been assumed that under the circumstances the probability of the uncertainty factors and deviations from the nominal being greater than considered is so small as to be of no serious consequence. Statistics per se have entered directly into the study in a few cases where large quantities of data are available, such as in the case of the heat transfer coefficient correlation, where a correlation representing 95% of the data was employed.³ In other cases, where correlations are based on more limited data, minimum data correlations have been used.

In applying the data correlations to the heat transfer analysis, five general categories of relevant factors have been considered:

1. The reactor nuclear characteristics and nuclear calculation tolerances.
2. The fuel element mechanical design parameters and associated tolerances.
3. Fuel plate defects (non-bonds and fuel segregation).
4. Changes in coolant channel dimensions caused by fuel plate deflections resulting from hydraulic or thermally-imposed loads.
5. Plant operating parameters and associated uncertainties (power level, fuel cycle length, coolant temperature, flow rates, pressure level, etc.).

In order to minimize the degree of conservatism and at the same time facilitate examination of the effects of individual design parameters, these general categories were subdivided into discrete factors, the effects of which could be described mathematically. The various heat

transfer parameters then became functions of all of those factors by which they could be influenced. This approach has the additional advantages of preventing the inclusion of conflicting factors and gives proper advantage credits for the secondary effects of the individual factors. For example, when using this approach, any given calculation is automatically prohibited from assuming adjacent wide and narrow channels for calculating pressure-induced fuel-plate deflection, and at the same time assuming adjacent narrow channels for calculating average plate temperatures. Also, a factor which causes an increase in bulk water temperature also results in an increase in heat transfer coefficient.

In subdividing the factors, it was necessary to include directly in the analysis several factors which are not usually considered. In addition to the effects of fuel plate deflections, local heat-flux peaking factors such as those resulting from non-bonds and fuel segregation were considered. The effects of oxide buildup on fuel plate strength and on buckling due to fuel-plate-to-side-plate temperature differences were included. In the case of those factors which could be limited to small plate areas by proper inspection techniques, both heat conduction in the plane of the plate and the effects of changes in local heat transfer coefficient were taken into account.

Reactor performance limitations are presently based on the calculated power level for the onset of boiling at the hot spot. The calculational procedures for establishing reactor power level limitations were originally based on correlations for burnout^{3,4} power level, the Zenkevich-Subbotin correlation being employed for high pressures and the Savannah River correlation for lower pressure operation; coefficients employed in these correlations were based on subcooled boiling burnout tests run specifically to simulate HFIR conditions. However, after including fuel plate deflection effects in the analysis, it became apparent that the calculated minimum coolant channel thicknesses at the calculated burnout power levels generally fell below the applicable range of the burnout correlations, which are generally limited to minimum channel thickness of about 30 mils. A plot of calculated end-of-cycle minimum coolant channel thickness as a function of reactor power level and

fuel region flow rate is shown in Figure 9. Data on burnout for very thin channels are very meager; however, on the basis of a few points that were available⁵ it appeared that a narrowing of the channels below 0.03 in. resulted in the burnout heat flux approaching the onset of boiling heat flux. Furthermore, these data indicated that for the very narrow channels expected in the HFIR during high power operation, the onset of nucleate boiling and the burnout heat flux would be very nearly equal. Therefore, the use of the incipient boiling point in lieu of the burnout point does not in reality constitute a significant or unjust limitation on achievable power.

Another problem associated with the application of the burnout correlation is that of instability due to bubble formation which cannot be calculated with any appreciable degree of accuracy. It is generally recognized⁶ that use of empirical burnout data correlations requires a very close examination of these correlations for applicability to the case under consideration. This provided another incentive for using the onset of nucleate boiling as a limiting condition. The correlation chosen for calculation of incipient boiling is that of Bergles and Rohsenow.⁷

In calculations relative to loss of flow and loss of pressure accidents, two principle operating flow rates have been considered in establishing fuel plate oxide build up. Calculations have been made for a fuel element flow rate of 10,800 gpm, which corresponds to an early value of the reactor design minimum flow rate. The HFIR main circulating pumps have subsequently been sized to deliver approximately a 13,000 gpm fuel element flow rate; calculations have also been made at this value.

In addition to investigation of the incipient boiling power level, calculations have been made to determine the hot spot heat flux peaking factors necessary to reach incipient boiling and burnout. This factor is defined as the quantity by which the hot spot heat flux must be multiplied in order to achieve the incipient boiling heat flux that corresponds to a specific steady state power level. This simplified procedure is sometimes used to predict "burnout" margins associated with an increase in power. However, since it does not account for changing core characteristics other than an increase in heat flux at the hot spot as the power

approaches burnout or incipient boiling, it predicts greater margins than predicted by the much preferred method discussed in this report.

To be able to interpret the final results of this study in terms of permissible operating power level it is necessary to consider certain aspects of the reactor control system and also to consider the basis upon which the heat transfer analysis was made. The control system limits power overshoot above normal full power through action of a multiple servo system; a rod reversal is provided at 110%, a scram on heat power is provided at 120%, and a neutron flux-to-flow scram is set at 130%. (A rate scram is also provided for rapid transients). The rod reversal points are provided in order to protect the reactor, without a scram occurring, against a slowly drifting power level; the nominal set points were established on the basis of instrument noise, etc.

In the heat transfer analysis all credible deleterious conditions were considered and were assumed to occur simultaneously, the probability of a worse condition existing being considered so small as to be tolerable in terms of the risk involved. Thus, it is quite reasonable to set the level scram point right at the calculated hot spot burnout power level. Since in this analysis it is assumed that burnout and incipient boiling are synonymous (at least for high power cases) the above approach will make nucleate boiling as well as burnout quite improbable in the vicinity of the level scram point.

In specifying a maximum steady state power level for normal operation, components other than the fuel element (control components, reflector, target and other experimental facilities, heat exchangers, cooling tower, etc.) must of course be considered. These have been designed for a nominal operating power level of 100 Mw, which is the originally specified normal operating power level for the reactor. This apparent limitation on associated components precludes operation of the fuel elements at a nominal power level above 100 Mw. Thus, it is only necessary that the calculated incipient boiling power level, for high power operation and under the conditions specified herein, be equal to or greater than 130 Mw. For low power operation at reduced flow and/or pressure, the safety instrumentation settings must reflect the corresponding reduction in calculated burnout point.

Independent variables that affect the incipient boiling and burnout power levels are the coolant flow rate and the system pressure. The results of these studies indicate that with the minimum expected flow from three of the four pumps and with a system inlet pressure of 600 psia (maximum design pressure is 1000 psi), the minimum incipient boiling power level is greater than 130 Mw.

METHOD OF ANALYSIS

A. Types of Factors Included in the Analysis

In describing mathematically the HFIR heat transfer conditions, the steady-state hydraulic and heat transfer equations are, first of all, written in terms of the nominal reactor design and operating parameters and the selected location* within the active core. These equations are then modified by all those factors (fabrication tolerances, variation in operating parameters uncertainties in data correlation, etc.) which can influence hot spot operating conditions. In modifying the nominal equations it is necessary to recognize the following three separate categories of influencing factors:

1. Hot plate factors are defined as those which influence heat transfer across the entire width of a coolant channel. These factors thus influence the overall response of the entire coolant channel (i.e., these factors affect total channel flow rate, fuel plate buckling, average channel outlet temperature, etc.).

2. Hot streak factors are defined as those which may affect heat transfer down a narrow element of a coolant channel from the top of the active fuel region to the hot spot elevation, the exact width of the streak being undefined but sufficiently narrow to preclude any measurable effects on fuel plate deflections (i.e., these factors do not affect plate deflection or total bulk flow through the entire channel, but they do affect local

*The calculational procedure permits pre-selection of the location within the active fuel region for which the calculations are to be made. No provision has been made for an automatic search for the hot spot location.

bulk water temperature and/or local coolant velocity).

3. Hot spot factors are defined as those which influence only a sufficiently small area of the plate such as to preclude any effects other than those on local coolant velocity or local heat flux (i.e., these factors are assumed to have no effect on bulk water temperatures or total channel flow rate or on fuel plate buckling).

These three types of factors are superimposed successively according to the assumption that all factors combine at the hot spot in the most unfavorable manner possible (i.e., the hot plate factors are superimposed on the nominal equations to give the hot plate equations, the hot streak factors are superimposed on the hot plate equations to give the hot streak equations, and the hot spot factors are superimposed on the hot streak equations). By proper selection of the values of the various factors, these modified equations can then be used to calculate fuel plate nominal, hot plate, hot streak, or hot spot conditions at any chosen location within the fuel element.

B. Variables to be Considered

The variables considered in these heat removal studies are listed in Table II. Although the distinction is not always clear-cut, these variables may be divided into the following five categories:

1. Physical Description of the Reactor

This category includes those parameters, both nominal values and tolerances, specified by the fuel element fabrication drawings which influence local heat transfer conditions, either in their effects on heat flux or on coolant flow rates or temperatures. Thus, as well as including fuel loading tolerances, this category also includes all dimensions and tolerances affecting coolant gap thickness, either directly or through their effects on fuel plate buckling.

2. Reactor Operating Conditions

As is the case with the previous category, those operating conditions are considered which influence heat flux or coolant conditions. As well as including the usual parameters of coolant inlet temperature, pressure, flow rate (as defined by available pressure differential), and

power level (as defined by the core average heat flux), this category also includes the calculated and/or experimental geometrical power distribution factors and the previous operating cycle history of the fuel element.

3. Uncertainties

In addition to the tolerances normally assigned to design and operating parameters which were covered under the previous two items, there are uncertainties involved in measurement of the operational variables and in the calculational procedures and correlations employed in predicting the actual fuel element heat transfer conditions. It is these operational, calculational, and correlation uncertainties which are included in this category.

4. Correlation Constants

Provision is made in the calculational procedure for varying the constants in some of the data correlations employed in these calculations. The correlations for which this is provided include those for calculation of local heat transfer coefficient, fuel plate oxide film buildup, and fuel plate deflection. These provisions serve two purposes. In the case of the correlations for heat transfer coefficient and oxide buildup the primary purpose is that of allowing a convenient means of modifying the equations to incorporate additional experimental data. In the case of the heat transfer coefficient, there is also provision for selecting one of two different forms for the correlation. The variable constants in the plate deflection equation also permit selection of values consistent with the radial location of the spot under consideration.

5. Hot Spot Location

As was mentioned previously, the calculational procedure employed allows pre-selection of the geometrical location within the fuel element for which the heat removal calculations are to be made. This is accomplished by specifying an axial location and fraction of total heat liberated above this elevation, the arrangement of adjacent wide and narrow channels to be considered, and by choice of proper values of nuclear flux peaking factors and plate deflection correlation constants corresponding to the chosen radial location.

C. Principal Assumptions

As has been indicated previously, the two principal assumptions involved in these heat transfer studies are as follows:

1. All individual hot spot factors are assumed to be superimposed at the "hot spot" in the most unfavorable, physically possible manner.
2. At anticipated HFIR operating conditions, the onset of nucleate boiling is in most cases a satisfactory substitute for the less well known burnout point.

In addition to these basic assumptions, it has been necessary to make a number of assumptions relative to the details of the heat transfer within the fuel element. The more important of these are summarized in the following paragraphs. (Again, the distinction as to the heading under which these assumptions should fall is not always clear-cut due to the interrelation of the topics to be considered).

Fluid Flow

The standard handbook equations have been employed for calculation of inlet, exit, and friction pressure drops, with modification of the standard friction factor according to experimental data obtained on thin rectangular channels.³ Friction drop calculations have been based on the core midplane bulk water temperature. In calculating the total flow rate through a given coolant channel, it is assumed that the average coolant channel thickness is not affected by fuel plate deflections. In the case of pressure-induced plate deflections, the deflected plate will assume an "S" shape relative to the original involute curvature, thus while one part of the coolant channel decreases in thickness, another part increases in thickness giving a net change in channel cross-sectional area of approximately zero. Some net change in channel dimensions resulting from different operating temperatures of adjacent fuel plates is to be expected since the resulting deflection is in one direction relative to the original involute; however, these temperature differences are not large enough to significantly affect average channel thickness. In the case of deflections resulting from fuel plate - side plate temperature differences the deflection pattern has been shown to assume a longitudinal sine wave pattern. These deflections then would be expected to affect

local coolant velocities but not overall coolant channel flow rates.

Two important postulates which have been employed in establishing equations to describe local coolant velocity, velocity pressure drop, and frictional pressure drop in these nominally flat channels are as follows:

(1) the static pressure is assumed to be independent of position across the width of the channel, and (2) frictional forces are transmitted solely across the thickness of the channel with none in the direction of width. (The width direction is defined as that along the involute arc.) These two postulates are justified for very thin channels which contain no abrupt changes in channel shape that would result in unrecoverable expansion or contraction losses. It is felt that the equations based on these postulates, provide a reasonably accurate analysis of the effects of deviations in plate contour and coolant-gap thickness on the hydrodynamics of the HFIR fuel element coolant channels.

Provision is made in the calculational procedures for specification of a degree of mixing across the channel width in terms of the fraction by which the hot streak bulk water temperature is modified toward the channel average bulk water temperature. At the normal operating coolant velocities of the HFIR fuel element dye flow tests have indicated that very little transverse mixing is to be anticipated. Consequently, all of the calculations have been based on the assumption of no mixing across the channel width.

There is also provision for including in the calculations a factor to account for flow maldistribution due to inlet plenum effects. This factor is included in the form of a fraction of the nominal flow rate to be applied to the hot streak calculations. Considerable effort has been expended in the design of the inlet plenum to minimize any such effects. Consequently, no inlet plenum flow effects have been included in the calculations.

Hot Spot Size

Even though incipient boiling rather than burnout is being used as a limiting design condition it is of interest to examine in at least a qualitative way some of the more important parameters effecting burnout.

It is possible that even with very narrow coolant channels there will be greater separation between incipient boiling and burnout than indicated by the limited uniformly-heated channel data. One parameter which might be important in this respect is the proximity of hot spots relative to each other. In arriving at the conclusion that for very narrow channels the incipient boiling point and burnout point would be nearly the same it was assumed that data from uniformly-heated-plate experiments were applicable. However, in the case of a small isolated hotspot, the flow of coolant would be expected to sweep away the bubbles as they are formed. Thus the film blanketing effect of boiling would be minimized. If, however, there were a second spot just upstream which was also generating vapor bubbles, these bubbles, in being swept over the second spot, would be expected to result in an appreciably lower burnout heat flux. Some preliminary experimental work on the effects of hot spot size and relative orientation of adjacent spots has confirmed these expectations⁸. Thus, if hot spots in the HFIR fuel plates are not grouped closely together, the actual margin on burnout will be significantly greater than calculated herein. At the present time the inspection techniques do not include an examination of hot spot relative position.

Hot Streak Width

As was mentioned previously, the exact width of the hot streak, employed for purposes of establishing bulk water temperatures, is undefined but assumed to be sufficiently narrow to preclude any measurable effect on fuel plate deflections. Factors included as hot streak values include those of fuel plate deflection due to pressure differential and fuel plate line average loading tolerance.

Fuel Plate Deflection

Fuel plate deflections of interest are those resulting from hydraulic pressure differentials, differential radial expansions between adjacent fuel plates and differential axial expansion between the fuel plates and the sideplates.

Calculations on elastically stable distortions¹⁰ have been based on elastic beam theory, assuming pinned ends and an initial curvature conforming to a true involute as shown on the fuel element drawings,¹¹

with the direction of deflection in adjacent plates chosen to give the most unfavorable heat transfer conditions. Calculations on fuel plate longitudinal buckling¹² are based on an experimental model arrived at through the use of theoretical and experimental results; the direction of buckling and creep considered gave the most unfavorable heat transfer conditions.

Three separate factors can be responsible for deflection of an individual fuel plate relative to its neighbors. They are:

1. Differences between fuel plate and side plate temperatures.
2. A difference in the average temperatures of adjacent fuel plates.
3. Pressure differentials across fuel plates.

Fuel plate buckling is assumed to be dependent upon the average fuel plate temperature at the elevation of the point under consideration. This average plate temperature is, in turn, assumed to be established by values of bulk water temperature and velocity, fuel plate power density, and heat transfer coefficient averaged across the entire channel width. The assumptions indicated under the heading of fluid flow are employed in establishing these average coolant properties and heat transfer coefficients. It is assumed that the maximum possible value of plate power density, averaged across the plate width, is fixed by the line average fuel loading tolerance (i.e., the time constant employed in the homogeneity scanning machine must be sufficiently short to prevent greater effective width averaged power densities).

As a fuel element comes up to power, a net temperature difference between the fuel plates and side plates comes into being. This temperature difference is potentially capable of generating two types of plate deflection. It may generate a "sine wave" type of buckling due to differences in axial expansion, and may also result in a deflection of the fuel plates due to differences in radial expansion between fuel plates and side plates. The generation of fuel plate stresses resulting from the difference in nominal fuel plate and side plate temperatures has been eliminated in HFIR by allowing relative rotation between the two side plates of a fuel element. Thus, the only deflections of a radial nature are those due to average temperature differences between adjacent fuel plates. In

determining the magnitude of these deflections, the slight changes in chord length and plate curvature due to differential radial expansions are secondary effects and are thus negligible. Average fuel plate temperature calculations are based on the previously-indicated hydraulic and heat transfer assumptions. Heat transfer from the side plates is based on a flat slab model (i.e., it is assumed that there is no transfer of heat between fuel plates and side plate. Two-dimensional heat transfer calculations have shown this to be good assumption for the HFIR geometries and operating conditions). Aluminum oxide build-up on the side plates reduces the temperature difference between the side plate and fuel plate. However, the effect is small and therefore was completely neglected. In addition bulk water temperatures, and heat generation rates were chosen to give minimum possible side plate temperatures. Natural convection heat transfer with a coefficient of $300 \text{ Btu hr}^{-1} \text{ ft}^{-2} (\text{°F})^{-1}$ was assumed for the side plate surfaces opposite the fuel plates except for the outer element outer side plate, where flow through the control region provides forced convection heat transfer. This forced convection coefficient is assumed proportional to the 0.27 power of the core pressure drop. The heat transfer coefficient on the fuel plate side is assumed equal to that calculated for a normal fuel plate, but the area was assumed to be just one-half of actual side plate surface area because of the existence of the fuel plate slots. Corner effects would be expected to result in an effective value lower than this assumed level, hence this assumption also leads toward a low calculated side plate temperature.

The bulk water temperature rise of the water flowing past the fuel plate side of the side plate was assumed to be more dependent on the temperature of the fuel region coolant than on heat transferred from the side plate. Therefore, the bulk temperature rise of this water was assigned a fractional portion of the nominal fuel region coolant bulk temperature rise. This fractional value, called the side plate cold streaking factor in the input data listing, is an input variable, thus permitting variation in the assumptions employed in calculating this bulk water temperature (i.e., a value of 1.0 would be assigned to this variable if complete mixing within the coolant channel was assumed).

In the case of coolant flow past the side of the side plate opposite the fuel plates, bulk temperature rise is assumed to be proportional to the reactor power level and inversely proportional to the 0.53 power of the fuel element pressure differential. An input variable is provided which permits selection of the bulk temperature increase; for a power level of 100 Mw and a flow rate of 10,800 gpm the bulk temperature increases are 80°F for the control region coolant and 100°F for all other side plates. These values were selected on the basis of calculated metal and water gamma and neutron heat generation rates.^{13,14}

The calculational procedure employed for determining the magnitude of the sine wave buckling, is not valid at points near the side plate - fuel plate attachment since the fuel plate buckling will be restricted at these locations by the side plate. In making these buckling calculations it is assumed that the magnitude of buckling will vary according to a sine curve between zero at the point of attachment to the theoretical value at about 3/4 inch from the point of attachment. Calculations have shown that the effects of variation in this model on calculated minimum incipient boiling power levels is quite small. The radial location of the point of minimum incipient boiling is apparently coincident with the point of maximum pressure-induced deflection for any reasonable model adopted for the buckling near the fuel plate - side plate attachment; this location is about 3/4 in. from the inner side plate. Even if the theoretical maximum buckling should occur at the point of attachment, the reduction in calculated incipient boiling power level over that of the assumed model has been shown to be only 0.77%.

In calculating the sine wave buckling it is assumed that the side plate nearest the point under consideration is the one which determines the magnitude of buckling. Since the calculated point of minimum incipient boiling is always well displaced from the radial center of the fuel plate, and since the two side plate temperatures are nearly equal, this appears to be a good assumption.

The pressure-induced fuel plate deflection calculations are based on the assumption of uniform average coolant channel thickness, with the magnitude of deflection being uniform down the length of the fuel plate and determined by the average pressure differential between the adjacent

coolant channels. The actual local pressure differential across a plate with adjacent coolant channels of uniform but different thickness is a maximum at the top of the channel and minimum at the channel exit. The assumed pressure differential is thus conservative when employed for the bottom half of the core. These maximum deflection values result in minimum calculated values of coolant velocity and maximum calculated coolant temperatures.

Operating Conditions

In establishing fuel element heat generation rates it was conservatively assumed that of the total power generated, 97.5% was deposited in the fuel plates, and the remaining 2.5% was deposited in other regions of the reactor. This assumption leads to both slightly high bulk water temperatures and heat flux levels.

The choice of system operating variables to be used in describing fuel element operating characteristics was governed by two principal criteria: (1) the variables used should be those actually measured and controlled during reactor operation, and (2) the performance of the fuel element was to be considered independently of the remainder of the primary coolant system. The basic system variables chosen on this basis are: reactor power level (indicated in terms of fuel element average heat flux), coolant inlet temperature, and core pressure drop. In the case of power level and inlet temperature, factors are also included to account for inaccuracies in measurement and control of these variables. No such provision was made in the case of core pressure drop since it was considered to be the independent variable. All of these calculations having been based on a $120^{\circ}\text{F} \pm 1\%$ maximum inlet temperature.

Flow of Heat Parallel to the Surface of the Fuel Plate

It was assumed in making these heat transfer calculations, that except in the case of local hot spots there was no heat transfer parallel to the surface of the fuel plate in both the fuel plate and coolant channel. This assumption is valid because the coolant film heat transfer coefficient is large compared to the thermal conductivity of the fuel plate and because the thermal conductivity and mixing in the coolant are also relatively small. In the case of non-bonds and local fuel segregation

such heat flow must be considered, particularly in view of the assumption regarding independence of boiling on hot spot size. Maximum heat flux peaking due to fuel segregation in the absence of non-bonds is fixed by the specified local fuel loading tolerances. The factors employed to account for additional heat flux peaking due to non-bonds are as shown in Figs. 3 and 4. These factors include the effects of local heat transfer in the plane of the fuel plate. These heat flux peaking factors have been based on two-dimensional heat transfer calculations,¹⁵ using the model shown in Fig. 5. The non-bond is assumed to occur at the fuel-filler piece interface, this being the most unfavorable location from the standpoint of maximum hot spot heat flux, with no heat transfer across the non-bond. A non-bond diameter of 1/16 inch was used, consistent with the fuel element drawing notes.¹¹ It is assumed that the non-bond inspection will result in rejection of any plates with more deleterious non-bonds such as comparative large areas containing many very small non-bonds, and that existing non-bonds are sufficiently far apart that effects of adjacent non-bonds may be neglected.

Circumferential symmetry was assumed, with the axis of the U_3O_8 segregation volume being coincident with that of the non-bond. In establishing the thermal conductivity and heat generation rate of the U_3O_8 segregation spot, it was assumed that the U_3O_8 was in the form of tightly packed spheres and the maximum packing fraction for spheres of 0.74 was used. Thermal conductivity of the segregation spot is assumed to be equal to the sum of the volume fraction times thermal conductivity values of the various materials (U_3O_8 and Al).

The diameter of the segregation spot in this model was chosen to be consistent with the specified +30% fuel loading tolerance over the corresponding area. The diameter turned out to be 5/64 in. This inspection spot size was established on the basis of two-dimensional calculations¹⁵ performed on a model with no non-bonds present and with a 10-mil-thick fuel region. These studies, summarized in Appendix B, have shown that, over the region of interest, the increase in local heat flux at such a spot is approximately proportional to the volume of U_3O_8 in the spot. It is shown in Appendix B that for a given packing fraction and meat thickness there

is a unique value of the inspection spot diameter that will make the maximum segregation-induced heat flux peaking value equal to the permissible local fuel loading tolerance. It was assumed that a maximum packing fraction would result in the highest peak value of the heat flux. The 10-mil thickness of the fuel region was chosen since as a result of being the thinnest portion of the fuel bearing section of the HFIR fuel plates it results in the smallest inspection spot size.

After having established the inspection spot size, calculations were made to determine the effect of grouping several hot spots together. In these studies a single hot spot was insulated at the inspection spot diameters. It was found that the increase in peak heat flux was only 2%.

The specific value of heat transfer coefficient chosen for the model shown in Fig. 5 is typical of nominal HFIR operating characteristics. This coefficient does, of course, exert some influence on local heat flux peaking due to non-bonds and local fuel segregation. It is assumed that the fractional increase in local heat flux due to non-bonds and segregation is directly proportional to the value of the local heat transfer coefficient. Thus, as would be expected, the degree of local heat flux peaking decreases with decreasing heat transfer coefficient.

Hot Spot Location

As has been indicated previously, any desired geometrical location within the fuel element may be selected by specifying an axial location and through proper choice of nuclear flux peaking constants and fuel plate buckling constants. In addition, any one of four possible arrangements of wide and narrow coolant channels may be selected. These are indicated in Fig. 6.

While the calculational procedure permits selection of the point for which the calculations are to be made, and this ultimately allows a search to be made for the actual hot spot location, all of the HFIR steady-state heat transfer calculations reported herein have been based on the hot spot being at the outlet end of the active fuel region. Nuclear calculations¹ have indicated a marked degree of nuclear flux peaking at the core ends. It has been assumed in the present study, based on the results of nuclear calculations and experiments and considering

the specified¹¹ fuel length tolerances, that the power density peaking at the core ends is equal to that at the core midplane. This assumption results in the most severe hot spot conditions since it gives maximum bulk water temperatures and minimum pressures coincident with the hot spot location.

D. General Computational Procedures

The radial location of the hot spot is a function of several factors, including the time in the fuel cycle. At the beginning of a cycle the radial power distribution is essentially flat in the inner fuel element and in the inner third of the outer element. Near the end of the cycle the power density near the three innermost side plates decreases significantly because of nonuniform burnup of the fuel. As indicated in a previous section of this report the radial location of the hot spot, assuming a radially flat power distribution but otherwise end of cycle conditions, is about 3/4 in. in from the inner side plate of either element. The inconsistency associated with the power distribution represents a conservative approach, although the actual differences involved are small.

The basic calculational procedure is outlined in the block diagram of Figure 7. It should be emphasized that this is a very simplified diagram showing only the principal steps in the procedure.* Steps which are primarily concerned with particular calculational techniques, such as convergence schemes and iterative procedures within the between adjacent major operating steps, have been omitted for reasons of clarity. Also omitted from this diagram are indications of simultaneous calculations of the same type, such as those involving wide and narrow coolant channels or hot, cold and average fuel plates. As has been pointed out previously, the same basic set of equations is employed for calculating fuel plate average, hot channel, hot streak and hot spot conditions. These equations are first employed to give information on plate average

*The equations employed in these calculations and the detailed steps in the procedure are indicated in Appendix A of this report.

operating characteristics on which the fuel plate deflection calculations are based. The calculated fuel plate deflections result in hot spot and hot streak flow factors which are used, along with the original specified design and operating parameters to give predicted hot spot operating conditions. Employing the incipient boiling correlation along with these calculated hot spot operating characteristics provides a measure of the nearness of approach to incipient boiling. If desired, the entire procedure can be repeated, using a corrected power level until the power level is found at which boiling would begin, thus the calculational procedure can be used either to calculate an incipient boiling power level or to determine the heat flux peaking factor necessary to reach incipient boiling at a given power level.

A listing of the input data variables is given in Table II along with the functions of the individual variables and typical values corresponding to HFTR operation at a 10,800 gpm fuel element flow rate with the spot location chosen at the outlet of the active fuel region and at the innermost point of maximum pressure-induced fuel plate deflection in the inner or outer fuel annulus. (Other locations within the fuel element have been considered during the course of these studies, the one chosen here having been demonstrated to be generally the most critical.)

RESULTS AND CONCLUSIONS

These studies have been aimed at two principal goals. First of all, they have been used during early stages of the design effort to determine the relative necessity for the various fabrication tolerances through examination of the effects of individual factors on burnout margin. Secondly, once the design details became relatively fixed, these studies were used to provide information indicating relative operability of the reactor under various modes of operation and as an aid in determining reactor control system requirements.

A. Specific Results

Calculated fuel element operating conditions are given in Table III. Fuel plate and coolant temperatures are given for the fuel element average, hot streak, and hot spot conditions for beginning and end of cycle and

for fuel region flow rates of 10,800 and 13,000 gpm. As would be expected, buildup of the oxide film on the fuel plates results in an increase in fuel plate temperatures thus resulting in increased longitudinal plate buckling and a decrease in incipient boiling power level as the fuel cycle progresses. (No advantage was taken for the beneficial effects associated with nonuniform burnup of the fuel.) The maximum increase in fuel plate temperature associated with the oxide build up was calculated to be 90°F. Since plate strength and deflection characteristics are dependent on the hot plate temperatures, which are somewhat lower than the hot streak values listed here, it appears from these figures that plate strength can be expected to remain at a reasonable value throughout the fuel cycle.

The effects of fuel element flow rate and operating pressure on incipient boiling power level are indicated in Figure 8. Also shown in this figure is the calculated allowable local incipient boiling hot spot heat flux peaking factor at 100 Mw, 600 psia reactor operation.

As would be expected, these curves indicate a decrease in the effectiveness of increased pressure in suppressing boiling as the operating pressure increases, a given pressure increase being about twice as effective at a 300-psia operating pressure as would be the same increase at 600 psia. At operating pressures above about 900 psia, there is very little to be gained in terms of incipient boiling power level margin by further increases in pressure. At an operating pressure level of 600 psi, the incipient boiling power levels for 10,800 and 13,000 gpm are 120 and 138 Mw, respectively. Increasing the operating pressure from 600 to 1000 psi increases the incipient boiling power level by 12 and 23% for 10,800 and 13,000 gpm flow rates, respectively.

The allowable values for local heat flux peaking for incipient boiling at 100 Mw operation are, as would be expected, somewhat above the level of local heat flux for the onset of boiling resulting from a reactor power level increase. If one confines the reactor to 100 Mw operation, this curve may be interpreted as an indication of the permissible unintentional and/or unknown departure from the specified local fuel loading, non-bond, and local channel thickness tolerances.

One of the most informative series of heat transfer studies from the standpoint of reactor operation under abnormal conditions has been that

covering the effects of reduced flow rate and operating pressures on incipient boiling power level. A typical set of these calculation results is indicated in Figure 10, where incipient boiling power level is plotted as a function of instantaneous fuel region flow rate for various operating pressures. (Vessel inlet pressure). These particular curves have been based on conditions at the end of a 15-day operating period at 100 Mw and at a fuel region flow rate of 10,800 gpm and an inlet water temperature of 120°F. For comparison purposes, three operating-pressure curves have also been given which have been based on a 15 day cycle with operation at a fuel region flow rate of 13,000 gpm. At operating pressures below 300 psia there is essentially no difference between these two sets of curves.

It will be noted that the above curves exhibit a peak in incipient boiling power level with increasing flow rate, the peaks occurring beyond the range of the graph at pressures above ~200 psia. This comes about because the indicated pressure is core inlet pressure rather than the pressure at the core, outlet, where the hot spot is presumed to be. As the flow rate increases the discharge pressure decreases, tending to decrease the incipient boiling power level. At some point prior to reaching the zero power level these curves would be expected to become discontinuous because of cavitation of the primary coolant pumps. This portion of the curves is of some interest in examining loss-of-pressure accidents; however, no attempt has been made here to estimate cavitation points, and the curves are simply extrapolated to the point of hot channel bulk boiling at the core outlet at zero power level. Actual pump cavitation points will be determined by hydraulic experiments on the primary system.

In order to establish the radial location of the hot spot, it was necessary to conduct a search across the width of the coolant channel at the bottom of the active fuel region. The results of this search for points near the inner side plate are shown in Fig. 11 (all points further removed from this side plate gave higher calculated incipient boiling power levels). In making this search, it was assumed that, in the case of the inner fuel annulus, there is no radial variation in nuclear flux

peaking constants. In the case of the outer annulus, the local power densities near the outside corners are depressed by the nearness of the control rods thus eliminating this region from consideration as a possible hot spot location.

As was mentioned previously, it was assumed in this study that axial thermal buckling of the fuel plate would vary between zero at the point of attachment to the theoretical value, at a point $3/4$ inches removed from the attachment, according to a sine curve. Calculations were also made assuming that the axial buckling was uniform all the way across the width of the plate. Results from the two cases are compared in Fig. 11. As indicated, the first assumption leads to a worst radial position associated with the latter assumption is adjacent to the side plate. It is of interest to note that the difference in incipient boiling power levels associated with the two worst positions is only 1%. Perhaps a more important observation and deduction is that near the side plate, where according to the first and more realistic assumption the buckling is restrained, it might be possible to increase the fuel loading tolerances and or the nominal power density. The former eases the fabrication problem and the latter results in a somewhat higher neutron flux in the island.

It has been pointed out previously that, due to the pronounced neutron flux peaking at the ends of the core, most of the calculations have been based on a hot spot located at the fuel region outlet end, with flux peaking values chosen on the basis of the nuclear calculation and experimental results and the fuel length fabrication tolerances¹¹ to give minimum incipient boiling power levels. Calculations were also made to determine the effect of axial position on incipient boiling power level. Figure 12 shows the relative incipient boiling power level in the inner fuel element as a function of elevation with respect to the core horizontal mid plane at the radial location of maximum pressure induced fuel plate deflection. It is apparent from this figure that efforts to reduce the fuel length tolerance or to further suppress the axial peaking at the bottom of the fuel element are probably warranted since elimination of this peaking could produce as much as a 25% increase

in incipient boiling power level.

The fuel element fabrication tolerances of most interest with respect to their effect on incipient boiling power level are those associated with coolant channel thickness and local fuel loading. The effects of changes in minimum and average coolant channel thickness tolerances are shown in Fig. 13, where relative incipient boiling power level has been plotted as a function of the average coolant channel thickness tolerance for various values of local coolant channel thickness tolerance. The relative power levels are based on the present values of 6 and 10 mils for the average and local thickness tolerances, respectively.

In evaluating the effects of fuel loading tolerance changes, the percentage change in incipient boiling power level has been shown to be essentially equal to the percentage change in local fuel loading tolerance (i.e., the 5/64-in.-diameter spot tolerance) and equal to about one-half the percentage change in line average loading tolerance, assuming a change in line average tolerance to apply to the radial as well as the axial hot streak.

B. General Conclusions

The results of these studies indicate that the HFTR should be capable of meeting the thermal design requirements of a 15-day, 100-Mw operating fuel cycle. As well as indicating general operability, these studies have given valuable information relative to required control system set points and accuracy requirements and required fuel element fabrication tolerances. They have also provided a basis for transient heat transfer studies covering such items as reactivity insertions, loss of pressure and loss of pumping power.

The incipient boiling power levels calculated here are believed to be generally conservative. While it was intended that the magnitude and treatment of each of the individual factors lead toward conservative results, the assumptions regarding hot spot coolant velocity and the probability of simultaneous occurrence of all of the influencing factors are particularly pessimistic. It must be recognized, however, that not all possible factors have been considered. The effects of dissolved radioactive gas might be to appreciably reduce the temperatures at which boiling

would occur. Data on inlet header flow distribution indicates no maldistribution effects and none have been included in the analysis; however, more conclusive evidence would have to be obtained before this possibility could be completely eliminated. Nuclear calculations indicate that the peak power density will remain constant during the cycle. There has also been no attempt to account for possible effects of radiation damage, which may prove to be a serious problem particularly in regard to blistering. These effects must be checked out during the approach-to-power runs. In applying the results of these studies it is essential that the possibility of occurrence of these unaccounted-for factors be recognized.

It is anticipated that the calculational program developed here will prove useful in future HFIR operations particularly in evaluation of fuel element design changes and in the programming of above design point operation or for the operation programming of substandard cores.

ACKNOWLEDGMENTS

The authors wish to express their gratitude to T. B. Fowler and C. D. Griffies for the conscientious manner in which they have undertaken the task of coding, revising, and expediting of the machine calculations carried out during the course of these studies over the past four years. We wish also to thank H. C. Claiborne for his most helpful review of the analysis philosophy and procedures and for his efforts in accomplishing inclusion of the incipient boiling correlation in the machine program. Thanks are also due to R. D. Cheverton for his many helpful suggestions made during the course of these studies and to all of the other co-workers whose cooperation and consulting services have made this report possible.

BIBLIOGRAPHY

1. R. D. Cheverton, "HFIR Preliminary Physics Report," USAEC Report ORNL-3006, Oak Ridge National Laboratory, October 4, 1960.
2. J. R. McWherter and T. G. Chapman, "Mechanical and Hydraulic Design of the HFIR," in Research Reactor Fuel Element Conference, September 17-19, 1962, Gatlinburg, Tennessee, TID-7642, Book I.
3. W. R. Gambill and R. D. Bundy, "HFIR Heat-Transfer Studies of Turbulent Water Flow in Thin Rectangular Channels," USAEC Report ORNL-3079, Oak Ridge National Laboratory, June 5, 1961.
4. W. R. Gambill, "Extension of HFIR Boiling Calculations," letter to H. C. Claiborne, September 18, 1963.
5. N. L. Kafengauz and I. D. Bauarov, "The Effect of the Height of a Flat Aperture on the Transformation of Heat Into Water," Teploenergetica, No. 3, 76-8, 1959.
6. R. P. Stein and P. A. Lottes, "Boiling 'Burnout' for Reactor Design," Reactor Technology, Selected Reviews - 1964.
7. A. E. Bergles and W. M. Rohsenow, "The Determination of Forced-Convection Surface-Boiling Heat Transfer," ASME Paper 63-HT-22, August 1963.
8. W. R. Gambill, "Boiling-Burnout Research at the Savannah River Laboratory," USAEC Report ORNL-CF-62-7-30, Oak Ridge National Laboratory, July 16, 1962.
9. W. R. Gambill, "Recommended HFIR Hot Spot Burnout Factors," letter to T. E. Cole, August 1, 1962.
10. T. G. Chapman, "Thermal Expansion and Pressure Differential Induced Stresses and Deflections of HFIR Involute-Shaped Fuel Plates," to be published.
11. Appendix E, Fuel Element Drawings.
12. R. N. Lyon, "Remarks on Thermal Buckling of Columns, Plates and Shells with Initial Sinusoidal Distortion (HFIR Fuel Plates)," Sept. 24, 1962, CF 62-9-53.

13. D. R. Vondy, "Gamma Ray and Neutron Heat Generation in the HFIR," USAEC Report ORNL-CF-63-2-52, Oak Ridge National Laboratory, Feb. 21, 1963.
14. L. A. Haack, "Some Temperature Aspects of the HFIR Control Plate System," USAEC Report ORNL-CF-61-4-73, Oak Ridge National Laboratory, April 18, 1961.
15. R. R. Liguori and J. W. Stephenson, "Heat Engineering and Transfer in Nine Geometries," Astra Inc., 417-5.0, Jan. 1, 1961.

TABLE I
FUEL ELEMENT DESIGN DATA

1. General Data

Geometry - Two concentric cylindrical elements containing involute shaped fuel plates.

Nominal dimensions

Inside diameter, in.	5.067
Outside diameter, in.	17.134
Height of fuel plates, in.	24.0
Height of active fuel, in.	20.0
Thickness of fuel plates, mils	50
Thickness of coolant channels, mils	50
Active core volume (minimum), liters	48.6

Materials of construction

Side Plates	6061-T6 Al
Fuel plate cladding and frames	6061-T0 Al
Fuel and filler piece matrix	Aluminum powder
Fuel (93% U-235 enrichment)	U_3O_8
Burnable poison (in inner annulus filler piece)	B_4C

Material Requirements

U ₃ O ₈ powder	
Particle size, mesh	- 100 to 325
Density, % of theoretical	> 90
Aluminum	
Maximum combined neutron cross section (Σ_a) of all elements other than aluminum and specified alloying constituents of 6061, cm ⁻¹	≤ 0.0005
Applicable specifications	
Powder - ALCOA atomized power No. 101	
Wrought - ASTM Specification B 209-58T Clad GS11A	
All Materials (except B ₄ C)	
Maximum boron content, ppm	< 30
Maximum cadmium content, ppm	< 80
Total fuel loading, Kg U-235	9.4

2. Mechanical Designa. Inner Annulus

Number of plates	171
Minimum heat transfer area, ft ²	138.4
Inner side plate ID, in.	5.067
Inner side plate OD, in.	5.443
Outer side plate ID, in.	10.074
Outer side plate OD, in.	10.590
Fuel plate curvature - involute, with straight sections in side plate grooves	
Involute generating circle radius, in.	2.722
Plate length, in.	24 ± 0.010
Plate width, in.	3.646
Plate thickness, in.	.050 ± .0005
Minimum clad thickness, in.	0.010
Fuel length, in.	20 ± 1/2
Fuel width, in.	3.067 ± 1/16

U ²³⁵ content per plate, g				15.18 g ± 1%
B ¹⁰ content per plate, mg				16.39 ± 10%
U ₃ O ₈ in fuel compact, wt%				31.1
Inner annulus fuel loading, Kg U-235				2.6
Fuel and poison distribution - see D-42114				
Weight of inner annulus assembly, lb				80
Side plate and adaptor rings				
Number				3
Location	Inner side plate		Outer side plate	
	<u>Top</u>	<u>Bottom</u>	<u>Top</u>	
Function	Support target, flow control	Support fuel element	Flow control	
Seat bearing area, in. ²	2.9	2.9		
Axial load, lb	2450	10,730		
Bearing stress, psi	845	3,700		
Seal pressure, psi	34	0	100	
Ambient water temp, °F				
Inside ring	120	130	120	
Outside ring	120	181	120	
Coolant velocity, ft/sec				
Inside ring	7	33	20	
Outside ring	20	20	2 below labyrinth	
Heat generation rate, watts/gm at midplane				70
Ring seat material				6061-T6 Al
Design pressure drop across fuel element, psi				100
Galvanic couples				
Al adaptor ring seats to SST fuel support grid				

b. Outer Annulus

Number of plates				369
Minimum heat transfer area, ft ²				276.6
Inner side plate ID, in.				11.250
Inner side plate OD, in.				11.746
Outer side plate ID, in.				16.622
Outer side plate OD, in.				17.134
Fuel plate curvature - involute, with straight sections in side plate grooves				
Involute generating circle radius, in.				5.873
Plate length, in.				24 ± 0.010
Plate width, in.				3.213
Plate thickness, in.				0.050 ± 0.0005
Minimum clad thickness, in.				0.010
Fuel length, in.				20 ± 1/2
Fuel width, in.				2.840 ± 1/16
²³⁵ U content per plate, g				18.44 g ± 1%
U ₃ O ₈ in fuel compact, wt %				42.3
Outer annulus fuel loading, Kg ²³⁵ U				6.8
Fuel distribution - see D-42122				
Weight of outer annulus assembly, lb				170
Side plate and adaptor rings				
Number				3
Location	Inner	Outer		
	side plate	side plate		
	<u>Top</u>	<u>Top</u>	<u>Bottom</u>	
Function	Flow con- trol	Flow control support shroud	Support element, flow control	
Seat bearing area, in. ²		9.7	9.7	
Axial load, lb		5135	19,235	
Bearing stress, psi		530	1980	
Seal pressure	100	~90	~5	

	<u>Inner</u>	<u>Outer Side Plate</u>	
	<u>Side</u>	<u>Top</u>	<u>Bottom</u>
	<u>Plate</u>		
Ambient water temp, °F			
Inside ring	120	120	181
Outside ring	120	120	156
Coolant velocity, ft/sec			
Inside ring	20	20	20
Outside ring	2 below labyrinth	15	15
Heat generation rate, w/gm at midplane		40	
Ring seat material		6061-T6 Al	
Design pressure drop across fuel element, psi		100	
Galvanic couples			
Al adaptor ring seats to 304 SST bearing rings			

c. Fuel Assembly

Nominal coolant channel thickness, mils	50
Maximum coolant channel local deviation, mils	10
Maximum coolant channel average deviation across width, mils	6
Minimum fuel plate-side plate joint strength, lb/lineal inch	100
Maximum center to center fuel plate - side plate attachment spacing, in.	1

3. Heat Transfer

Design heat load, Mw	97.5
Anticipated fuel region flow rate, gpm at 120°F	10,800 - 13,000

Core pressure drop, psi	72 -- 100
Inlet water temperature, °F	120
Minimum heat transfer area, ft ²	415
Minimum active core volume, liters	48.6
Core average power density, Mw/liter	2
Calculated core max/avg power density ratio (nuclear)	1.45
Active core metal heat capacity, Btu/°F	35.7
Heat fluxes, Btu/hr-ft ²	
Core average	0.8 x 10 ⁶
Hot Spot	1.9 x 10 ⁶
Minimum Incipient Boiling Power Level at end of 15 day fuel cycle, Mw	
Operation at fuel region flow rate of 10,800 gpm	
900 psi vessel inlet	131
600 psi vessel inlet	120
Operation at fuel region flow rate of 13,000 gpm	
900 psi vessel inlet	155
600 psi vessel inlet	139

TABLE II. INPUT DATA FOR HFIR STEADY STATE HEAT TRANSFER STUDIES

Symbol	Definition and Dimensions	Discussion	Typical Value
Physical Description of Reactor			
W	Plate thickness, mils	Include allowance for oxide film buildup in these values. The procedure could be revised to use calculated oxide thickness but would require an additional iterative procedure with negligible improvement in results.	51.5
a	Coolant channel thickness, mils		48.5
L	Active core length, in.	Length of fuel bearing region of the fuel plates is specified here.	20.0
2H	Coolant channel length, ft	This dimension includes entire distance from top to bottom of fuel plates.	2.0
b	Side plate thickness, in.	This value is that of total plate thickness, and not a strengthwise effective thickness.	0.1875
β	Side plate slot factor (1.0 = no slots, 0.0 = complete slots)	This factor specifies degree of restraint for relative longitudinal expansion between fuel plates and side plates (1.0 = max restraint, 0.0 = no restraint).	1.0
Reactor Operating Conditions			
ΔP core	Core pressure drop, psi	The flow model includes shroud inlet losses in this value (see appendix).	73.5
T_i	Coolant inlet temp, °F	The maximum control set value is chosen for this variable.	120.0
P	Operating pressure at core inlet, psia	The control set point is specified here.	900.0
Q/A	Fuel element avg heat flux, Btu/hr-ft ²	This value may be a specified power level or a first guess. At 100 Mw, Q/A = 8.0 x 10 ⁵ .	8.0 x 10 ⁵
A	Side plate heat generation rate, Btu/hr-in. ³	A minimum value for 100 Mw operation is specified to give minimum side plate temperature.	7600.0
β	Constant in side plate heat transfer coeff equation	These constants may be varied to correspond to existing heat transfer conditions on the surface of the side plate opposite the fuel plates.	0.0
γ	Constant in side plate bulk water temp equation		100.0
N	Side plate cold streaking factor	The ratio of bulk water temperature rise of the side plate to that in the average coolant channel is specified here.	0.35
$[q_w/q_c]_c$	Ratio of spot power density to core avg power density	These calculated or experimental nuclear flux peaking values are normally specified for beginning of fuel cycle conditions. Provision for timewise changes in local power density are included elsewhere.	1.45
$[q_w/q_c]_{bc}$	Ratio of channel avg power density to core avg power density		1.15
$[q_w/q_c]_{bc}$	Ratio of spot power density to avg power density across channel at spot elevation		1.0
I	Number of time steps for oxide buildup calculations	Up to 1000 discrete operating periods may be considered in calculating oxide buildup.	1
$Q/A(i)$	Duration of i th period of operation, hr	These values specify operating conditions during each of the time steps to be considered (i.e., one set of these values is given for each time step).	360.0
U2(i)	Ratio of spot power density during i th period of operation to start of cycle value		1.0
ΔP Core (i)	Core pressure drop during i th period of operation, psi		73.5
Uncertainties and Tolerances			
U1	Fuel element flow distribution	Hot streak water vel and temp	This factor is combined with the average channel thickness tolerance and plate deflections to give a hot streak flow factor.
U2	Local flow disturbance factor	Hot spot water vel	This factor is combined with the local channel thickness tolerance and plate deflections to give a hot spot flow factor.
U3	Channel roughness factor	Friction factor	Experimental data ³ indicates a value of 1.15 is applicable to HFIR.
U4	Channel mixing factor	Hot streak bulk temp	A value of 1.0 corresponds to complete cross-channel mixing, 0.0 to no mixing.
U5	Power level measurement and control accuracy	Heat flux	Values of these factors should correspond to anticipated control system performance.
U6	Inlet temp measurement and control accuracy	Bulk water temp	
U7	Pressure measurement and control accuracy	Hot spot operating pressure	0.9
U8	Uncertainty in heat transfer coeff correlation	Heat transfer coeff	The recommended correlation ³ has been incorporated, hence no multiplying factor correction is required.
U9	Uncertainty in burnout correlation	Burnout heat flux	This value not used in calculating incipient boiling. Value of 0.7702 gives recommended burnout correlation.
U10	This input variable not used in calculations		This value is not used in the calculations. Place a 1.0 in appropriate blank on data sheet.
U11	Uncertainty in nuclear calculations	Power densities	An accuracy of ±10% has been assumed pending results of critical experiments.
U12	Timewise spot power density	Hot spot power density	Nuclear calculations to date indicate no increases in hot spot power density with time.
U13	Uncertainty in streak avg fuel loading	Hot streak water vel and temp	This value is governed by the line average fuel loading tolerance.
U14	Uncertainty in plate fuel loading	Hot plate water temp	This value is governed by the fuel plate fuel loading tolerance.
U15	Uncertainty in fuel loading across plate	Hot plate temp	This value is governed by the line average fuel loading tolerance and time constants.
U16	Segregation flux peaking, hot side of plate	Hot spot heat flux	This value is governed by the fuel plate spot loading tolerance.
U17	Segregation flux peaking, cold side of plate	Hot spot heat flux	This value is governed by the fuel plate spot loading tolerance.
U18	Nonband flux peaking, hot side of plate	Hot spot heat flux	These values are determined by two dimensional matrix heat transfer constants and are dependent on thickness of the fuel bearing portion of the fuel plate.
U19	Nonband flux peaking, cold side of plate	Hot spot heat flux	
Δx avg	Tolerance on avg coolant channel thickness, mils	Hot streak flow rate	These are the fabrication tolerance values. They are combined with plate deflections to give corrected hot streak and hot spot flow rates.
Δx local	Tolerance on local coolant channel thickness, mils	Hot spot flow rate	10.0
Hot Spot Location			
σ	Distance from top of core to spot, ft	These values are employed in calculating bulk water temperature and pressure at the hot spot location.	1.833
f	Fraction of total heat liberated above hot spot		1.0
a1	Adjacent channel arrangement - narrow, wide, narrow, wide, narrow	These four variables are employed to specify the arrangement of wide and narrow channels to be considered. A value of 1.0 is assigned to the variable corresponding to the desired arrangement, all others being assigned values of 0.0.	0.0
a2	Adjacent channel arrangement - wide, wide, narrow, wide, wide		0.0
a3	Adjacent channel arrangement - narrow, wide, narrow, narrow, wide, narrow		1.0
a4	Adjacent channel arrangement - all narrow		0.0
Correlation Constants			
A_{ht}	Constant in heat transfer coeff correlation	The recommended correlation is as follows: $h = K [A + B T_B - C T_B^2] \left[\frac{1}{(x)} \right] \left[\left(\frac{0.4 \rho v^4}{\mu} \right)^D - 125 \right] \left[1 + 7.854 \times 10^{-4} \right]$ $+ \frac{1}{3} \left(\frac{1.667 \times 10^{-4}}{\mu} \right)^D \left[\left(\frac{1}{x} \right)^E \right]$ where K is a constant. This equation is selected by setting $E_{ht} = 0.164$. Selecting $D_{ht} = 0.164$ provides for use of the following alternate equation: $h = [A + B T_B - C T_B^2] \left[\left(\frac{1}{x} \right)^D \right] \left[\left(\frac{1}{x} \right)^E \right]$ Typical input values for this alternate equation are 1402.0, 12.759, 0.014836, 0.164 and 0.654 for A_{ht} , B_{ht} , C_{ht} , D_{ht} , and E_{ht} , respectively.	478.205
B_{ht}	Constant in heat transfer coeff correlation		0.91233
C_{ht}	Constant in heat transfer coeff correlation		0.667
D_{ht}	Constant in heat transfer coeff correlation		0.164
E_{ht}	Constant in heat transfer coeff correlation		0.164
Q	Fuel plate pressure deflection constant, mils/psi	These values are based on elastic beam theory, and are dependent upon position along the involute arc.	0.52981
Z	Fuel plate thermal deflection constant, mils/°F		0.02823
ξ	Fuel plate volumetric expansion coeff, in. ³ /in. ³ -°F	This value is assumed equal to 3 times the linear coefficient of expansion for calculating closing of gap.	3.9 x 10 ⁻⁵
C1	Constant in oxide buildup correlation	The recommended correlation constants ¹⁰ have been modified to correspond to minimum data points.	8290.0
C2	Constant in oxide buildup correlation		0.03124
Computational Procedure Mechanics			
Initial v_i	Initial guess of channel inlet vel, ft/sec	Choice of this variable is critical only at low flow rates.	40.0
Initial T_{sh}	Initial guess at plate surface temp, °F	Choice of this variable is not critical. A value of 400.0 is generally satisfactory.	400.0
Initial K	Initial guess at ratio of incipient boiling heat flux to hot spot heat flux	A value of 1.0 is generally employed when solving for incipient boiling power level.	1.0
B.O. Indicator	Specific correlation to be employed for incipient boiling or burnout	Use -2.0 when calculating incipient boiling. See appendix for burnout calculation options.	-2.0
Max. Iter.	Max permissible number of iterations	Convergence is generally obtained in less than 15 iterations.	31.0
Conv.	Constant in equation for calculating corrected reactor power level	This variable determines degree of correction to be applied on next iteration. Value of 0.5 generally satisfactory.	0.5
Conv. Power	Permissible error between assumed and calculated incipient boiling power	A value of 1 x 10 ⁻⁵ gives satisfactory convergence on an incipient boiling power level. If a calculation at a specific power level is desired, a large number, such as 10.0, should be used here.	1.0 x 10 ⁻⁵

TABLE III. HFIR FUEL ELEMENT OPERATING CONDITIONS AT 100 Mw

	Start of Cycle			End of 15-day Cycle		
	Fuel Average	Hot Streak	Hot Spot	Fuel Average	Hot Streak	Hot Spot
1. 10,800 gpm Fuel Region Flow Rate						
Heat flux, Btu/hr-ft ²	0.8 x 10 ⁶	0.9 x 10 ⁶	1.9 x 10 ⁶	0.8 x 10 ⁶	0.9 x 10 ⁶	1.9 x 10 ⁶
Water inlet temp., °F	120	121	121	120	121	121
Water outlet temp., °F	189	266	266	189	268	268
Oxide-water interface temp., °F	206	328	400	206	330	413
Metal-oxide interface temp., °F	206	328	400	213	397	540
Mean fuel plate temp., °F	214	337	419	221	406	559
Calculated permissible incipient boiling local heat flux peaking factor	1.338			1.275		
Calculated incipient boiling power level at 600 psia, Mw	131.5			120		
2. 13,000 gpm Fuel Region Flow Rate						
Heat flux, Btu/hr-ft ²	0.8 x 10 ⁶	0.9 x 10 ⁶	1.9 x 10 ⁶	0.8 x 10 ⁶	0.9 x 10 ⁶	1.9 x 10 ⁶
Water inlet temp., °F	120	121	121	120	121	121
Water outlet temp., °F	178	246	246	178	246	246
Oxide-water interface temp., °F	197	303	371	197	303	377
Metal-oxide interface temp., °F	197	303	371	204	351	461
Mean fuel plate temp., °F	205	312	390	212	360	480
Calculated permissible incipient boiling local heat flux peaking factor	1.490			1.451		
Calculated incipient boiling power level at 600 psia, Mw	146.0			139		

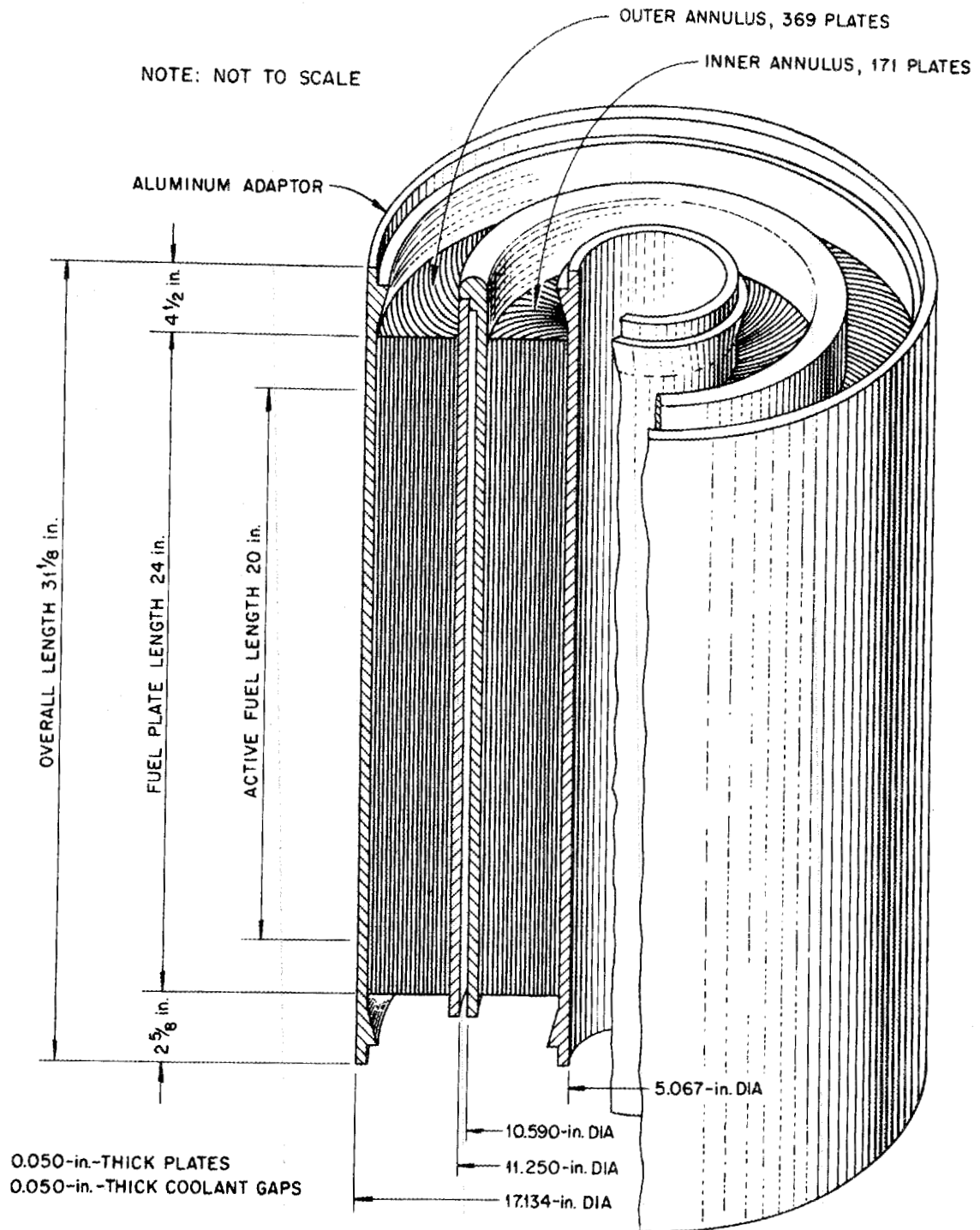


Fig. 1. Dimensional Illustration of the Assembled High Flux Isotope Reactor Fuel Element.

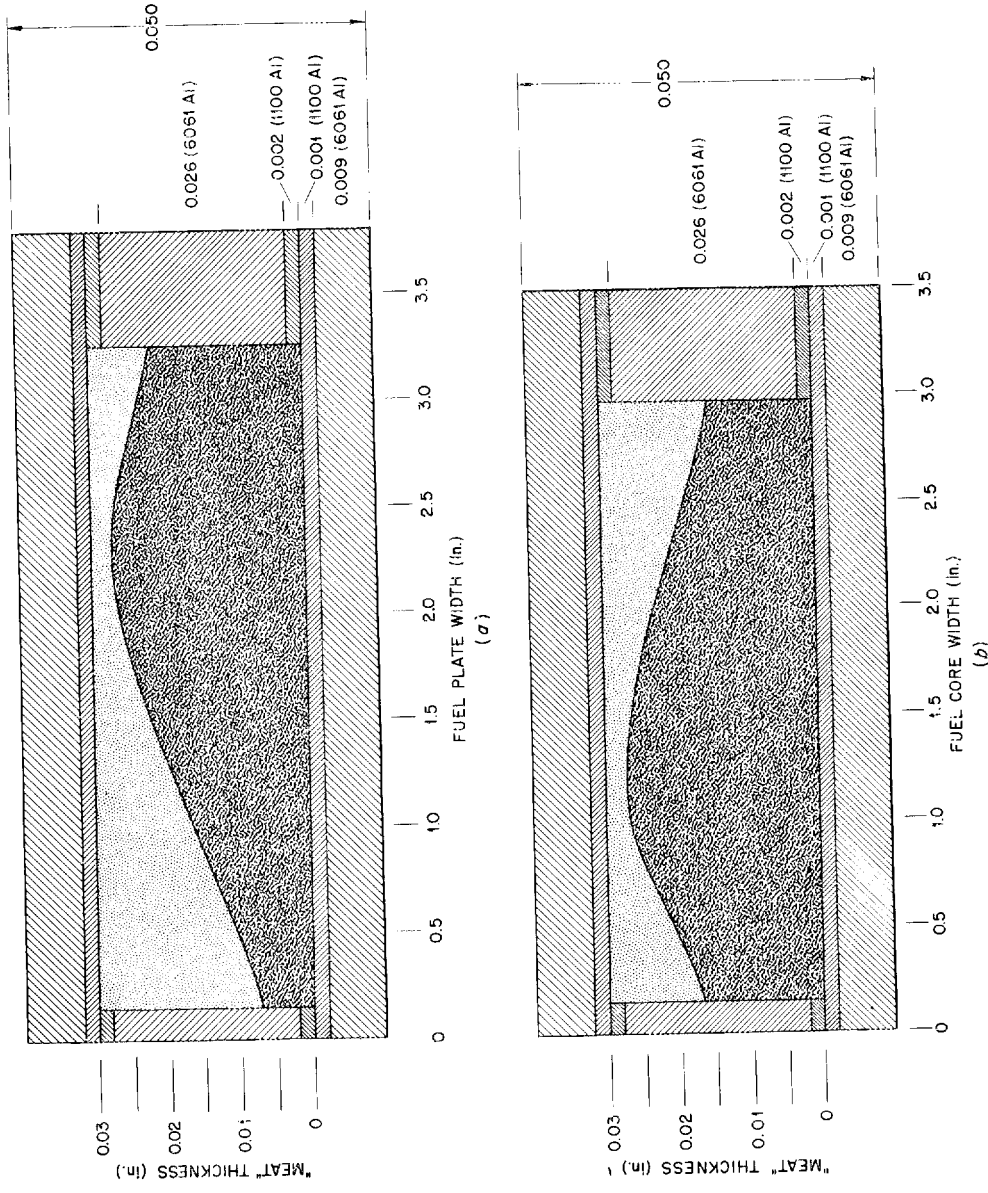


Fig. 2. Idealized Cross Sections for Experimental HFIR Fuel Plates.
(a) Inner Annulus; (b) Outer Annulus.

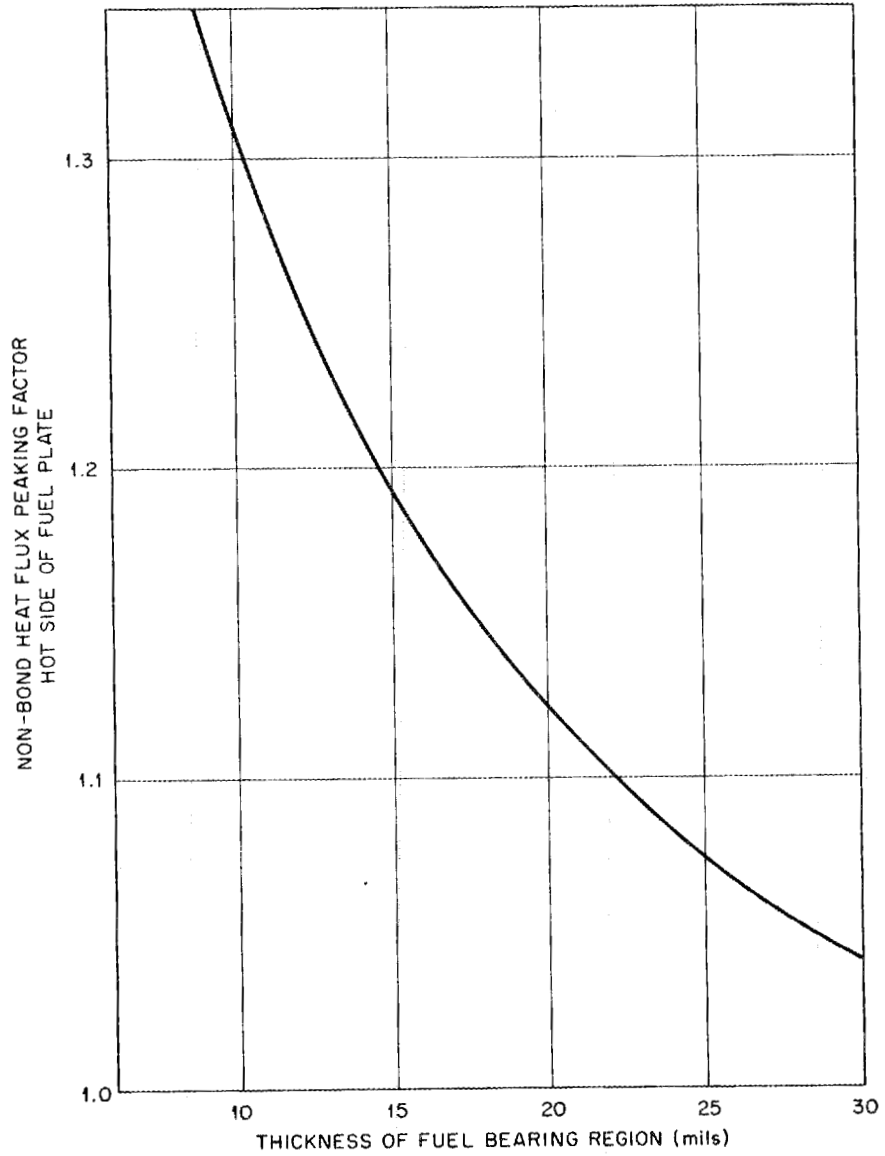


Fig. 3. Heat Flux Peaking on Hot Side of Fuel Plate Due to Non-Bonds.

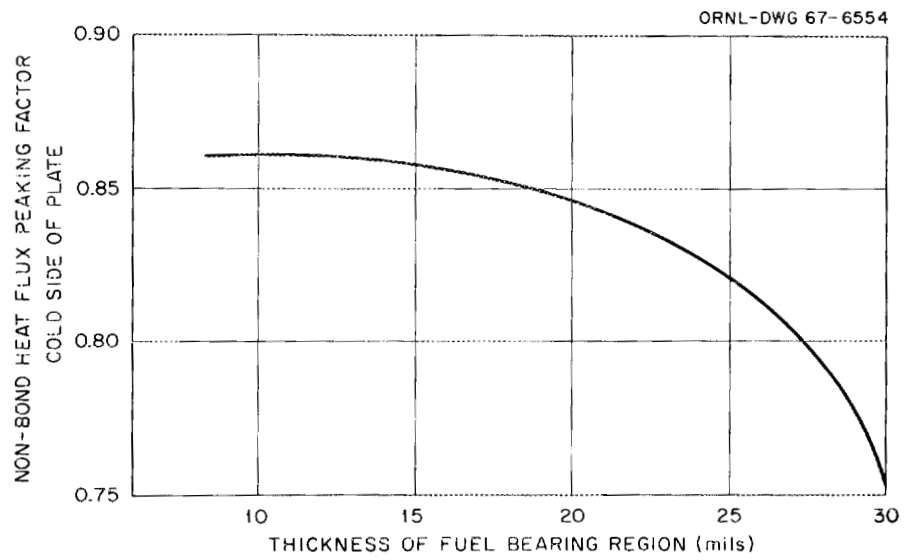
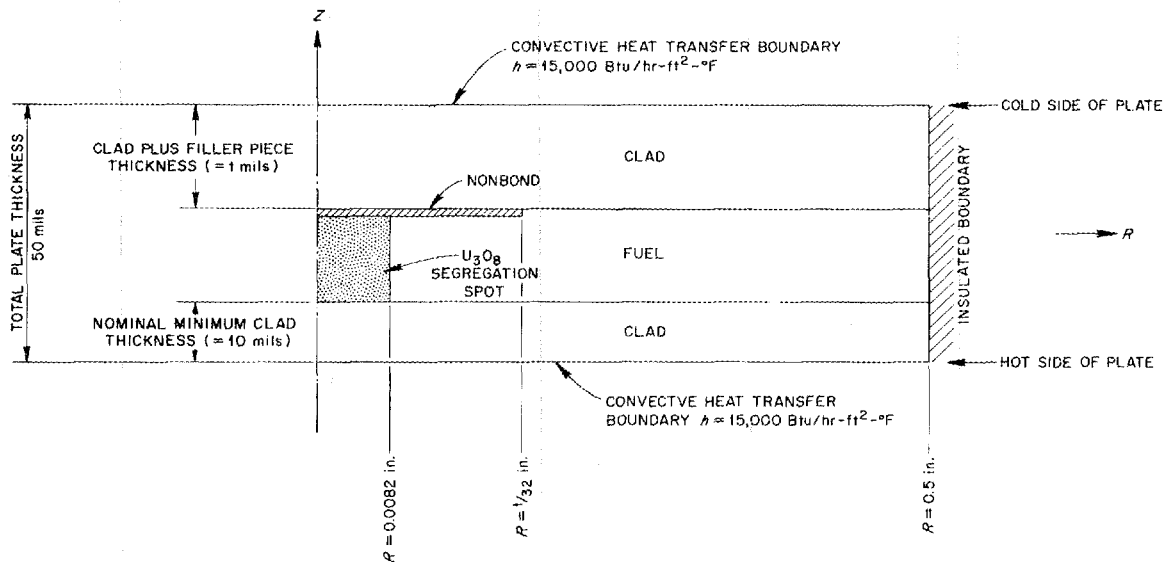


Fig. 4. Heat Flux Peaking on Cold Side of Fuel Plate Due to Non-Bonds.

ORNL-DWG 67-6556



BASIC ASSUMPTIONS:

1. NO HEAT TRANSFER ACROSS NON-BOND
2. CIRCUMFERENTIAL SYMMETRY
3. PACKING FRACTION OF U_3O_8 PARTICLES IN SEGREGATION SPOT = 0.74

REGION	THERMAL CONDUCTIVITY		HEAT GENERATION RATE AT 100 MW (Btu/hr in. ³)
	(Btu/hr-in.-°F)	(Btu/hr-ft-°F)	
FUEL	8.08	97.0	$1.82 \times 10^{17} / (50-t-10)$
U_3O_8 SEGREGATION	2.26	27.1	$1.87 \times 10^{18} / (50-t-10)$
CLAD	8.08	97.0	1.51×10^4

Fig. 5. Model Employed for Calculation of Non-Bond and Fuel Segregation Heat Flux Peaking Factors.

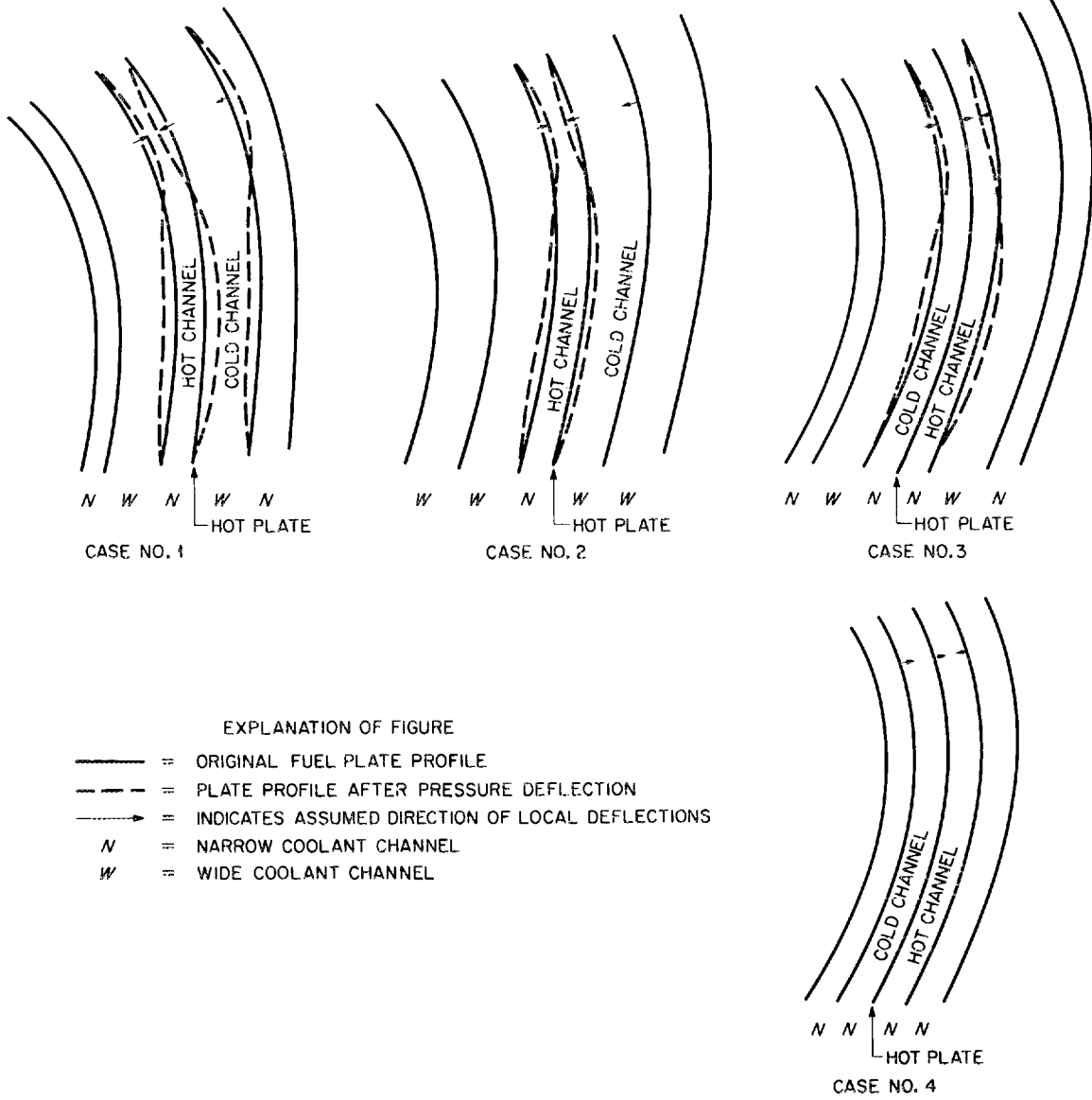


Fig. 6. Alternate Arrangements of Adjacent Coolant Channels.

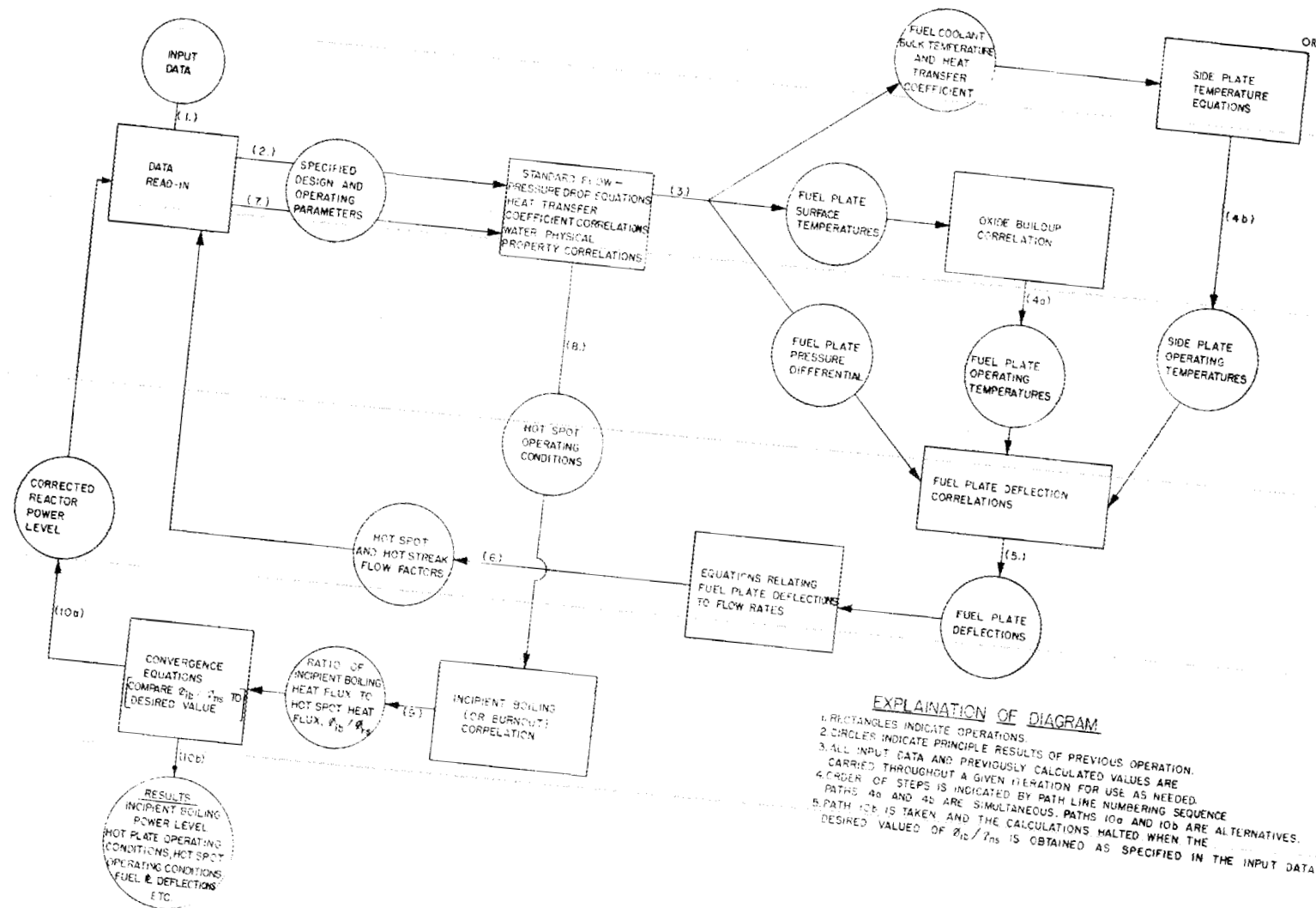


Fig. 7. Calculational Procedure - Simplified Block Diagram.

INCIDENT BOILING POWER LEVEL, ($\text{MW} \times 10^{-2}$)
OR
ALLOWABLE LOCAL HEAT FLUX PEAKING FACTOR AT 100 MW.

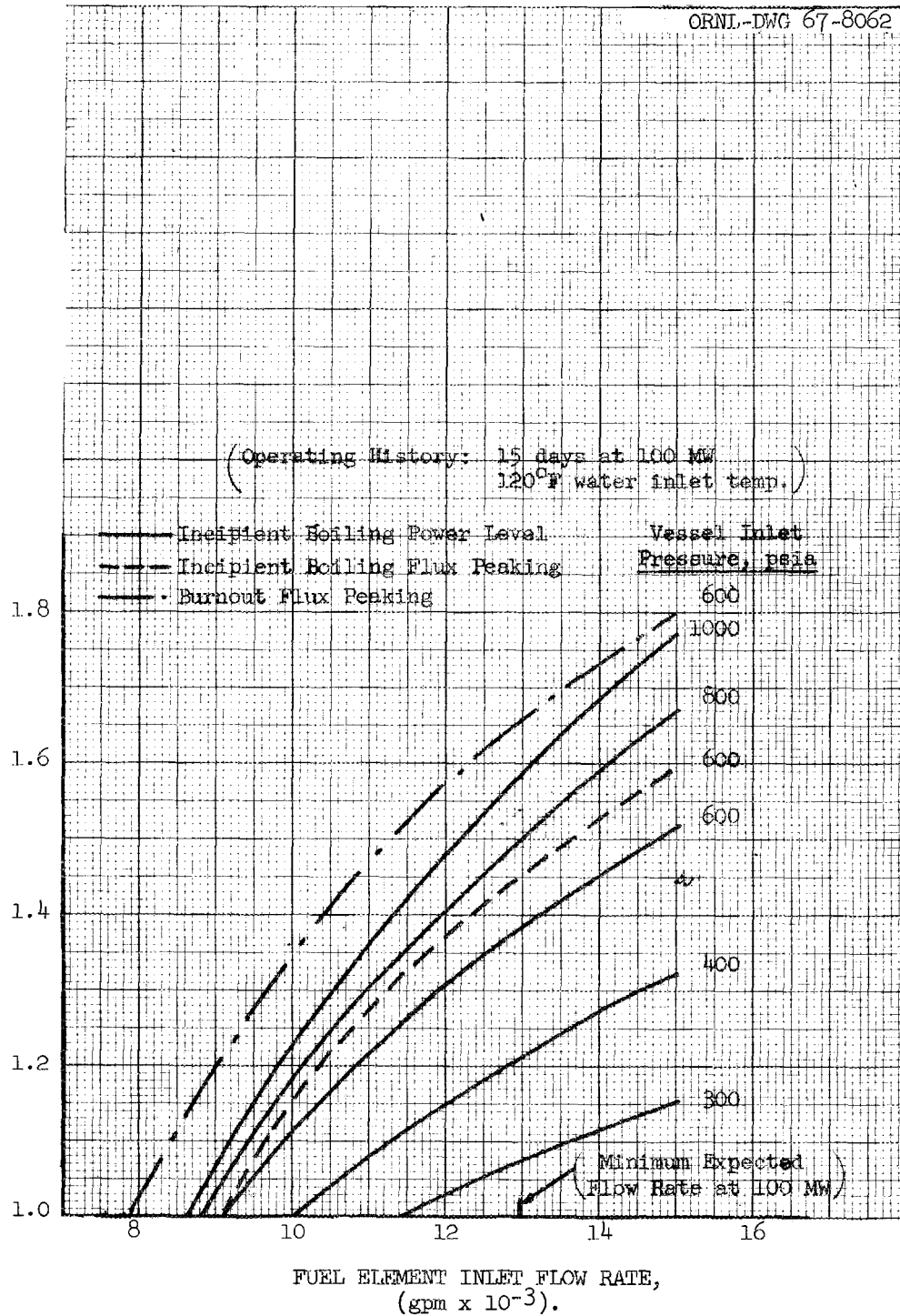


Fig. 8. Effect of Fuel Element Flow Rate on Incipient Boiling Power Level and Allowable Local Heat Flux Peaking Factors for Incipient Boiling and Burnout at 100 Mw.

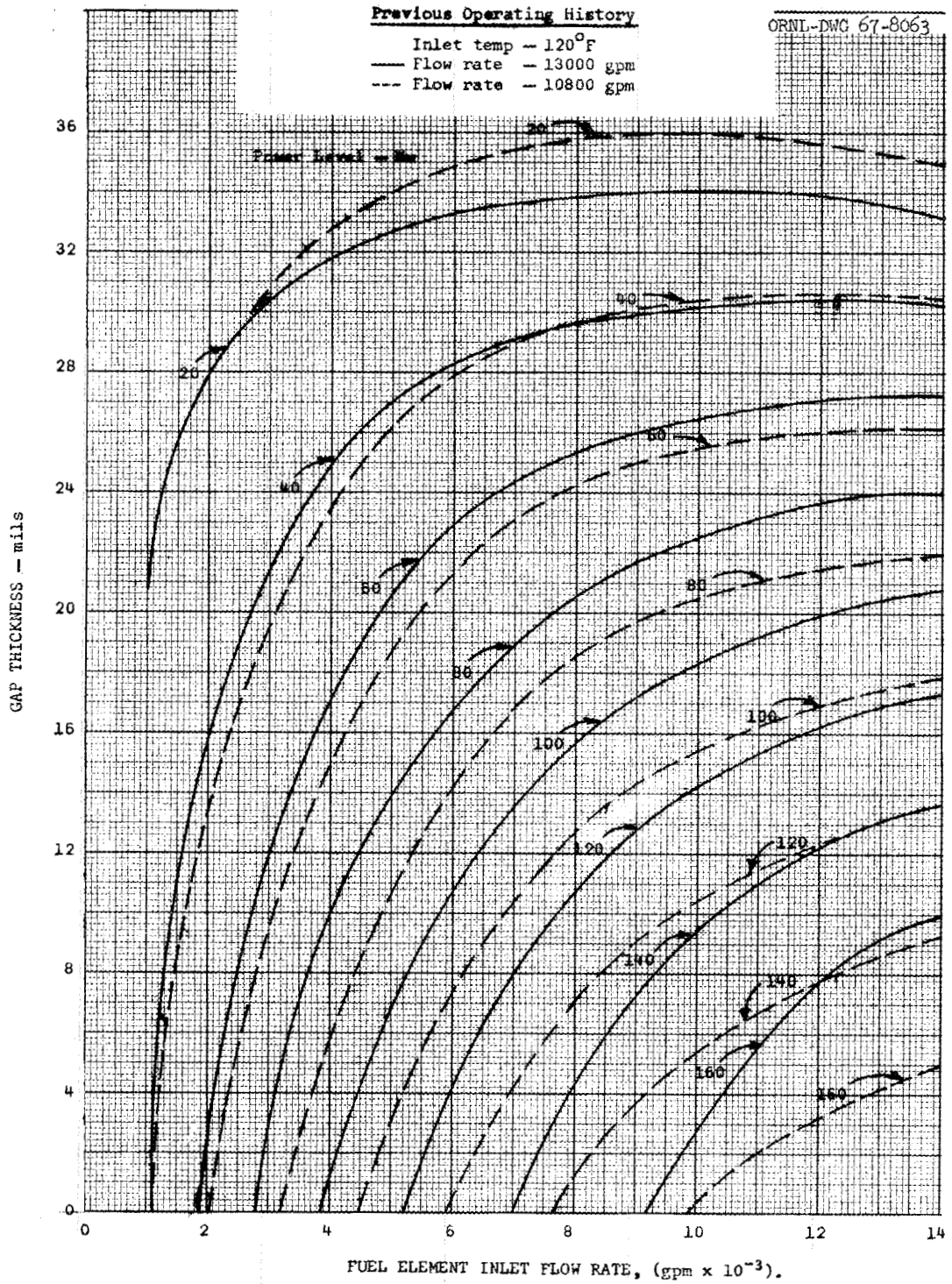


Fig. 9. Minimum Calculated Coolant Gap Thickness After 15-Day Operation at 100 Mw.

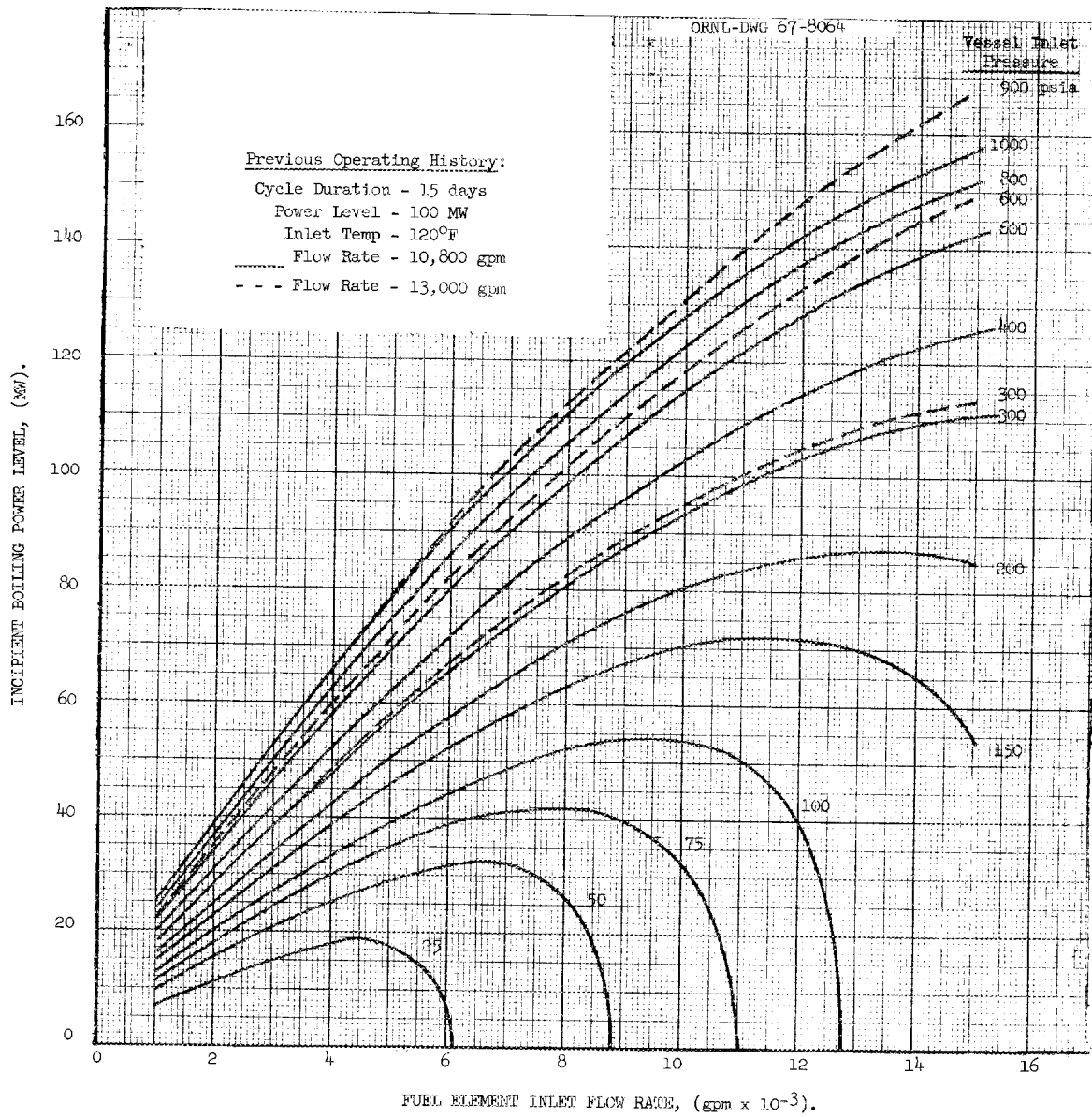


Fig. 10. Effect of Flow Rate and Operating Pressure on Incipient Boiling Power Level.

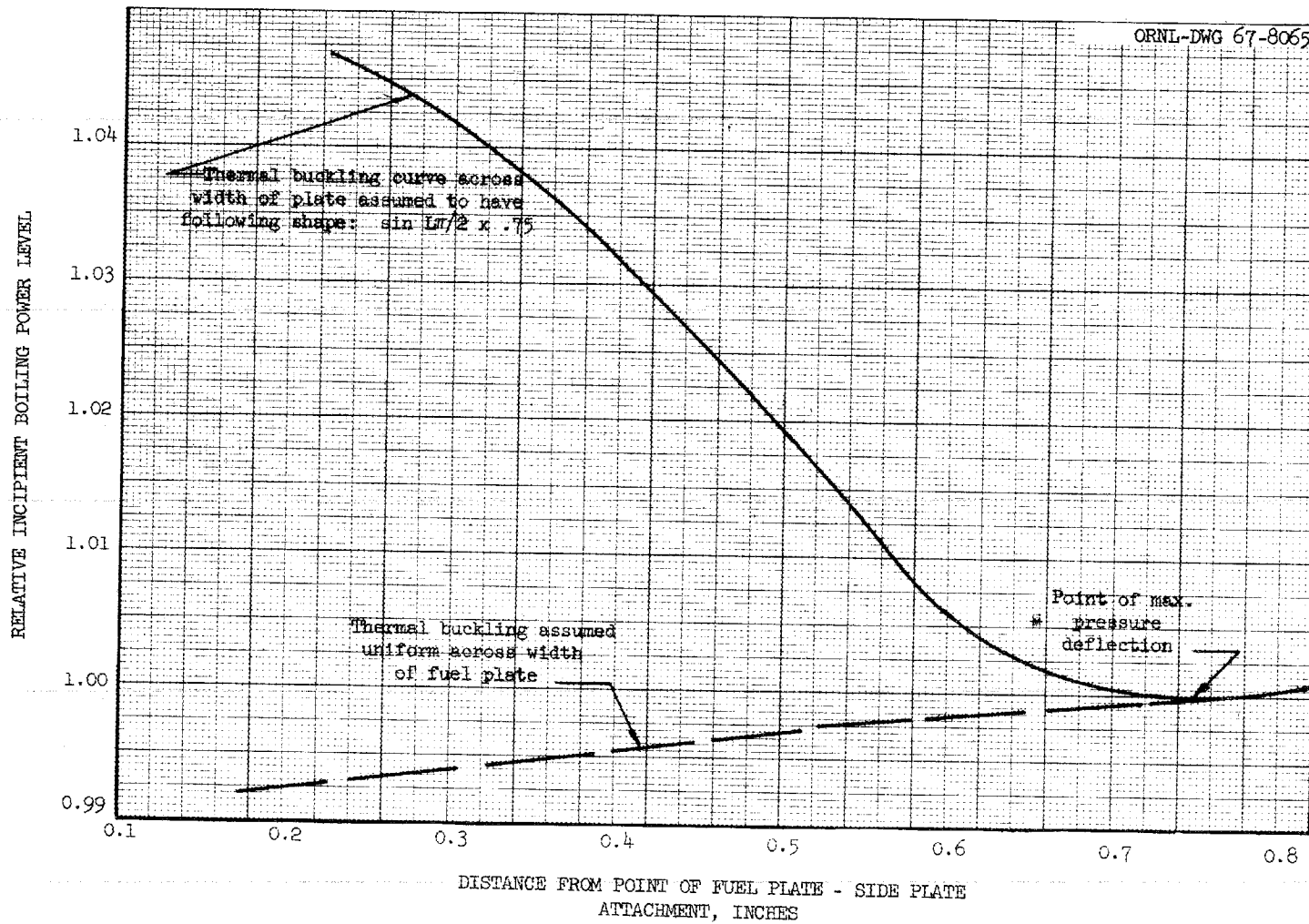


Fig. 11. Effect of Alternative Assumptions on Fuel Plate Axial Thermal Buckling Calculated Incipient Boiling Power Level.

ORNL-DWG 67-8066

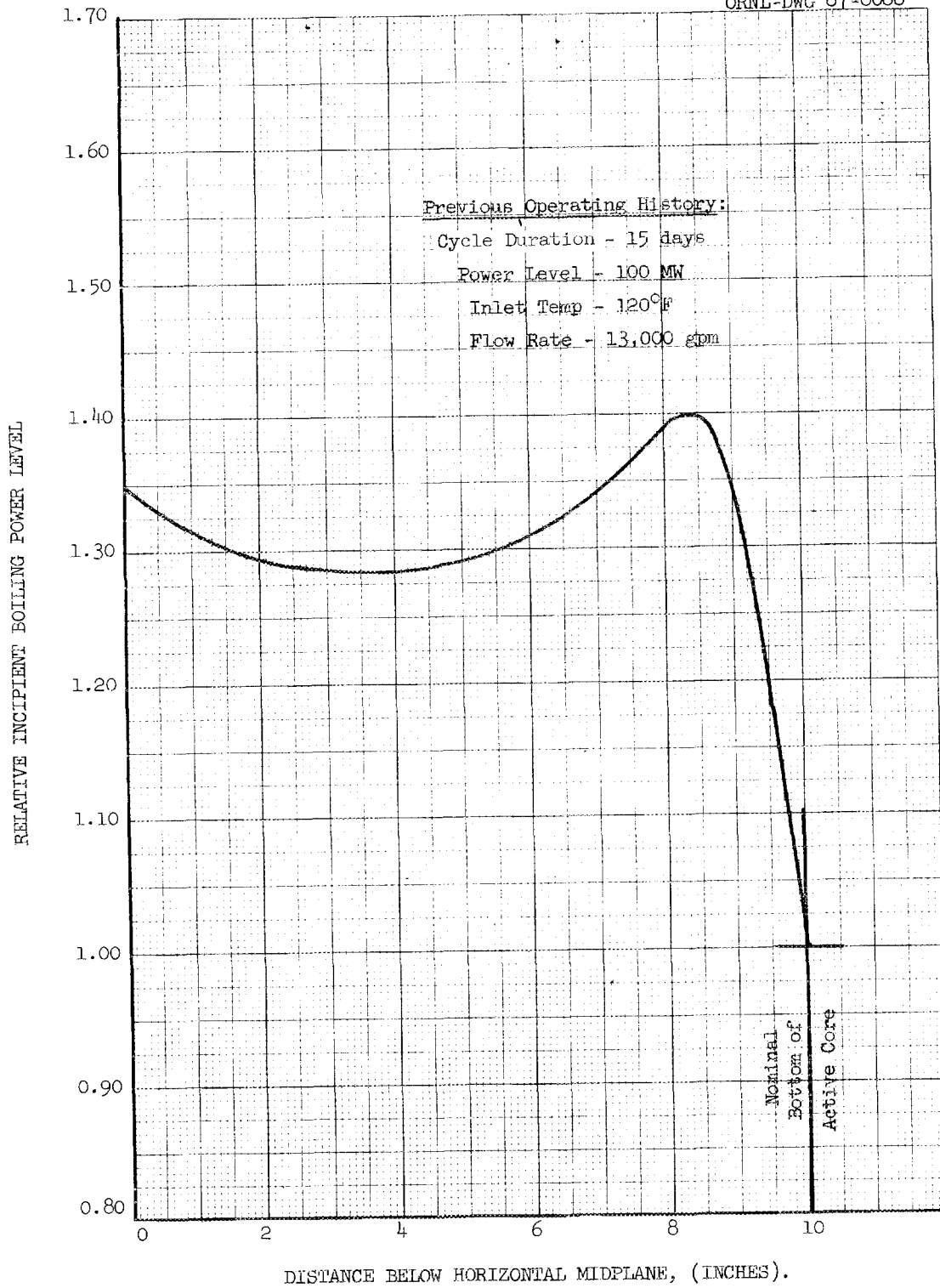


Fig. 12. Effect of Hot Spot Elevation on Incipient Boiling Power Level.

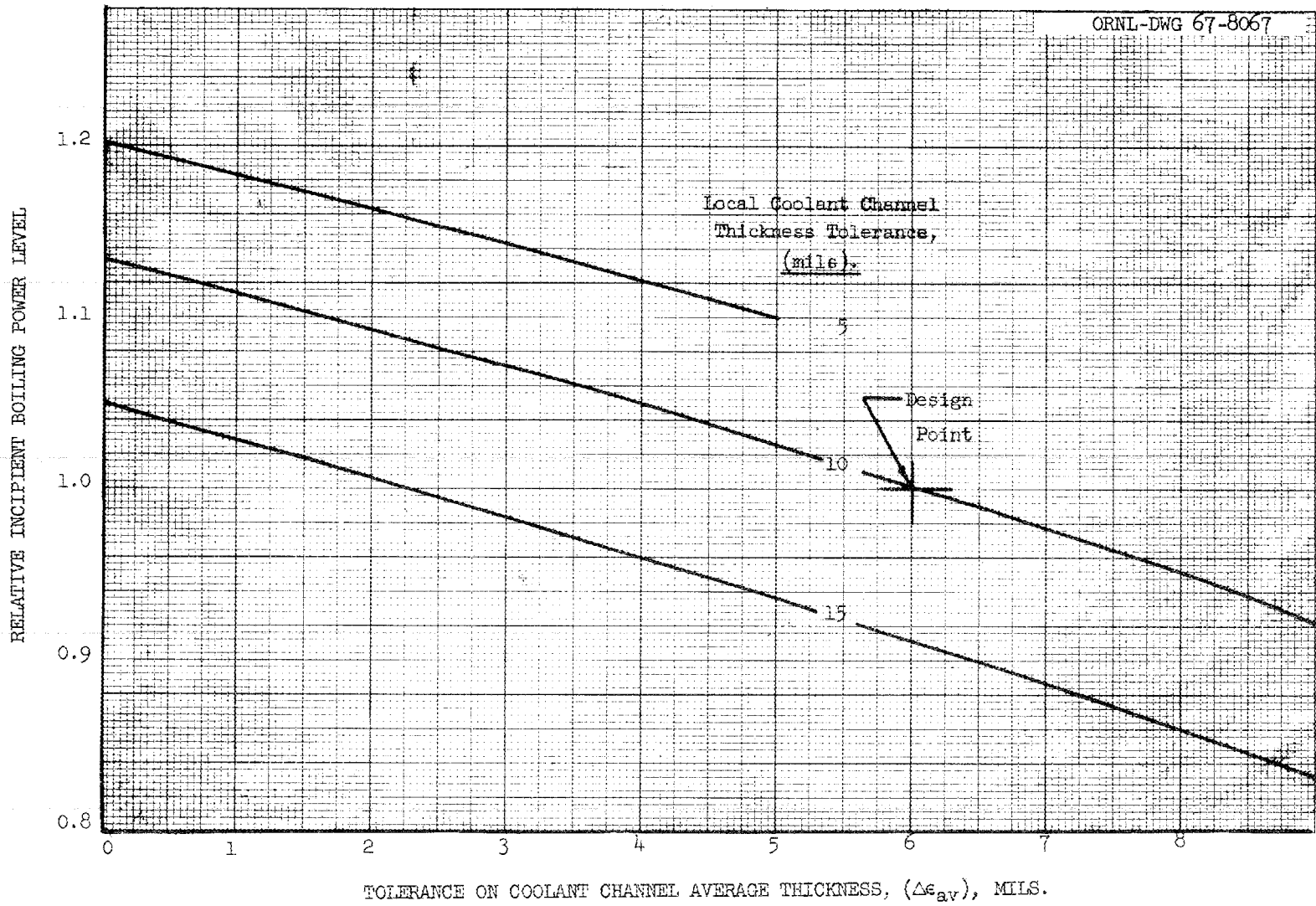


Fig. 13. Effect of Coolant Channel Tolerances on Incipient Boiling Power Level.

APPENDICES

APPENDIX A

DETAILS OF HEAT REMOVAL ANALYSIS PROCEDURE

Before considering the details of the analysis procedure, it is essential that the reader realize that this study is one of those which, like Topsy, just grew and which, after having grown, has not been subjected to the plastic surgery which would be desirable from the standpoint of beauty of form. Consequently, a brief review of the history of this growth is probably in order. These studies began as a part of the HFIR feasibility and initial design effort. At this stage, the emphasis in these studies was on establishment of overall design feasibility, without inclusion of certain design details and factors which ultimately required consideration. A calculational procedure, referred to as the HOT SPOT code, based on standard hydraulic and heat transfer equations and the best available burnout correlations, was developed to meet these early needs. Subsequently, there were two major changes in approach which resulted in drastic revision of this calculational procedure. The first of these was inclusion of the effects of fuel plate deflections and time in the fuel cycle (i.e., oxide buildup). In calculating plate deflections and oxide buildup, the original HOT SPOT procedure became simply a subroutine in the overall calculation, referred to as the HOT SPOT program. The second revision was the result of the decision to base the heat transfer studies on the calculated point of incipient boiling rather than on burnout. This necessitated changes in some of the mechanics of the calculations due to the nature of the correlation employed in calculating incipient boiling. The following presentation of the details of the procedure follows this historical pattern in that the basic subroutine is presented first, then comes the method of employing this subroutine along with the fuel plate deflection and oxide buildup equations to give calculated burnout power levels, and finally the revisions made to permit calculation of the minimum incipient boiling power level. It should also be noted here that while the following presentation would seem to indicate a complete integration of the incipient boiling and burnout calculations into a single machine program such

is actually not the case. Separate program decks are available for boiling and burnout calculations, but as yet there is no single deck which will accomplish both.

The following pages consist of a listing of the basic steps employed in these heat removal studies and the equations employed in each of these steps. The principal assumptions utilized in arriving at these equations have been discussed in the body of this report. Notations employed in these equations are defined in the table of nomenclature, with more detailed information regarding the input variables being supplied in Table II. The exact procedures employed for obtaining convergence have not been indicated in this listing. These can be determined if desired by examination of a Fortran listing for the program.

I. HOT SPOT SUBROUTINE

Part A. Nominal Operating Conditions

1. The density of the inlet coolant water, ρ_i , is calculated according to the following correlation:

$$\rho_T = 62.99 - (0.5350 \times 10^{-2})T - (0.4525 \times 10^{-4})T^2 \quad (1)$$

2. Assuming a value of inlet velocity, v_i , calculate the nominal bulk temperature rise across the channel, $\Delta T_{B \text{ nom}}$, according to the following equation:

$$\Delta T_{B \text{ nom}} = \frac{1.44 \times 10^5}{v_i \rho_i \epsilon} \frac{Q}{A} \frac{(q_a)_{hc}}{(q_a)_c} L (0.3858 \times 10^{-5}) U_5 U_{11} U_{12} U_{14} \quad (2)$$

3. Calculate the core midplane bulk temperature, T_{mp} , as follows:

$$T_{mp} = (U_6)T_i + 1/2 \Delta T_{B \text{ nom}} \quad (3)$$

4. Calculate the midplane bulk water density, ρ_{mp} via equation (1).

5. Calculate the bulk water exit temperature, T_{exit} , as follows:

$$T_{\text{exit}} = (U_6) T_i + \Delta T_{\text{B nom}} \quad (4)$$

6. Calculate the exit bulk water density, ρ_{exit} , via equation (1).

7. Calculate the midplane bulk coolant viscosity, μ_{mp} , from the following correlation:

$$\mu(T) = 366 T^{-1.172} \quad (5)$$

8. Calculate a new value of inlet velocity, v_i , from the following equation:

$$144 \frac{\Delta P_{\text{core}}}{\rho_i} = \left\{ \left(v_i \frac{\epsilon}{\epsilon + w} \right)^2 (7.764 \times 10^{-3}) + \right. \\ \left. v_i^2 \left(1.25 - \frac{\epsilon}{\epsilon + w} \right) (6.211 \times 10^{-3}) + \right. \\ \left. v_i^2 \frac{\rho_i}{\rho_{\text{exit}}} \left(1 - \frac{\epsilon}{\epsilon + w} \right)^2 (0.01553) + \right. \\ \left. \frac{U_3 (20.0) \mu_{\text{mp}}^{0.2} v_i^{1.8} \rho_i^{0.8} (2H)}{\rho_{\text{mp}} \epsilon^{1.2}} - \right. \\ \left. \frac{(2H) \rho_{\text{mp}}}{\rho_i} \right\} \quad (6)$$

(The flow model employed in establishing this equation is shown in Figure A-1.)

9. Reiterate steps 2 through 8 until

$$\left| \frac{v_i(n) - v_i(n-1)}{v_i(n)} \right| \leq 10^{-6} \quad .$$

10. Using final value of v_i , calculate the maximum possible bulk temperature rise from core inlet to the hot spot, $\Delta T_{B \text{ hs}}$, as follows:

$$\Delta T_{B \text{ hs max}} = \frac{U_{13}}{U_1} \Delta T_{B \text{ nom}} f \left(\frac{q_{in}}{q_a} \right) r, hc \quad (7)$$

11. Calculate the actual hot spot bulk water temperature from the following equations:

$$\Delta T_{B \text{ hs}} = \Delta T_{B \text{ hs max}} - (U_4) \left[\Delta T_{B \text{ hs max}} - f \left(\Delta T_{B \text{ nom}} \right) \right], \quad (8)$$

$$T_{B \text{ hs}} = (U_6) T_i + \Delta T_{B \text{ hs}} \quad (8a)$$

12. Calculate the bulk water density at the hot spot, $\rho_{B \text{ hs}}$, from Eq. (1).
 13. Calculate the hot spot coolant velocity, v_{hs} , as follows:

$$v_{hs} = \left(\frac{v_i \rho_i}{\rho_{B \text{ hs}}} \right) (U_1)(U_2) \quad (9)$$

14. Assuming a value of hot spot plate surface temperature, $T_{s \text{ hs}}$, calculate the hot spot heat transfer coefficient, h_{hs} , from either of the equations listed below.

$$h_{hs} = U_8 \left\{ A_{ht} + B_{ht} T_{B \text{ hs}} - C_{ht} T_{B \text{ hs}}^2 \right\} \left(\frac{T_{s \text{ hs}}}{T_{B \text{ hs}}} \right)^{D_{ht}} \frac{(v_{B \text{ hs}})^{E_{ht}}}{\epsilon^{0.348}} \quad (10)$$

$$h_{hs} = U_8 \left\{ A_{ht} + B_{ht} T_{B \text{ hs}} - C_{ht} T_{B \text{ hs}}^2 \right\} \frac{1}{\epsilon} \left[\left(\frac{0.6 v_{B \text{ hs}} \rho_{B \text{ hs}} \epsilon}{\mu_{B \text{ hs}}} \right)^{D_{ht}} - 125 \right] \left[1 + \frac{1}{3} \left(\frac{1.667 \times 10^{-4} \epsilon}{a} \right)^{D_{ht}} \right] \left(\frac{T_{s \text{ hs}}}{T_{B \text{ hs}}} \right)^{E_{ht}} (0.9633) \quad (10a)$$

[The exponent of the $(T_{s\text{ hs}}/T_{B\text{ hs}})$ term is 0.164 in both of these correlations. The choice of Eq. (10) or (10a) is made automatically depending on whether D_{ht} or E_{ht} is specified as 0.164. Equation (10) is based on the G. E. correlation, while Eq. (10a) is the recommended correlation for HFIR calculations.³]

15. Calculate the hot spot water film temperature drop, $\Delta T_{\text{film hs}}$, as follows:

$$\Delta T_{\text{film hs}} = \frac{(Q/A)_{\text{max hs}}}{h_{\text{hs}}}, \quad (11)$$

where

$$\left(\frac{Q}{A}\right)_{\text{max hs}} = \left(\frac{Q}{A}\right) \left(\frac{q_m}{q_a}\right)_c U_5 U_{11} U_{12} U_{15} \left[1.0 + (U_{10} - 1.0) \frac{h_{\text{hs}}}{15,000}\right] \quad (12)$$

- NOTES: 1. Various of the U_n values are set at 1.0 depending on whether the equation is being used to calculate hot spot, hot streak, or hot channel conditions.
2. The value of U_{10} , unless otherwise specified for a particular calculation, is actually the product of the segregation and nonbond heat flux peaking factors (i.e., $U_{10} = U_{16}U_{18}$ for the hot channel and $U_{10} = U_{17}U_{19}$ for the cold channel).

16. Calculate a new value of hot spot surface temperature, $T_{s\text{ hs}}$, as follows:

$$T_{s\text{ hs}} = T_{B\text{ hs}} + \Delta T_{\text{film hs}} \quad (13)$$

17. Reiterate setps 14 through 16 until

$$\frac{T_{s\text{ hs}}(n) - T_{s\text{ hs}}(n-1)}{T_{s\text{ hs}}(n)} \leq 10^{-6} .$$

Part B. Burnout Conditions

Whether this part of the subroutine is used and what section of it is used is determined by the value specified for burnout indicator in input No. 35 (see sample input data form) according to the following table.

<u>Burnout Indicator</u>	<u>Burnout Correlation Employed</u>
2.0	No burnout calculation made
1.0	Savannah River correlation
0.0	Zenkevich-Subbotin correlation
-2.0	Incipient boiling calculation (This correlation is separate from Part B and requires a separate program deck.)

a. Zenkevich-Subbotin Burnout Correlation (valid at pressures ≥ 250 psia)

- a-1. Assuming a value for the ratio of burnout heat flux to hot spot heat flux, K, repeat steps 1 through 13 of Part A using as the input value for Q/A the value employed in Part A times the assumed value of K. (The subscript "bo" is added to all values calculated here to indicate that these are burnout calculations.)
- a-2. Calculate the static pressure at the hot spot, $P_{hs\ bo}$, at these assumed burnout conditions as follows:

$$P_{hs\ bo} = U_7 P - \left[\left(v_{i\ bo} \frac{\epsilon}{\epsilon + w} \right)^2 (7.764 \times 10^{-3}) \frac{\rho_{i\ bo}}{144} + v_i^2 \right. \\ \left. \left(1.25 - \frac{\epsilon}{\epsilon + w} \right) (6.211 \times 10^{-3}) \frac{\rho_{i\ bo}}{144} + \frac{v_{i\ bo}^2 \rho_{i\ bo}}{9.2736 \times 10^3} + \right. \\ \left. \frac{a U_3 (20.0) \mu_{mp\ bo}^{0.2} v_{i\ bo}^{1.8} \rho_{i\ bo}^{1.8}}{\rho_{mp\ bo} \epsilon^{1.2} 144} - \frac{a \rho_{mp\ bo}}{144} \right] \quad (14)$$

- a-3. Calculate the coolant saturation temperature at the hot spot, T_{sat} , according to the following correlation:

$$T_{\text{sat}} = 118.43 P_{\text{hs bo}}^{0.221} \quad (15)$$

- a-4. Calculate the coolant density at the saturation temperature of the previous step, $\rho_{T \text{ sat}}$, via Eq. (1).
 a-5. Calculate the saturated vapor density at the temperature from step a-3, $\rho_v T \text{ sat}$, from the following correlation:

$$\rho_v T \text{ sat} = 1.7357 \times 10^{-3} P_{\text{hs bo}}^{1.038} \quad (16)$$

- a-6. Calculate the burnout heat flux $(Q/A)_{\text{bo}}$ from the Zenkevich-Subbotin correlation as follows:

$$\left(\frac{Q}{A}\right)_{\text{bo}} = 396 (U_9) \left[3600 v_{\text{hs bo}} \rho_{B \text{ hs bo}} \right]^{0.5} \left[T_{\text{sat}} - T_{B \text{ hs bo}} \right]^{0.3} \left[\frac{\rho_{T \text{ sat}} - \rho_v T \text{ sat}}{\rho_{T \text{ sat}}} \right]^{1.8} \quad (17)$$

- a-7. Calculate a new value of K as follows:

$$K = \frac{(Q/A)_{\text{bo}}}{(Q/A)_{\text{max hs}}} \quad (18)$$

NOTE: The value of $(Q/A)_{\text{max hs}}$ is that which comes from the original Q/A input value and not the revised value of step a-1.

- a-8. Reiterate steps a-1 through a-7 until

$$\left| \frac{K_{(n-1)} - K_{(n)}}{K_{(n)}} \right| \leq 10^{-6} .$$

- a-9. Calculate a value of burnout hot spot surface temperature, $T_{S \text{ bo}}$, from the Bernath correlation as follows:

$$T_{S \text{ bo}} = \left[57 \ln P_{hs \text{ bo}} - 54 \left(\frac{P_{hs \text{ bo}}}{P_{hs \text{ bo}} + 15} \right) - \frac{v_{hs \text{ bo}}}{4} \right] (1.8) + 32 \quad (20)$$

NOTE: This value is calculated for advisory purposes only. It is never used in subsequent calculations in this program and is not to be interpreted as an exact value.

- b. Savannah River Correlation (valid at pressures from 25 to 85 psia and for a minimum velocity of ~5.5 ft/sec)

b-1. Same as a-1.

b-2. Same as a-2.

b-3. Same as a-3.

b-4. Calculate a value of burnout heat flux, $(Q/A)_{bo}$, according to the Savannah River correlation as follows:

$$\left(\frac{Q}{A} \right)_{bo} = (479,000) \left\{ 1 + 0.0365 v_{hs \text{ bo}} \right\} \left[1 + 0.00507 (T_{sat} - T_{B \text{ hs bo}}) \right] (1 + 0.0131 P_{hs \text{ bo}}) (U_9) \quad (21)$$

b-5. Same as a-7.

b-6. Same as a-8.

b-7. Same as a-9.

End of HOT SPOT Subroutine

II. HOT SLOT BURNOUT CALCULATION PROCEDURE

1. Run HOT SPOT program to determine hot plate operating conditions per input specified by input data sheet, input numbers 1 through 37, (sample input data sheets will be found in Figs. A-2 and A-3 of this report) with the following exceptions:

Variable	Value
ϵ	as specified $\pm \Delta\epsilon_{av}$
U_1	1.0
U_2	1.0
U_{10}	1.0
U_{13}	1.0
$(q_m, q_a)_r, hc$	1.0
B.O. indicator	2.0

The HOT SPOT program is run twice, as indicated by the values to be employed for ϵ . Results based on the specified value of $\epsilon - \Delta\epsilon_{av}$ are referred to as the narrow channel results and are given the subscript n. Results based on the specified value of $\epsilon + \Delta\epsilon_{av}$ are referred to as the wide channel results and are given the subscript w. The following results from these calculations will be utilized in subsequent steps.

$$\epsilon_n = \epsilon - \Delta\epsilon_{av}$$

$$v_{i,n}, T_{S,hs,n}, \rho_{i,n}, (Q/A)_{max,hs,n}, \rho_{exit,n}$$

$$\epsilon_w = \epsilon + \Delta\epsilon_{av}$$

$$v_{i,w}, \Delta T_{B,nom,w}, T_{S,hs,w}, h_{hs,w}, \rho_{i,w}, \rho_{exit,w}$$

2. Calculate the average pressure differential across a fuel plate, dp , from the following equations:

$$dp = (\alpha_1 + \alpha_2 + \alpha_3) \frac{\rho_{i,n} + \rho_{exit,n} + \rho_{i,w} + \rho_{exit,w}}{1152} (P_i + P_{exit})$$

where

$$P_i = \left[1 + 0.4 \left(1.25 - \frac{\epsilon_w}{\epsilon_w + w} \right) \right] \frac{v_w^2}{64.4} - \left[1 + 0.4 \left(1.25 - \frac{\epsilon_n}{\epsilon_n + w} \right) \right] \frac{v_n^2}{64.4}$$

$$P_{\text{exit}} = \left[1 - \left(1 - \frac{\epsilon_w}{\epsilon_w + w} \right)^2 \right] \frac{v_w^2}{64.4} - \left[1 - \left(1 - \frac{\epsilon_n}{\epsilon_n + w} \right)^2 \right] \frac{v_n^2}{64.4}$$

and

$$v_n = \frac{v_{i,n}}{2} \left(1 + \frac{\rho_{i,n}}{\rho_{\text{exit},n}} \right)$$

$$v_w = \frac{v_{i,w}}{2} \left(1 + \frac{\rho_{i,w}}{\rho_{\text{exit},w}} \right)$$

3. Calculate the hot plate oxide film temperature drop for plates bounded by narrow, wide and average coolant channels ΔT_{fn} , ΔT_{fw} , and ΔT_{fa} as follows:

Rerun HOT SPOT for wide and narrow channels for each specified time interval with the same input values as those of step 1 except that the values of (Q/A) , U_{12} , and ΔP_{core} are to be those specified in conjunction with the particular time step. From these calculations, values of hot plate surface temperature are obtained for the wide and narrow channel cases for each of the time steps $T_{S \text{ hs}, w(i)}$ and $T_{S \text{ hs}, n(i)}$.

$$\Delta T_{fn} = C_2 \left(\frac{Q}{A} \right) \frac{(q_a)_{hc}}{(q_a)_c} U_5 U_{11} U_{12} U_{14} \sum_{(i)} [t(i)]^{0.778} e^{-\frac{C_1}{T_{S \text{ hs}, n(i)} + 460}}$$

$$\Delta T_{fa} = C_2 \left(\frac{Q}{A} \right) \frac{(q_a)_{hc}}{(q_a)_c} U_5 U_{11} U_{12} U_{14} \sum_{(i)} [t(i)]^{0.778} e^{-\frac{2C_1}{T_{S \text{ hs}, n(i)} + T_{S \text{ hs}, w(i)} + 920}}$$

$$\Delta T_{fw} = C_2 \left(\frac{Q}{A} \right) \frac{(q_a)_{hc}}{(q_a)_c} U_5 U_{11} U_{12} U_{14} \sum_{(i)} \frac{C_1}{[t(i)]^{0.778} e^{T_{s\ hs,w(i)} + 460}}$$

NOTE: The value of (Q/A) in the above equations is that employed in step 1 and not a time step value.

4. Calculate hot plate metal temperatures for plates bounded by narrow, average, and wide coolant channels ($T_{\text{plate n}}$, $T_{\text{plate a}}$, and $T_{\text{plate w}}$) as follows:

$$T_{\text{plate n}} = T_{s\ hs,n} + \Delta T_{fn}$$

$$T_{\text{plate a}} = \left(\frac{T_{s\ hs,n} + T_{s\ hs,w}}{2} \right) + \Delta T_{fa}$$

$$T_{\text{plate w}} = T_{s\ hs,w} + \Delta T_{fw}$$

5. Calculate side plate temperature, $t_{\text{side plate}}$, as follows:

$$T_{\text{side plate}} = -\left(\frac{Q}{A} \right) \frac{A b^2}{38.78 \times 10^6} + \frac{c_1 b}{2} + c_2,$$

where

$$c_1 = \frac{1}{b + \frac{8.08}{v_b} + \frac{16.16}{h_{hs,w}}} \left[T_b - (\Delta T_{B,w}) Nf - T_i + \frac{b A (Q/A)}{0.8 \times 10^6} \left(\frac{1}{U_b} + \frac{b}{16.16} \right) \right]$$

$$c_2 = T_i + (\Delta T_{B,w}) Nf + \frac{16.16 c_1}{h_{hs,w}}$$

and

$$U_b = \left(\frac{\Delta P_{\text{core}}}{73.5} \right)^{0.27} \beta + 2$$

$$T_b = \left(\frac{73.5}{\Delta P_{\text{core}}} \right)^{0.53} \frac{(Q/A)}{0.8 \times 10^6} \gamma f + T_i .$$

6. Calculate fuel plate buckling due to fuel plate-side plate temperature differences for plates bounded by narrow, average, and wide channels (δ_{Tn} , δ_{Ta} , and δ_{Tw}) from the following correlations:

$$\delta_{Tn} = 0.0063 \left[T_{\text{plate n}} - T_{\text{side plate}} \right]^{1.31} \theta$$

$$\delta_{Ta} = 0.0063 \left[T_{\text{plate a}} - T_{\text{side plate}} \right]^{1.31} \theta$$

$$\delta_{Tw} = 0.0063 \left[T_{\text{plate w}} - T_{\text{side plate}} \right]^{1.31} \theta$$

7. Calculate fuel plate pressure induced deflection due to adjacent narrow and wide channels, δ_p , as follows:

$$\delta_p = \frac{(\Omega)(dp)}{E.R.}$$

where

$$E.R. = -(1.642 \times 10^{-6})(T_{\text{plate a}})^2 + (4.719 \times 10^{-4})(T_{\text{plate a}}) + 0.9737, \text{ and}$$

dp = pressure differential from step 2.

8. Calculate fuel plate deflections due to differences in fuel plate temperatures for plates bounded by narrow or by wide channels as compared to plates bounded by average channels ($\delta_{T,n-a}$ and $\delta_{T,w-a}$) as follows:

$$\delta_{T,n-a} = \frac{(z)(T_{\text{plate n}} - T_{\text{plate a}})}{E.R.}$$

$$\delta_{T,w-a} = \frac{(z)(T_{\text{plate a}} - T_{\text{plate w}})}{E.R.},$$

where E.R. is the same as in step 7.

9. Calculate the effective volumetric expansion due to heating from room temperature of plates bounded by narrow, average, and wide channels (δ_{Vn} , δ_{Va} , and δ_{Vw}) as follows:

$$\delta_{Vn} = \frac{(\xi)(T_{\text{plate } n} - 70)(w)}{2}$$

$$\delta_{Va} = \frac{(\xi)(T_{\text{plate } a} - 70)(w)}{2}$$

$$\delta_{Vw} = \frac{(\xi)(T_{\text{plate } w} - 70)(w)}{2}$$

10. Calculate the effective hot streak fuel plate deflections in the hot and cold channels ($\delta_{\text{streak},H}$ and $\delta_{\text{streak},C}$) for the preselected arrangement of adjacent channels as follows:

$$\delta_{\text{streak},H} = (1 + \alpha_1 + \alpha_2) \delta_p + (1 + \alpha_1 + \alpha_2 - \alpha_4) \delta_{Va} + (\alpha_3 + 2\alpha_4) \delta_{Vn} + \alpha_3 \delta_{T,n-a} + \Delta\epsilon_{\text{local}} - \Delta\epsilon_{\text{av}}$$

$$\delta_{\text{streak},C} = (2\alpha_1 + \alpha_2 - \alpha_3) \delta_p + (-2\alpha_1 - \alpha_2 - \alpha_3) \delta_{Va} + (-\alpha_3 - 2\alpha_4) \delta_{Vn} + (-\alpha_2) \delta_{Vw} + (-\alpha_2) \delta_{T,w-a} + (\alpha_3) \delta_{T,n-a} - \Delta\epsilon_{\text{local}} + (-\alpha_1 - \alpha_2 + \alpha_3 + \alpha_4) \Delta\epsilon_{\text{avg}}$$

NOTE: See Fig. 6 for assumed directions of plate deflections, etc.

11. Calculate the effective hot spot plate deflections in both the hot and cold channels ($\delta_{hs,H}$ and $\delta_{hs,C}$) as follows:

$$\delta_{hs,H} = (2\alpha_1 + 2\alpha_2 + \alpha_3) \delta_{Ta} + (\alpha_3 + 2\alpha_4) \delta_{Tn}$$

$$\delta_{hs,C} = (\alpha_2 - \alpha_3) \delta_{Ta} - \alpha_2 \delta_{Tw} + \alpha_3 \delta_{Tn}$$

12. Calculate values of average coolant channel width for the hot and cold channels (ϵ_H and ϵ_C) of Fig. 6 as follows:

$$\epsilon_H = \epsilon - \Delta\epsilon_{av}$$

$$\epsilon_C = \epsilon + (\alpha_1 + \alpha_2 - \alpha_3 - \alpha_4) \Delta\epsilon_{av}$$

13. Calculate values of the hot spot flow factor for the hot and cold channels ($U_{1,H}$ and $U_{1,C}$) of Fig. 6 as follows:

$$U_{1,H} = U_1 \left(\frac{\epsilon_H - \delta_{streak,H}}{\epsilon_H} \right)^{0.667}$$

$$U_{1,C} = U_1 \left(\frac{\epsilon_C + \delta_{streak,C}}{\epsilon_C} \right)^{0.667}$$

14. Calculate values of the hot spot flow factor for the hot and cold channels ($U_{2,H}$ and $U_{2,C}$) of Fig. 6 as follows:

$$U_{2,H} = U_2 \left(\frac{\epsilon_H - \delta_{streak,H} - \delta_{hs,H}}{\epsilon_H - \delta_{streak,H}} \right)^{0.667}$$

$$U_{2,C} = U_2 \left(\frac{\epsilon_C + \delta_{streak,C} + \delta_{hs,C}}{\epsilon_C + \delta_{streak,C}} \right)^{0.667}$$

NOTE: Up to this point the procedures for burnout and incipient boiling calculations are identical. The remainder of this section applies only to burnout calculations. Incipient boiling calculations are outlined in Section III of this appendix.

15. Run HOT SPOT for the hot and cold channels using the values specified by the input data except set U_{14} and U_{15} at 1.0 and replace the values of ϵ , U_1 , and U_2 with the respective values calculated in steps 12, 13, and 14. These calculations yield values of the ratio of burnout to maximum heat flux values for the hot and cold channels (i.e., $K_{bo,H}$ and $K_{bo,C}$). In calculating the hot spot heat transfer coefficients,

h_{hs} , use as the value of channel thickness e for the hot channel $\epsilon_H - \delta_{streak,H} - \delta_{hs,H}$, and for the cold channel use $\epsilon_C + \delta_{streak,C} + \delta_{hc,C}$.

16. Calculate the overall ratio of burnout to maximum heat flux for the fuel plate, K , as follows:

$$K = \frac{K_{bo,H} + K_{bo,C}}{2}$$

17. Choose a new value for (Q/A) as follows:

$$\left(\frac{Q}{A}\right)_{new} = \left(\frac{Q}{A}\right) [1 + (K - 1)(Conv.)]$$

18. Reiterate, beginning with step 1 using the new value of (Q/A) and continue iterations until

$$1 - Conv. Power \leq K \leq 1 + Conv. Power$$

where K is the value determined in step 16.

19. Print out results of final iteration as outlined in Section IV of this appendix.

End of HOT SLOT Burnout Program

III. HOT SLOT INCIPIENT BOILING CALCULATION PROCEDURE

- 1-14. Identical to HOT SLOT burnout calculation procedure of Section II.
15. Run HOT SPOT for the hot channel using the values specified by the input data except set U_{15} and U_{25} at 1.0, B.O. indicator = 2.0, and values of ϵ , U_1 , and U_2 at the values calculated for this channel in steps 12, 13, and 14.

NOTE: In calculating the hot spot heat transfer coefficient, employ the same values of ϵ as outlined in step 15 of HOT SLOT.

16. Calculate the hot spot pressure at these conditions, $P_{hs\ ib}$, from Eq. (14) of HOT SPOT.

NOTE: The subscript bo of HOT SPOT has been replaced by ib to indicate that these are incipient boiling calculations.

17. Calculate the coolant saturation temperature at the hot spot, T_{sat} , via Eq. (15) of HOT SPOT.
18. Calculate the hot spot plate surface temperature, $T_{S\ hs}$, from the incipient boiling correlation as follows:

$$T_{S\ hs,ib} = T_{sat} + e \frac{P_{hs\ ib}^{0.0234}}{2.3} \ln \left(\frac{(Q/A)_{max,hs}}{15.6 (P_{hs\ ib})^{1.156}} \right)$$

19. Calculate new value of hot spot heat transfer coefficient, $h_{hs,ib}$, via Eq. (10) or (10a) of HOT SPOT using the value of hot spot surface temperature calculated in step 18.
20. Calculate a new value of $(Q/A)_{max,hs}$ from Eq. (12) of HOT SPOT using the value of $h_{hs,ib}$ from step 19.
21. Reiterate from step 18 using the new value of $(Q/A)_{max,hs}$ until

$$\left| \frac{T_{S\ hs,ib(n-1)}}{T_{S\ hs,ib(n)}} - 1 \right| \leq 10^{-6}.$$

22. Calculate the incipient boiling bulk water temperature, $T_{B\ hs\ ib}$, as follows:

$$T_{B\ hs\ ib} = T_{s\ hs\ ib} - \frac{(Q/A)_{max,hs}}{h_{hs,ib}},$$

where $(Q/A)_{max,hs}$ and h_{hs} are the final values from steps 20 and 19 respectively.

23. Calculate the incipient boiling value of bulk temperature rise, $\Delta T_{B\ hs\ ib}$, as follows:

$$\Delta T_{B\ hs\ ib} = T_{B\ hs\ ib} - (U_6) T_i$$

24. Calculate the nominal incipient boiling bulk temperature rise, $\Delta T_{B \text{ nom ib}}$, as follows:

$$\Delta T_{B \text{ nom ib}} = \Delta T_{B \text{ hs ib}} \left/ \left[\frac{U_{13}}{U_1} f \left(\frac{q_m}{q_a} \right)_{r, hc} (1 - U_4) + U_4 f \right] \right.$$

25. Calculate the core average heat flux, (Q/A) , from the following equation:

$$\left(\frac{Q}{A} \right)_{ib} = \frac{\Delta T_{B \text{ nom ib}}^{v_i \rho_i \epsilon}}{1.44 \times 10^5 \frac{(q_a)_{hc}}{(q_a)_c} L (0.3858 \times 10^{-5}) U_5 U_{11} U_{12} U_{14}}$$

26. Choose a new value of $(Q/A)_{\text{new}}$ according to the following equation:

$$\left(\frac{Q}{A} \right)_{\text{new}} = \left(\frac{Q}{A} \right) \left[1 + (K - 1)(\text{Conv.}) \right],$$

where

$$K = (Q/A)_{ib} / (Q/A).$$

27. Reiterate to step 16 until

$$\left| \frac{(Q/A)_{ib(n)}}{(Q/A)_{ib(n-1)}} - 1 \right| \leq 10^{-5}$$

28. Take the final value of $(Q/A)_{ib}$ from step 27 and go back to step 1 using this value as the input value of (Q/A) . Continue until

$$|K - 1| \leq \text{Conv. power}$$

where

$$K = (Q/A)_{(n)} / (Q/A)_{(n-1)}$$

29. Print out results of final overall iteration for the hot channel.
30. Start over at step 1 with the original input data. At step 15 use the calculated cold channel values of ϵ , U_1 , and U_2 .

31. Continue through step 28 and print out results of final overall iteration for the cold channel.

End of HOT SLOT Incipient Boiling Calculation

IV. INPUT DATA

Sample input data forms for HOT SLOT are shown in Figs. A-2 and A-3. The form of Fig. A-2 provides for specification of all of the input variables listed in Table II. It will be noted that the arrangement of variables on the input form does not follow a consistent pattern such as that of Table II, this again being due to the manner in which the calculation procedure grew during the course of the studies. The form shown as Fig. A-3 provides a means for supplying data to permit running a series of different calculations by changing only selected input values from the previous calculation, without the necessity for relisting all of the unchanged input numbers. The procedures for accomplishing this are indicated in Figs. A-4 and A-5 where input forms are filled in for a series of three sample problems.

The first of the sample problems, listed in Fig. A-4, uses the typical input data values of Table II and comprises the basic case for the series of calculations; in each subsequent case the input data values listed are only those in which there has been a change over the previous case. A new title card is required at the beginning of each problem. Changes in input numbers A(1) through A(61) are accomplished by listing the input number in columns 1 and 2 and the desired value of this input number in columns 3 through 12. A change in the reactor operating history (i.e., time steps) is indicated by a card containing -1 in columns 1 and 2 (e.g., Card 15). This card is followed by a card for each of the time steps which is to be changed (e.g., Card 16). This card contains the number of the time step to be changed and the desired time step data in the columns indicated in Fig. A-5. It should be noted that all input data numbers are of the floating point form except for Card 11 which contains the number of time steps and the time step numbers in cards changing the time step data such as Card 16. Each case, except for the first, must be followed by a card containing zeros in columns 1 and 2 (e.g., Cards 17 and 20). The series of

calculations is ended by inserting a blank card followed by a card containing -2 in columns 1 and 2 (e.g., Cards 21 and 22). The final case of this series illustrates the method employed for calculating reactor operating conditions at a fixed power level (i.e., at a given value of core average heat flux) rather than the usual procedure which calls for a search for incipient boiling or burnout power level.

V. OUTPUT DATA

The output data from the last iteration on a single HOT SLOT burnout calculation is printed out on a series of three sheets. Incipient boiling calculations require a six-page output, three sheets for the hot channel and three for the cold channel. Output data from the sample problems of Figs. A-4 and A-5 are given in Fig. A-6 for incipient boiling calculations and in Fig. A-7 for burnout calculations on the same cases. Figure A-8 consists of a duplicate of the output from the burnout calculations of the first sample case which has been marked up to indicate the calculation step from which the output number is obtained and the symbol employed for this number in the equations of Sections I, II, and III. Figure A-9 is similar to Fig. A-8 except that this set of output data is for the first sample incipient boiling calculation.

NOMENCLATURE

A	Side plate heat generation rate at 100 Mw, Btu hr ⁻¹ in. ⁻³
A _{ht} to E _{ht}	Heat transfer coefficient correlation constants
a	Distance from core inlet to hot spot, ft
b	Side plate thickness, in.
C	Constant in oxide buildup equation
c	Constant in side plate temperature equation
Conv.	Constant governing speed of convergence
Conv. Power	Constant governing degree of convergence
E.R.	Elasticity reduction factor with temperature
f	Fraction of total heat liberated upstream of preselected hot spot location
2H	Total length of coolant channel, ft
h	Heat transfer coefficient, Btu hr ⁻¹ ft ⁻² (°F) ⁻¹
K	Ratio of incipient boiling or burnout heat flux to hot spot heat flux
L	Coolant channel length, in.
N	Side plate cold streaking factor
P	Core inlet pressure, psia
P	Pressure differential across fuel plate, psi
(Q/A)	Heat flux, Btu hr ⁻¹ ft ⁻²
q	Power density, Btu hr ⁻¹ in. ⁻³
T	Temperature, °F
t	Duration of operating period, hours
U	Heat transfer coefficient, Btu hr ⁻¹ ft ⁻² (°F) ⁻¹
U _n	Uncertainty factor (Table II)
v	Velocity, ft/sec
W	Coolant channel width, in.
w	Thickness of fuel plate, mils
z	Fuel plate thermal deflection constant, mils °F
α	Specifies choice of adjacent channel arrangement (See Table II and Fig. 6)
β	Constant in side plate heat transfer coefficient equation
γ	Constant in side plate bulk H ₂ O temperature equation
δ	Fuel plate deflection, mils

NOMENCLATURE (continued)

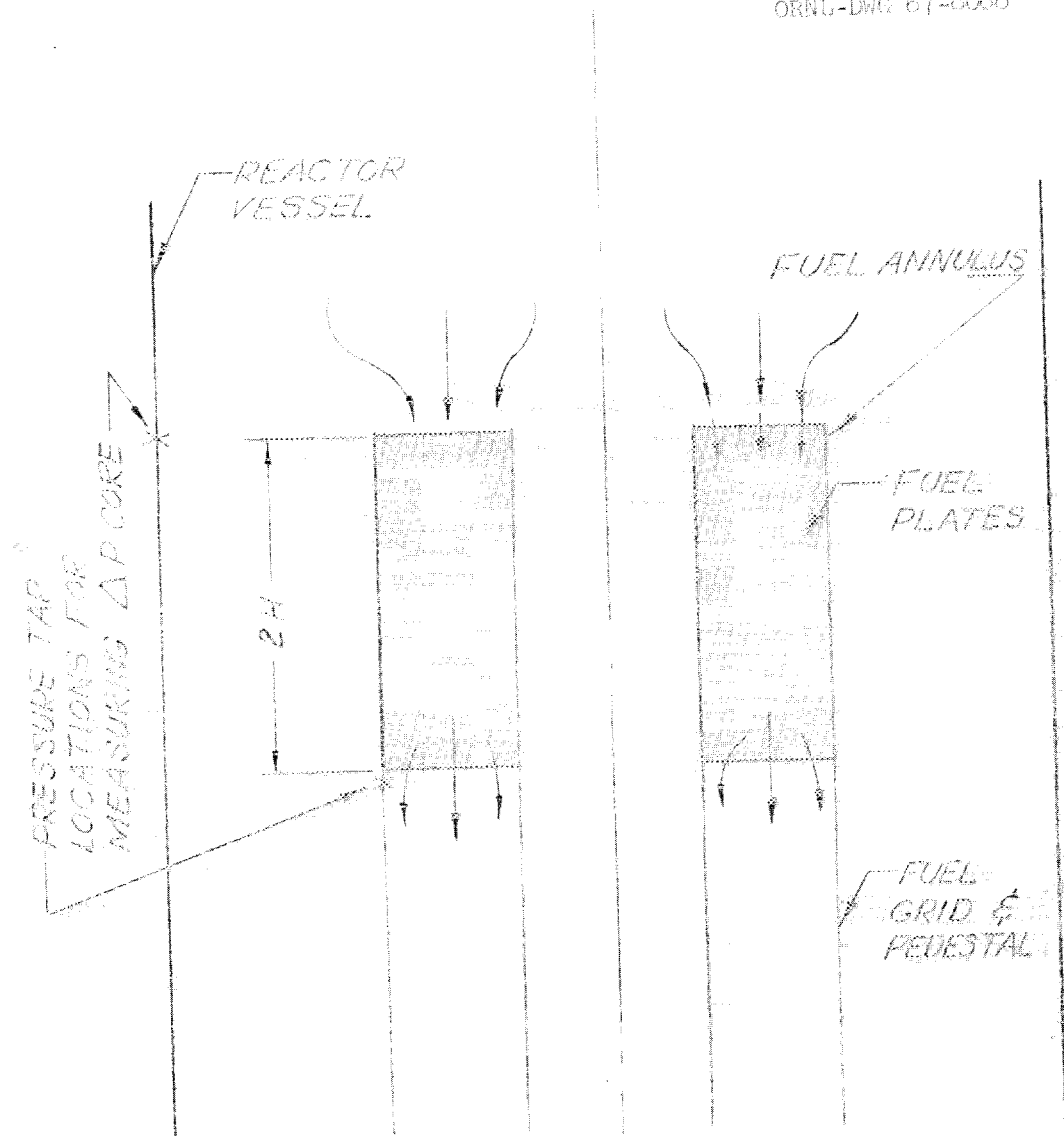
ϵ	Coolant channel thickness, mils
ζ	Fuel plate volumetric expansion coefficient, $\text{in.}^3/\text{in.}^3$, $^{\circ}\text{F}$
θ	Side plate slot factor (see Table II)
μ	Viscosity, $\text{lb ft}^{-1} \text{hr}^{-1}$
ρ	Density, lb/ft^3
Ω	Fuel plate pressure deflection constant, mils/psi
ΔP_{core}	Pressure drop across core, psi
ΔT	Temperature rise or temperature differential, $^{\circ}\text{F}$

SUBSCRIPTS

a	Average or average channel
B	Bulk coolant in coolant channel
b	Bulk coolant outside fuel annulus
bo	At burnout (or assumed burnout) conditions
C	Cold channel (see Fig. 6)
c	Core
exit	At core exit
f	Oxide film
film	Water film
H	Hot channel (see Fig. 6)
hc	Hot channel conditions
hs	At the preselected hot spot location
ht	Heat transfer coefficient correlation constant
i	At core inlet
(i)	Time step number
ib	At incipient boiling conditions
m	Maximum
mp	At core midplane
n	Narrow channel
(n)	n th iteration
(n-1)	(n-1) th iteration

SUBSCRIPTS (continued)

nom	Nominal value
P	Due to pressure differential
plate	Fuel plate metal
r	Radially
s	At the plate surface
side plate	Fuel element side plate
streak	Pertaining to hot streak calculations
T	At temperature T or due to temperature
Tsat	At saturation temperature
V	Volumetric
v	Vapor
w	Wide channel



$$\Delta P \text{ CONTRACTION} = \frac{V_2^2}{2g} \left(0.4 \left(1.25 \frac{S_2}{S_1} \right)^2 \right)$$

$$\Delta P \text{ EXPANSION} = \frac{V_1^2}{2g} \left(1 - \frac{S_1}{S_2} \right)^2$$

WHERE V_1 = INITIAL VELOCITY
 V_2 = FINAL VELOCITY
 S_1 = INITIAL FLOW AREA
 S_2 = FINAL FLOW AREA

Fig. A-1. Model Employed for Flow Calculations.

TYPICAL CASE - INPUT VALUES FROM TABLE II

24 ITERATIONS

INPUT DATA

1.833000E 00	5.150000E 01	4.950000E 01	2.000000E 01	2.000000E 00	7.350000E 01	1.200000E 02	1.450000E 00
1.150000E 00	9.000000E 02	8.000000E 05	1.000000E 00	1.000000E 00	1.150000E 00	0.	1.050000E 00
1.010000E 00	9.000000E-01	1.000000E 00	7.702000E-01	1.000000E 00	1.100000E 00	1.000000E 00	1.100000E 00
1.010000E 00	1.000000E 00	4.782050E 02	9.123300E-01	7.954000E-04	6.670000E-01	1.640000E-01	4.000000E 01
4.000000E 02	1.000000E 00	-2.000000E 00	3.100000E 01	1.000000E 00	6.000000E 00	1.000000E 01	0.
0.	1.000000E 00	0.	7.600000E 03	1.875000E-01	0.	1.000000E 02	5.298100E-01
2.823000E-02	3.900000E-05	3.500000E-01	1.000000E 00	8.280000E 03	3.124000E-02	5.000000E-01	1.000000E-05
1.100000E 00	1.300000E 00	1.300000E 00	1.118000E 00	8.460000E-01	0.	0.	

DATA FOR OXIDE FILM BUILD-UP CALCULATION

TIME INCREMENT	TIME (I)	Q/A (I)	U12 (I)	DPC (I)
1	3.600000E 02	8.000000E 05	1.000000E 00	7.350000E 01

FIGURE A-6
(PAGE 1 OF 18)

Fig. A-6. Output Data from Sample Problems, Burnout Calculations.

TYPICAL CASE - INPUT VALUES FROM TABLE II
 THE FOLLOWING OUTPUT IS FOR THE COLD CHANNEL CALCULATION
 HOT PLATE - NARROW CHANNEL

DEL T BN	V I	DEL T BHS	V BHS	H HS	DEL T FHS	TS HS	QMAX
2.085967E 02	3.905200E 01	2.085967E 02	4.277864E 01	1.731638E 04	1.524024E 02	4.821990E 02	2.639057E 06

HOT PLATE - WIDE CHANNEL

DEL T BN	V I	DEL T BHS	V BHS	H HS	DEL T FHS	TS HS	QMAX
1.413951E 02	4.492713E 01	1.413951E 02	4.739541E 01	1.665394E 04	1.584644E 02	4.210595E 02	2.639057E 06

FACTORS CAUSING DEFLECTIONS

PRESS. DIFF.	DELTA TF N	DELTA TF A	DELTA TF W	T SIDE PLATE
3.229024E 00	1.793707E 02	1.423097E 02	1.117220E 02	1.917641E 02

PLATE DEFLECTIONS

PRESS. DEFL.	FP BUCKL N	FP BUCKL A	FP BUCKL W	HC DEFL H	HC DEFL C
2.511804E 00	1.993211E 01	1.626013E 01	1.310019E 01	1.043522E 01	-4.828684E 00

TEMP DIFF N	TEMP DIFF W	VOL EXP N	VOL EXP A	VOL EXP W	HS DEFL H	HS DEFL C
2.803170E 00	2.534866E 00	5.940839E-01	5.261657E-01	4.647483E-01	3.619224E 01	3.671980E 00

EPS HOT	U1 HOT	U2 HOT	EPS COLD	U1 COLD	U2 COLD
4.250000E 01	8.727756E-01	1.000000E 00	4.250000E 01	9.227036E-01	1.064004E 00

00
 10

FIGURE A-6
 (PAGE 2 OF 18)

TYPICAL CASE - INPUT VALUES FROM TABLE II

HOT CHANNEL

DEL T BN	V I	DEL T BHS	V BHS	H HS	DEL T FHS	TS HS	QMAX
2.065869E 02	3.904150E 01	2.462823E 02	4.305039E 01	1.773827E 04	1.512146E 02	5.186969E 02	2.682286E 06

BERGLES-R. BURNOUT CORRELATION K # 1.00003E 00

DEL T BN	V I	DEL T BHS	V BHS	P HS	T S	T SAT	Q
2.065887E 02	3.904150E 01	2.462845E 02	4.305043E 01	7.351948E 02	5.945447E 02	5.092566E 02	2.682303E 06

COLD CHANNEL

DEL T BN	V I	DEL T BHS	V BHS	H HS	DEL T FHS	TS HS	QMAX
2.065869E 02	3.904150E 01	2.462823E 02	4.305039E 01	1.773827E 04	1.512146E 02	5.186969E 02	2.682286E 06

BERGLES-R. BURNOUT CORRELATION K # 1.00003E 00

DEL T BN	V I	DEL T BHS	V BHS	P HS	T S	T SAT	Q
2.065887E 02	3.904150E 01	2.462845E 02	4.305043E 01	7.351948E 02	5.945447E 02	5.092566E 02	2.682303E 06

AT CONVERGENCE, Q/A # 1.432543E 06 AND K(0) # 1.000009E 00

00

FIGURE A-6
(PAGE 3 OF 18)

TYPICAL CASE - INPUT VALUES FROM TABLE II

7 ITERATIONS

INPUT DATA

1.833000E 00	5.150000E 01	4.850000E 01	2.000000E 01	2.000000E 00	7.350000E 01	1.200000E 02	1.450000E 00
1.150000E 00	9.000000E 02	8.000000E 05	1.000000E 00	1.000000E 00	1.150000E 00	0.	1.050000E 00
1.010000E 00	9.000000E-01	1.000000E 00	7.702000E-01	1.000000E 00	1.100000E 00	1.000000E 00	1.100000E 00
1.010000E 00	1.000000E 00	4.782050E 02	9.123300E-01	7.854000E-04	6.670000E-01	1.640000E-01	4.000000E 01
4.000000E 02	1.000000E 00	-2.000000E 00	3.100000E 01	1.000000E 00	6.000000E 00	1.000000E 01	0.
0.	1.000000E 00	0.	7.600000E 03	1.875000E-01	0.	1.000000E 02	5.298100E-01
2.823000E-02	3.900000E-05	3.500000E-01	1.000000E 00	8.280000E 03	3.124000E-02	5.000000E-01	1.000000E-05
1.100000E 00	1.300000E 00	1.300000E 00	1.118000E 00	8.460000E-01	-0.	-0.	

DATA FOR OXIDE FILM BUILD-UP CALCULATION

TIME INCREMENT	TIME (I)	Q/A (I)	U12 (I)	DPC (I)
1	3.600000E 02	8.000000E 05	1.000000E 00	7.350000E 01

FIGURE A-6
(PAGE 4 OF 18)

TYPICAL CASE - INPUT VALUES FROM TABLE II
 THE FOLLOWING OUTPUT IS FOR THE HOT CHANNEL CALCULATION
 HOT PLATE - NARROW CHANNEL

DEL T BN	V I	DEL T BHS	V BHS	H HS	DEL T FHS	TS HS	QMAX
1.519145E 02	3.870300E 01	1.519145E 02	4.104787E 01	1.608338E 04	1.184308E 02	3.915453E 02	1.904768E 06

HOT PLATE - WIDE CHANNEL

DEL T BN	V I	DEL T BHS	V BHS	H HS	DEL T FHS	TS HS	QMAX
1.028856E 02	4.456373E 01	1.028856E 02	4.617945E 01	1.547390E 04	1.230955E 02	3.471811E 02	1.904768E 06

FACTORS CAUSING DEFLECTIONS

PRESS. DIFF.	DELTA TF N	DELTA TF A	DELTA TF W	T SIDE PLATE
3.336116E 00	1.294627E 02	1.027136E 02	8.063653E 01	1.720990E 02

PLATE DEFLECTIONS

PRESS. DEFL.	FP BUCKL N	FP BUCKL A	FP BUCKL W	HC DEFL H	HC DEFL C
2.117906E 00	1.349875E 01	1.107458E 01	8.984816E 00	8.629787E 00	-5.319447E 00

TEMP DIFF N	TEMP DIFF W	VOL EXP N	VOL EXP A	VOL EXP W	HS DEFL H	HS DEFL C
1.655170E 00	1.497129E 00	4.529248E-01	4.037856E-01	3.593384E-01	2.457332E 01	2.424169E 00

EPS HOT	U1 HOT	U2 HOT	EPS COLD	U1 COLD	U2 COLD
4.250000E 01	8.595144E-01	4.221752E-01	4.250000E 01	9.227036E-01	1.064004E 00

FIGURE A-6
 (PAGE 5 OF 18)

TYPICAL CASE - INPUT VALUES FROM TABLE II

HGT CHANNEL

DEL T BN	V I	DEL T BHS	V BHS	H HS	DEL T FHS	TS HS	QMAX
1.504514E 02	3.869244E 01	1.925466E 02	1.523032E 01	1.139503E 04	2.043022E 02	5.180488E 02	2.328031E 06

BERGLES-R. BURNOUT CORRELATION K # 1.000009E 00

DEL T BN	V I	DEL T BHS	V BHS	P HS	T S	T SAT	Q
1.504528E 02	3.869244E 01	1.925484E 02	1.523032E 01	7.352333E 02	6.070690E 02	5.092624E 02	2.328031E 06

COLD CHANNEL

DEL T BN	V I	DEL T BHS	V BHS	H HS	DEL T FHS	TS HS	QMAX
1.504514E 02	3.869244E 01	1.925466E 02	1.523032E 01	1.139503E 04	2.043022E 02	5.180488E 02	2.328031E 06

BERGLES-R. BURNOUT CORRELATION K # 1.000009E 00

DEL T BN	V I	DEL T BHS	V BHS	P HS	T S	T SAT	Q
1.504528E 02	3.869244E 01	1.925484E 02	1.523032E 01	7.352333E 02	6.070690E 02	5.092624E 02	2.328031E 06

AT CONVERGENCE, Q/A # 1.033952E 06 AND K(D) # 1.000005E 00

FIGURE A-6
(PAGE 6 OF 18)

TYPICAL CASE - START OF FUEL CYCLE - 600 PSI PRESSURE

17 ITERATIONS

INPUT DATA

1.833000E 00	5.150000E 01	4.850000E 01	2.000000E 01	2.000000E 00	7.350000E 01	1.200000E 02	1.450000E 00
1.150000E 00	6.000000E 02	8.000000E 05	1.000000E 00	1.000000E 00	1.150000E 00	0.	1.050000E 00
1.010000E 00	9.000000E-01	1.000000E 00	7.702000E-01	1.000000E 00	1.100000E 00	1.000000E 00	1.100000E 00
1.010000E 00	1.000000E 00	4.782050E 02	9.123300E-01	7.854000E-04	6.670000E-01	1.640000E-01	4.000000E 01
4.000000E 02	1.000000E 00	-2.000000E 00	3.100000E 01	1.000000E 00	6.000000E 00	1.000000E 01	0.
0.	1.000000E 00	0.	7.600000E 03	1.875000E-01	0.	1.000000E 02	5.298100E-01
2.823000E-02	3.900000E-05	3.500000E-01	1.000000E 00	8.280000E 03	3.124000E-02	5.000000E-01	1.000000E-05
1.100000E 00	1.300000E 00	1.300000E 00	1.118000E 00	8.460000E-01	-0.	-0.	

DATA FOR OXIDE FILM BUILD-UP CALCULATION

TIME INCREMENT	TIME (I)	Q/A (I)	U12 (I)	OPC (I)
1	0.	8.000000E 05	1.000000E 00	7.350000E 01

TYPICAL CASE - START OF FUEL CYCLE - 600 PSI PRESSURE
 THE FOLLOWING OUTPUT IS FOR THE COLD CHANNEL CALCULATION
 HOT PLATE - NARROW CHANNEL

DEL T BN	V I	DEL T BHS	V BHS	H HS	DEL T FHS	TS HS	QMAX
1.790722E 02	3.888434E 01	1.790722E 02	4.185187E 01	1.671373E 04	1.349670E 02	4.352393E 02	2.255802E 06

HOT PLATE - WIDE CHANNEL

DEL T BN	V I	DEL T BHS	V BHS	H HS	DEL T FHS	TS HS	QMAX
1.213480E 02	4.474686E 01	1.213480E 02	4.675303E 01	1.607362E 04	1.403419E 02	3.823899E 02	2.255602E 06

FACTORS CAUSING DEFLECTIONS

PRESS. DIFF.	DELTA TF N	DELTA TF A	DELTA TF W	T SIDE PLATE
3.288986E 00	0.	0.	0.	1.815188E 02

PLATE DEFLECTIONS

PRESS. DEFL.	FP BUCKL N	FP BUCKL A	FP BUCKL W	HC DEFL H	HC DEFL C
1.946997E 00	8.892957E 00	7.710822E 00	6.570173E 00	7.479904E 00	-5.828683E 00

TEMP DIFF N	TEMP DIFF W	VOL EXP N	VOL EXP A	VOL EXP W	HS DEFL H	HS DEFL C
8.256104E-01	8.256104E-01	3.667915E-01	3.405056E-01	3.142197E-01	1.660378E 01	1.182135E 00

EPS HOT	U1 HOT	U2 HOT	EPS COLD	U1 COLD	U2 COLD
4.250000E 01	8.595144E-01	4.221752E-01	4.250000E 01	9.062966E-01	1.021388E 00

FIGURE A-6
 (PAGE 8 OF 18)

TYPICAL CASE - START OF FUEL CYCLE - 600 PSI PRESSURE

HOT CHANNEL

DEL T BN	V I	DEL T BHS	V BHS	H HS	DEL T FHS	TS HS	QMAX
1.773482E 02	3.887360E 01	2.152530E 02	3.958455E 01	1.691242E 04	1.349000E 02	4.713530E 02	2.281485E 06

BERGLES-R. BURNOUT CORRELATION K # 1.000002E 00

DEL T BN	V I	DEL T BHS	V BHS	P HS	T S	T SAT	Q
1.773495E 02	3.887360E 01	2.152546E 02	3.958458E 01	4.652067E 02	5.502417E 02	4.602687E 02	2.281497E 06

COLD CHANNEL

DEL T BN	V I	DEL T BHS	V BHS	H HS	DEL T FHS	TS HS	QMAX
1.773482E 02	3.887360E 01	2.152530E 02	3.958455E 01	1.691242E 04	1.349000E 02	4.713530E 02	2.281485E 06

BERGLES-R. BURNOUT CORRELATION K # 1.000002E 00

DEL T BN	V I	DEL T BHS	V BHS	P HS	T S	T SAT	Q
1.773495E 02	3.887360E 01	2.152546E 02	3.958458E 01	4.652067E 02	5.502417E 02	4.602687E 02	2.281497E 06

AT CONVERGENCE, Q/A # 1.224503E 06 AND K(D) # 1.000006E 00

89

TYPICAL CASE - START OF FUEL CYCLE - 600 PSI PRESSURE

15 ITERATIONS

INPUT DATA

1.833000E 00	5.150000E 01	4.850000E 01	2.000000E 01	2.000000E 00	7.350000E 01	1.200000E 02	1.450000E 00
1.150000E 00	6.000000E 02	8.000000E 05	1.000000E 00	1.000000E 00	1.150000E 00	0.	1.050000E 00
1.010000E 00	9.000000E-01	1.000000E 00	7.702000E-01	1.000000E 00	1.100000E 00	1.000000E 00	1.100000E 00
1.010000E 00	1.000000E 00	4.782050E 02	9.123300E-01	7.854000E-04	6.670000E-01	1.640000E-01	4.000000E 01
4.000000E 02	1.000000E 00	-2.000000E 00	3.100000E 01	1.000000E 00	6.000000E 00	1.000000E 01	0.
0.	1.000000E 00	0.	7.600000E 03	1.875000E-01	0.	1.000000E 02	5.298100E-01
2.823000E-02	3.900000E-05	3.500000E-01	1.000000E 00	8.280000E 03	3.124000E-02	5.000000E-01	1.000000E-05
1.100000E 00	1.300000E 00	1.300000E 00	1.118000E 00	8.460000E-01	-0.	-0.	

DATA FOR OXIDE FILM BUILD-UP CALCULATION

TIME INCREMENT	TIME (I)	Q/A (I)	U12 (I)	DPC (I)
1	0.	8.000000E 05	1.000000E 00	7.350000E 01

FIGURE A-6
(PAGE 10 OF 18)

TYPICAL CASE - START OF FUEL CYCLE - 600 PSI PRESSURE
 THE FOLLOWING OUTPUT IS FOR THE HOT CHANNEL CALCULATION

HOT PLATE - NARROW CHANNEL

DEL T BN	V I	DEL T BHS	V BHS	H HS	DEL T FHS	TS HS	QMAX
1.474259E 02	3.868500E 01	1.494259E 02	4.097625E 01	1.602113E 04	1.168890E 02	3.875149E 02	1.872693E 06

HOT PLATE - WIDE CHANNEL

DEL T BN	V I	DEL T BHS	V BHS	H HS	DEL T FHS	TS HS	QMAX
1.011932E 02	4.454610E 01	1.011932E 02	4.612767E 01	1.541542E 04	1.214819E 02	3.438751E 02	1.872694E 06

FACTORS CAUSING DEFLECTIONS

PRESS. DIFF.	DELTA TF N	DELTA TF A	DELTA TF W	T SIDE PLATE
3.340127E 00	0.	0.	0.	1.712363E 02

PLATE DEFLECTIONS

PRESS. DEFL.	FP BUCKL N	FP BUCKL A	FP BUCKL W	HC DEFL H	HC DEFL C
1.904696E 00	7.214531E 00	6.276307E 00	5.370213E 00	7.183501E 00	-5.857522E 00

TEMP DIFF N	TEMP DIFF W	VOL EXP N	VOL EXP A	VOL EXP W	HS DEFL H	HS DEFL C
6.629894E-01	6.629893E-01	3.188643E-01	2.969517E-01	2.750390E-01	1.349084E 01	9.382240E-01

EPS HOT	U1 HOT	U2 HOT	EPS COLD	U1 COLD	U2 COLD
4.250000E 01	8.838238E-01	7.254211E-01	4.250000E 01	9.062966E-01	1.021388E 00

FIGURE A-6
 (PAGE II OF 18)

TYPICAL CASE - START OF FUEL CYCLE - 600 PSI PRESSURE

HOT CHANNEL

DEL T BN	V I	DEL T BHS	V BHS	H HS	DEL T FHS	TS HS	QMAX
1.479866E 02	3.867450E 01	1.841830E 02	2.676648E 01	1.480966E 04	1.664146E 02	4.717976E 02	2.464544E 06

BERGLES-R. BURNOUT CORRELATION K # 1.000009E 00

DEL T BN	V I	DEL T BHS	V BHS	P HS	T S	T SAT	Q
1.479879E 02	3.867450E 01	1.841846E 02	2.676648E 01	4.652364E 02	5.560162E 02	4.602752E 02	2.464544E 06

COLD CHANNEL

DEL T BN	V I	DEL T BHS	V BHS	H HS	DEL T FHS	TS HS	QMAX
1.479866E 02	3.867450E 01	1.841830E 02	2.676648E 01	1.480966E 04	1.664146E 02	4.717976E 02	2.464544E 06

BERGLES-R. BURNOUT CORRELATION K # 1.000009E 00

DEL T BN	V I	DEL T BHS	V BHS	P HS	T S	T SAT	Q
1.479879E 02	3.867450E 01	1.841846E 02	2.676648E 01	4.652364E 02	5.560162E 02	4.602752E 02	2.464544E 06

AT CONVERGENCE, C/A # 1.016541E 06 AND K(D) # 1.000004E 00

FIGURE A-6
(PAGE 12 OF 18)

TYPICAL CASE - START OF FUEL CYCLE - 600 PSI PRESSURE - ICOMW OPERATION

1 ITERATIONS

INPUT DATA

1.833000E 00	5.150000E 01	4.850000E 01	2.000000E 01	2.000000E 00	7.350000E 01	1.200000E 02	1.450000E 00
1.150000E 00	6.000000E 02	8.000000E 05	1.000000E 00	1.000000E 00	1.150000E 00	0.	1.050000E 00
1.010000E 00	9.000000E-01	1.000000E 00	7.702000E-01	1.000000E 00	1.100000E 00	1.000000E 00	1.100000E 00
1.010000E 00	1.000000E 00	4.782050E 02	9.123300E-01	7.854000E-04	6.670000E-01	1.640000E-01	4.000000E 01
4.000000E 02	1.000000E 00	-2.000000E 00	3.100000E 01	1.000000E 00	6.000000E 00	1.000000E 01	0.
0.	1.000000E 00	0.	7.600000E 03	1.875000E-01	0.	1.000000E 02	5.298100E-01
2.823000E-02	3.900000E-05	3.500000E-01	1.000000E 00	8.280000E 03	3.124000E-02	5.000000E-01	1.000000E 01
1.100000E 00	1.300000E 00	1.300000E 00	1.118000E 00	8.460000E-01	-0.	-0.	

DATA FOR OXIDE FILM BUILD-UP CALCULATION

TIME INCREMENT	TIME (I)	Q/A (I)	U12 (I)	DPC (I)
1	0.	8.000000E 05	1.000000E 00	7.350000E 01

FIGURE A-6
(PAGE 13 OF 18)

TYPICAL CASE - START OF FUEL CYCLE - 600 PSI PRESSURE - ICDMW OPERATION
 THE FOLLOWING OUTPUT IS FOR THE COLD CHANNEL CALCULATION
 HOT PLATE - NARROW CHANNEL

DEL T BN	V I	DEL T BHS	V BHS	H HS	DEL T FHS	TS HS	QMAX
1.183466E 02	3.843957E 01	1.183466E 02	4.010757E 01	1.516697E 04	9.717036E 01	3.367170E 02	1.473780E 06

HOT PLATE - WIDE CHANNEL

DEL T BN	V I	DEL T BHS	V BHS	H HS	DEL T FHS	TS HS	QMAX
8.005694E 01	4.431267E 01	8.005694E 01	4.549013E 01	1.462857E 04	1.007467E 02	3.020036E 02	1.473780E 06

FACTORS CAUSING DEFLECTIONS

PRESS. DIFF.	DELTA TF N	DELTA TF A	DELTA TF W	T SIDE PLATE
3.385969E 00	0.	0.	0.	1.604761E 02

PLATE DEFLECTIONS

PRESS. DEFL.	FP BUCKL N	FP BUCKL A	FP BUCKL W	HC DEFL H	HC DEFL C
1.871059E 00	5.517471E 00	4.816771E 00	4.139442E 00	6.900378E 00	-5.878281E 00

TEMP DIFF N	TEMP DIFF W	VOL EXP N	VOL EXP A	VOL EXP W	HS DEFL H	HS DEFL C
5.110484E-01	5.110482E-01	2.678505E-01	2.504201E-01	2.329896E-01	1.033424E 01	7.006996E-01

EPS HOT	U1 HOT	U2 HOT	EPS COLD	U1 COLD	U2 COLD
4.250000E 01	8.838238E-01	7.254211E-01	4.250000E 01	9.054788E-01	1.012722E 00

FIGURE A-6
 (PAGE 14 OF 18)

TYPICAL CASE - START OF FUEL CYCLE - 600 PSI PRESSURE - ICQMW OPERATION

HOT CHANNEL

DEL T BN	V I	DEL T BHS	V BHS	H HS	DEL T FHS	TS HS	QMAX
1.172047E 02	3.842981E 01	1.423834E 02	3.719447E 01	1.529853E 04	9.649119E 01	3.600746E 02	1.476173E 06

BERGLES-R. BURNOUT CORRELATION K # 1.000007E 00

DEL T BN	V I	DEL T BHS	V BHS	P HS	T S	T SAT	G
1.770918E 02	3.887201E 01	2.151358E 02	3.920871E 01	4.652067E 02	5.504109E 02	4.602687E 02	2.277486E 06

COLD CHANNEL

DEL T BN	V I	DEL T BHS	V BHS	H HS	DEL T FHS	TS HS	QMAX
1.172047E 02	3.842981E 01	1.423834E 02	3.719447E 01	1.529853E 04	9.649119E 01	3.600746E 02	1.476173E 06

BERGLES-R. BURNOUT CORRELATION K # 1.000007E 00

DEL T BN	V I	DEL T BHS	V BHS	P HS	T S	T SAT	G
1.770918E 02	3.887201E 01	2.151358E 02	3.920871E 01	4.652067E 02	5.504109E 02	4.602687E 02	2.277486E 06

AT CONVERGENCE, C/A # 1.011337E 06 AND K(D) # 1.528342E 00

95

FIGURE A-6
(PAGE 15 OF 18)

TYPICAL CASE - START OF FUEL CYCLE - 600 PSI PRESSURE - 10MW OPERATION

1 ITERATIONS

INPUT DATA

1.833000E 00	5.150000E 01	4.850000E 01	2.000000E 01	2.000000E 00	7.350000E 01	1.200000E 02	1.450000E 00
1.150000E 00	6.000000E 02	8.000000E 05	1.000000E 00	1.000000E 00	1.150000E 00	0.	1.050000E 00
1.010000E 00	9.000000E-01	1.000000E 00	7.702000E-01	1.000000E 00	1.100000E 00	1.000000E 00	1.100000E 00
1.010000E 00	1.000000E 00	4.782050E 02	9.123300E-01	7.854000E-04	6.670000E-01	1.640000E-01	4.000000E 01
4.000000E 02	1.000000E 00	-2.000000E 00	3.100000E 01	1.000000E 00	6.000000E 00	1.000000E 01	0.
0.	1.000000E 00	0.	7.600000E 03	1.875000E-01	0.	1.000000E 02	5.298100E-01
2.823000E-02	3.900000E-05	3.500000E-01	1.000000E 00	8.280000E 03	3.124000E-02	5.000000E-01	1.000000E 01
1.100000E 00	1.300000E 00	1.300000E 00	1.118000E 00	8.460000E-01	-0.	-0.	

DATA FOR OXIDE FILM BUILD-UP CALCULATION

TIME INCREMENT	TIME (I)	Q/A (I)	U12 (I)	DPC (I)
1	0.	8.000000E 05	1.000000E 00	7.350000E 01

96

FIGURE A-6
(PAGE 16 OF 18)

TYPICAL CASE - START OF FUEL CYCLE - 600 PSI PRESSURE - ICOMW OPERATION
 THE FOLLOWING OUTPUT IS FOR THE HOT CHANNEL CALCULATION

HOT PLATE - NARROW CHANNEL

DEL T BN	V I	DEL T BHS	V BHS	F HS	DEL T FHS	TS HS	QMAX
1.183466E 02	3.843957E 01	1.183466E 02	4.010757E 01	1.516697E 04	9.717036E 01	3.367170E 02	1.473780E 06

HOT PLATE - WIDE CHANNEL

DEL T BN	V I	DEL T BHS	V BHS	F HS	DEL T FHS	TS HS	QMAX
8.005694E 01	4.431267E 01	8.005694E 01	4.549013E 01	1.462857E 04	1.007467E 02	3.020036E 02	1.473780E 06

FACTORS CAUSING DEFLECTIONS

PRESS. DIFF.	DELTA TF N	DELTA TF A	DELTA TF W	T SIDE PLATE
3.385969E 00	0.	0.	0.	1.604761E 02

PLATE DEFLECTIONS

PRESS. DEFL.	FP BUCKL N	FP BUCKL A	FP BUCKL W	HC DEFL H	HC DEFL C
1.871059E 00	5.517471E 00	4.816771E 00	4.139442E 00	6.900378E 00	-5.878281E 00

TEMP DIFF N	TEMP DIFF W	VOL EXP N	VOL EXP A	VOL EXP W	HS DEFL H	HS DEFL C
5.110484E-01	5.110482E-01	2.678505E-01	2.504201E-01	2.329896E-01	1.033424E 01	7.006996E-01

EPS HOT	U1 HOT	U2 HOT	EPS COLD	U1 COLD	U2 COLD
4.250000E 01	8.885434E-01	7.955558E-01	4.250000E 01	9.054788E-01	1.012722E 00

FIGURE A-6
 (PAGE 17 OF 18)

97

TYPICAL CASE - START OF FUEL CYCLE - 600 PSI PRESSURE - 100MW OPERATION

HOT CHANNEL

DEL T BN	V I	DEL T BHS	V BHS	P HS	DEL T FHS	TS HS	QMAX
1.172047E 02	3.842981E 01	1.450972E 02	2.871119E 01	1.438251E 04	1.336525E 02	3.999497E 02	1.922258E 06

BERGLES-R. BURNOUT CORRELATION K # 1.000004E 00

DEL T BN	V I	DEL T BHS	V BHS	P HS	T S	T SAT	Q
1.501202E 02	3.869006E 01	1.858460E 02	2.955136E 01	4.652336E 02	5.547624E 02	4.602746E 02	2.528389E 06

COLD CHANNEL

DEL T BN	V I	DEL T BHS	V BHS	H HS	DEL T FHS	TS HS	QMAX
1.172047E 02	3.842981E 01	1.450972E 02	2.871119E 01	1.438251E 04	1.336525E 02	3.999497E 02	1.922258E 06

BERGLES-R. BURNOUT CORRELATION K # 1.000004E 00

DEL T BN	V I	DEL T BHS	V BHS	P HS	T S	T SAT	Q
1.501202E 02	3.869006E 01	1.858460E 02	2.955136E 01	4.652336E 02	5.547624E 02	4.602746E 02	2.528389E 06

AT CONVERGENCE, Q/A # 9.158040E 05 AND K(D) # 1.289510E 00

88

FIGURE A-6
(PAGE 18 OF 18)

TYPICAL CASE -INPUT VALUES FROM TABLE II

9 ITERATIONS

INPUT DATA

1.833000E 00	5.150000E 01	4.850000E 01	2.000000E 01	2.000000E 00	7.350000E 01	1.200000E 02	1.450000E 00
1.150000E 00	9.000000E 02	8.000000E 05	1.000000E 00	1.000000E 00	1.150000E 00	0.	1.050000E 00
1.010000E 00	9.000000E-01	1.000000E 00	7.702000E-01	1.000000E 00	1.100000E 00	1.000000E 00	1.100000E 00
1.010000E 00	1.000000E 00	4.782050E 02	9.123300E-01	7.854000E-04	6.670000E-01	1.640000E-01	4.000000E 01
4.000000E 02	1.000000E 00	0.	3.100000E 01	1.000000E 00	6.000000E 00	1.000000E 01	0.
0.	1.000000E 00	0.	7.600000E 03	1.875000E-01	0.	1.000000E 02	5.298100E-01
2.823000E-02	3.900000E-05	3.500000E-01	1.000000E 00	8.280000E 03	3.124000E-02	5.000000E-01	1.000000E-05
1.100000E 00	1.300000E 00	1.300000E 00	1.118000E 00	8.460000E-01	-0.	-0.	

DATA FOR OXIDE FILM BUILD-UP CALCULATION

TIME INCREMENT	TIME (I)	Q/A (I)	U12 (I)	DPC (I)
1	3.600000E 02	8.000000E 05	1.000000E 00	7.350000E 01

FIGURE A-7
(PAGE 1 OF 9)

Fig. A-7. Output Data from Sample Problems, Incipient Boiling Calculations.

TYPICAL CASE - INPUT VALUES FROM TABLE II

HOT PLATE - NARROW CHANNEL

DEL T BN	V I	DEL T BHS	V BHS	H HS	DEL T FHS	TS HS	QMAX
1.853836E 02	3.892267E 01	1.853836E 02	4.204506E 01	1.684887E 04	1.387399E 02	4.453235E 02	2.337610E 06

HOT PLATE - WIDE CHANNEL

DEL T BN	V I	DEL T BHS	V BHS	H HS	DEL T FHS	TS HS	QMAX
1.256361E 02	4.478701E 01	1.256361E 02	4.688863E 01	1.620354E 04	1.442654E 02	3.911015E 02	2.337610E 06

FACTORS CAUSING DEFLECTIONS

PRESS. DIFF.	DELTA TF N	DELTA TF A	DELTA TF W	T SIDE PLATE
3.277002E 00	1.588821E 02	1.260544E 02	9.896053E 01	1.837089E 02

PLATE DEFLECTIONS

PRESS. DEFL.	FP BUCKL N	FP BUCKL A	FP BUCKL W	HC DEFL H	HC DEFL C
2.316561E 00	1.723731E 01	1.409217E 01	1.138392E 01	9.587014E 00	-5.071625E 00

TEMP DIFF N	TEMP DIFF W	VOL EXP N	VOL EXP A	VOL EXP W	HS DEFL H	HS DEFL C
2.257695E 00	2.041720E 00	5.364759E-01	4.762825E-01	4.218473E-01	3.132948E 01	3.145139E 00

EPS HOT	U1 HOT	U2 HOT	EPS COLD	U1 COLD	U2 COLD
4.250000E 01	8.432349E-01	1.321485E-01	4.250000E 01	9.187337E-01	1.355292E 00

FIGURE A-7
(PAGE 2 OF 9)

TYPICAL CASE - INPUT VALUES FROM TABLE II

HOT CHANNEL

DEL T BN	V I	DEL T BHS	V BHS	H HS	DEL T FHS	TS HS	QMAX
1.835985E 02	3.891199E 01	2.395043E 02	4.847203E 00	1.937655E 03	1.160973E 03	1.521677E 03	2.249565E 06

ZENKEVICH-SUBBOTIN BURNOUT CORRELATION K # 6.380630E-01

DEL T BN	V I	DEL T BHS	V BHS	P HS	T S	T SAT	Q
1.185809E 02	3.844159E 01	1.546888E 02	4.549716E 00	7.352849E 02	6.118823E 02	5.092704E 02	1.435364E 06

COLD CHANNEL

DEL T BN	V I	DEL T BHS	V BHS	H HS	DEL T FHS	TS HS	QMAX
1.835985E 02	3.891199E 01	2.198226E 02	4.162289E 01	1.720806E 04	1.376335E 02	4.786560E 02	2.368405E 06

ZENKEVICH-SUBBOTIN BURNOUT CORRELATION K # 1.361932E 00

DEL T BN	V I	DEL T BHS	V BHS	P HS	T S	T SAT	Q
2.480106E 02	3.923175E 01	2.969432E 02	4.439656E 01	7.352078E 02	5.939407E 02	5.092586E 02	3.225647E 06

AT CONVERGENCE, Q/A # 1.268904E 06 AND K(0) # 9.999973E-01

101

FIGURE A-7
(PAGE 3 OF 9)

TYPICAL CASE - START OF FUEL CYCLE - 600 PSI PRESSURE

7 ITERATIONS

INPUT DATA

1.833000E 00	5.150000E 01	4.850000E 01	2.000000E 01	2.000000E 00	7.350000E 01	1.200000E 02	1.450000E 00
1.150000E 00	6.000000E 02	8.000000E 05	1.000000E 00	1.000000E 00	1.150000E 00	0.	1.050000E 00
1.010000E 00	9.000000E-01	1.000000E 00	7.702000E-01	1.000000E 00	1.100000E 00	1.000000E 00	1.100000E 00
1.010000E 00	1.000000E 00	4.782050E 02	9.123300E-01	7.854000E-04	6.670000E-01	1.640000E-01	4.000000E 01
4.000000E 02	1.000000E 00	0.	3.100000E 01	1.000000E 00	6.000000E 00	1.000000E 01	0.
0.	1.000000E 00	0.	7.600000E 03	1.875000E-01	0.	1.000000E 02	5.298100E-01
2.823000E-02	3.900000E-05	3.500000E-01	1.000000E 00	8.280000E 03	3.124000E-02	5.000000E-01	1.000000E-05
1.100000E 00	1.300000E 00	1.300000E 00	1.118000E 00	8.460000E-01	-0.	-0.	

DATA FOR OXIDE FILM BUILD-UP CALCULATION

TIME INCREMENT	TIME (I)	Q/A (I)	U12 (I)	DPC (I)
1	0.	8.000000E 05	1.000000E 00	7.350000E 01

FIGURE A-7
(PAGE 4 OF 9)

TYPICAL CASE - START OF FUEL CYCLE - 600 PSI PRESSURE

HOT PLATE - NARROW CHANNEL

DEL T BN	V I	DEL T BHS	V BHS	H HS	DEL T FHS	TS HS	QMAX
1.962745E 02	3.898560E 01	1.962745E 02	4.238459E 01	1.707358E 04	1.451916E 02	4.626660E 02	2.478940E 06

HOT PLATE - WIDE CHANNEL

DEL T BN	V I	DEL T BHS	V BHS	H HS	DEL T FHS	TS HS	QMAX
1.330323E 02	4.485422E 01	1.330323E 02	4.712479E 01	1.642005E 04	1.509704E 02	4.052026E 02	2.478940E 06

FACTORS CAUSING DEFLECTIONS

PRESS. DIFF.	DELTA TF N	DELTA TF A	DELTA TF W	T SIDE PLATE
3.255295E 00	0.	0.	0.	1.874882E 02

PLATE DEFLECTIONS

PRESS. DEFL.	FP BUCKL N	FP BUCKL A	FP BUCKL W	HC DEFL H	HC DEFL C
1.976321E 00	9.890859E 00	8.560442E 00	7.277340E 00	7.665572E 00	-5.806702E 00

TEMP DIFF N	TEMP DIFF W	VOL EXP N	VOL EXP A	VOL EXP W	HS DEFL H	HS DEFL C
9.294352E-01	9.294351E-01	3.943349E-01	3.654810E-01	3.366272E-01	1.845130E 01	1.330417E 00

EPS HOT	U1 HOT	U2 HOT	EPS COLD	U1 COLD	U2 COLD
4.250000E 01	8.757585E-01	6.046205E-01	4.250000E 01	9.066589E-01	1.024040E 00

103

FIGURE A-7
(PAGE 5 OF 9)

TYPICAL CASE - START OF FUEL CYCLE - 600 PSI PRESSURE

HOT CHANNEL

DEL T BN	V I	DEL T BHS	V BHS	H HS	DEL T FHS	TS HS	QMAX
1.943841E 02	3.897498E 01	2.441569E 02	2.314469E 01	1.493517E 04	2.190092E 02	5.843661E 02	3.270940E 06

ZENKEVICH-SUBBOTIN BURNOUT CORRELATION K # 8.348615E-01

DEL T BN	V I	DEL T BHS	V BHS	P HS	T S	T SAT	Q
1.630957E 02	3.876094E 01	2.048571E 02	2.244193E 01	4.652188E 02	5.579585E 02	4.602714E 02	2.730773E 06

COLD CHANNEL

DEL T BN	V I	DEL T BHS	V BHS	H HS	DEL T FHS	TS HS	QMAX
1.943841E 02	3.897498E 01	2.358357E 02	4.035085E 01	1.729806E 04	1.452733E 02	5.023090E 02	2.512946E 06

ZENKEVICH-SUBBOTIN BURNOUT CORRELATION K # 1.165143E 00

DEL T BN	V I	DEL T BHS	V BHS	P HS	T S	T SAT	Q
2.255574E 02	3.913531E 01	2.736566E 02	4.163784E 01	4.651964E 02	5.493155E 02	4.602665E 02	2.927939E 06

AT CONVERGENCE, Q/A # 1.345625E 06 AND K(D) # 1.000002E 00

104

FIGURE A-7
(PAGE 6 OF 9)

TYPICAL CASE - START OF FUEL CYCLE - 600 PSI PRESSURE - 100MW OPERATION

1 ITERATIONS

INPUT DATA

1.833000E 00	5.150000E 01	4.850000E 01	2.000000E 01	2.000000E 00	7.350000E 01	1.200000E 02	1.450000E 00
1.150000E 00	6.000000E 02	8.000000E 05	1.000000E 00	1.000000E 00	1.150000E 00	0.	1.050000E 00
1.010000E 00	9.000000E-01	1.000000E 00	7.702000E-01	1.000000E 00	1.100000E 00	1.000000E 00	1.100000E 00
1.010000E 00	1.000000E 00	4.782050E 02	9.123300E-01	7.854000E-04	6.670000E-01	1.640000E-01	4.000000E 01
4.000000E 02	1.000000E 00	0.	3.100000E 01	1.000000E 00	6.000000E 00	1.000000E 01	0.
0.	1.000000E 00	0.	7.600000E 03	1.875000E-01	0.	1.000000E 02	5.298100E-01
2.823000E-02	3.900000E-05	3.500000E-01	1.000000E 00	8.280000E 03	3.124000E-02	5.000000E-01	1.000000E 01
1.100000E 00	1.300000E 00	1.300000E 00	1.118000E 00	8.460000E-01	-0.	-0.	

DATA FOR OXIDE FILM BUILD-UP CALCULATION

TIME INCREMENT	TIME (I)	Q/A (I)	U12 (I)	DPC (I)
1	0.	8.000000E 05	1.000000E 00	7.350000E 01

TYPICAL CASE - START OF FUEL CYCLE - 600 PSI PRESSURE - 100MW OPERATION

HOT PLATE - NARROW CHANNEL

DEL T BN	V I	DEL T BHS	V BHS	H HS	DEL T FHS	TS HS	QMAX
1.183466E 02	3.843957E 01	1.183466E 02	4.010757E 01	1.516697E 04	9.717036E 01	3.367170E 02	1.473780E 06

HOT PLATE - WIDE CHANNEL

DEL T BN	V I	DEL T BHS	V BHS	H HS	DEL T FHS	TS HS	QMAX
8.005694E 01	4.431267E 01	8.005694E 01	4.549013E 01	1.462857E 04	1.007467E 02	3.020036E 02	1.473780E 06

FACTORS CAUSING DEFLECTIONS

PRESS. DIFF.	DELTA TF N	DELTA TF A	DELTA TF W	T SIDE PLATE
3.385969E 00	0.	0.	0.	1.604761E 02

PLATE DEFLECTIONS

PRESS. DEFL.	FP BUCKL N	FP BUCKL A	FP BUCKL W	HC DEFL H	HC DEFL C
1.871059E 00	5.517471E 00	4.816771E 00	4.139442E 00	6.900378E 00	-5.878281E 00

TEMP DIFF N	TEMP DIFF W	VOL EXP N	VOL EXP A	VOL EXP W	HS DEFL H	HS DEFL C
5.110484E-01	5.110482E-01	2.678505E-01	2.504201E-01	2.329896E-01	1.033424E 01	7.006996E-01

EPS HOT	U1 HOT	U2 HOT	EPS COLD	U1 COLD	U2 COLD
4.250000E 01	8.885434E-01	7.955558E-01	4.250000E 01	9.054788E-01	1.012722E 00

FIGURE A-7
(PAGE 8 OF 9)

TYPICAL CASE - START OF FUEL CYCLE - 600 PSI PRESSURE - 100MM OPERATION

HOT CHANNEL

DEL T BN	V I	DEL T BHS	V BHS	H HS	DEL T FHS	TS HS	QMAX
1.172047E 02	3.842981E 01	1.450972E 02	2.871119E 01	1.438251E 04	1.336525E 02	3.999497E 02	1.922258E 06

ZENKEVICH-SUBBOTIN BURNOUT CORRELATION K # 1.567100E 00

DEL T BN	V I	DEL T BHS	V BHS	P HS	T S	T SAT	Q
1.814561E 02	3.889899E 01	2.246392E 02	3.043262E 01	4.652038E 02	5.543595E 02	4.602681E 02	3.012370E 06

COLD CHANNEL

DEL T BN	V I	DEL T BHS	V BHS	H HS	DEL T FHS	TS HS	QMAX
1.172047E 02	3.842981E 01	1.423834E 02	3.719447E 01	1.529853E 04	9.649119E 01	3.600746E 02	1.476173E 06

ZENKEVICH-SUBBOTIN BURNOUT CORRELATION K # 1.963466E 00

DEL T BN	V I	DEL T BHS	V BHS	P HS	T S	T SAT	Q
2.259678E 02	3.913721E 01	2.745118E 02	4.115291E 01	4.651965E 02	5.495338E 02	4.602665E 02	2.898422E 06

AT CONVERGENCE, Q/A # 1.106113E 06 AND K(0) # 1.765283E 00

107

TYPICAL CASE - INPUT VALUES FROM TABLE II

(TITLE CARD)

9 ITERATIONS		(NUMBER OF OVERALL ITERATIONS PERFORMED)						
INPUT DATA		(LISTED IN SAME ORDER AS ON INPUT DATA SHEET)						
A (1)	A (2)	A (3)	A (4)	A (5)	A (6)	A (7)	A (8)	
1.833000E 00	5.150000E 01	4.850000E 01	2.000000E 01	2.000000E 00	7.350000E 01	1.200000E 02	1.450000E 00	
A (9)							A (16)	
1.150000E 00	9.000000E 02	8.000000E 05	1.000000E 00	1.000000E 00	1.150000E 00	0.	1.050000E 00	
A (17)							A (24)	
1.010000E 00	9.000000E-01	1.000000E 00	7.702000E-01	1.000000E 00	1.100000E 00	1.000000E 00	1.100000E 00	
A (25)							A (32)	
1.010000E 00	1.000000E 00	4.782050E 02	9.123300E-01	7.854000E-04	6.070000E-01	1.640000E-01	4.000000E 01	
A (33)							A (40)	
4.000000E 02	1.000000E 00	0.	3.100000E 01	1.000000E 00	6.000000E 00	1.000000E 01	0.	
A (41)							A (48)	
0.	1.000000E 00	0.	7.600000E 03	1.875000E-01	0.	1.000000E 02	5.298180E-01	
A (49)							A (56)	
2.823000E-02	3.900000E-05	3.500000E-01	1.000000E 00	6.280000E 03	3.124000E-02	5.000000E-01	1.000000E-05	
A (57)				A (61)				
1.100000E 00	1.300000E 00	1.300000E 00	1.118000E 00	8.460000E-01	-0.	-0.		

DATA FOR OXIDE FILM BUILD-UP CALCULATION

TIME INCREMENT	TIME (I)	Q/A (I)	U ₁₂ (I)	OPC (I)
1	3.600000E 02	8.000000E 05	1.000000E 00	7.350000E 01
(TIME STEP NO.)	t (i)	(Q/A)(i)	U ₁₂ (i)	ΔP _{CORE} (i)

NOTE:

1. ALL CALCULATION STEP NUMBERS APPEARING ON THE FOLLOWING 2 PAGES CORRESPOND TO THOSE OF SECTION I "HOT SPOT SUBROUTINE" AND OF SECTION II "HOT SLOT BURNOUT CALCULATION PROCEDURE".
2. STEPS ARE LISTED BY SECTION AND NUMBER (EG. II-5 SIGNIFIES SECTION II, STEP 5)
3. SYMBOLS GIVEN FOR OUTPUT NUMBERS ARE THOSE EMPLOYED IN THE EQUATIONS OF SECTIONS I AND II. FIGURE A-8
4. ALL OUTPUT NUMBERS ARE FROM THE FINAL ITERATION. (PAGE 1 OF 3)

Fig. A-8. Correlation of Burnout Output Data with Calculation Steps.

TYPICAL CASE - INPUT VALUES FROM TABLE II

HOT PLATE - NARROW CHANNEL (ALL NUMBERS UNDER THIS HEADING FROM STEP II-1, NARROW CHANNEL CALCULATION)

DEL T BN	V I	DEL T BHS	V BHS	H HS	DEL T FHS	TS HS	QMAX
1.853836E 02	3.892267E 01	1.853836E 02	4.204506E 01	1.684887E 04	1.387399E 02	4.453235E 02	2.337610E 06
I-2	I-9	I-11	I-13	I-14	I-15	I-17	I-15
$\Delta T_{B \text{ nom}}$	V_i	$\Delta T_{B \text{ hs}}$	V_{hs}	h_{hs}	$\Delta T_{\text{film hs}}$	$T_{\text{s hs}}$	$(Q/A)_{\text{max hs}}$

HOT PLATE - WIDE CHANNEL (ALL NUMBERS UNDER THIS HEADING FROM STEP II-1, WIDE CHANNEL CALCULATION)

DEL T BN	V I	DEL T BHS	V BHS	H HS	DEL T FHS	TS HS	QMAX
1.256361E 02	4.478701E 01	1.256361E 02	4.688863E 01	1.620354E 04	1.442654E 02	3.911015E 02	2.337610E 06
(STEP NUMBERS AND SYMBOLS IDENTICAL TO THOSE FOR NARROW CHANNEL)							

FACTORS CAUSING DEFLECTIONS

PRESS. DIFF.	DELTA TF N	DELTA TF A	DELTA TF W	T SIDE PLATE
3.277002E 00	1.588821E 02	1.260544E 02	9.896053E 01	1.837089E 02
II-2	II-3	II-3	II-3	II-5
Δp	ΔT_{fn}	ΔT_{fa}	ΔT_{fw}	$T_{\text{side plate}}$

PLATE DEFLECTIONS

PRESS. DEFL.	FP BUCKL N	FP BUCKL A	FP BUCKL W	HC DEFL H	HC DEFL C	
2.316561E 00	1.723731E 01	1.409217E 01	1.138392E 01	9.587014E 00	-5.071625E 00	
II-7	II-6	II-6	II-6	II-10	II-10	
δ_p	δ_{Tn}	δ_{Ta}	δ_{Tw}	$\delta_{\text{streak,H}}$	$\delta_{\text{streak,C}}$	
TEMP DIFF N	TEMP DIFF W	VOL EXP N	VOL EXP A	VOL EXP W	HS DEFL H	HS DEFL C
2.257695E 00	2.041720E 00	5.364759E -01	4.762825E -01	4.218473E -01	3.132948E 01	3.145139E 00
II-8	II-8	II-9	II-9	II-9	II-11	II-11
$\delta_{\text{T,n-a}}$	$\delta_{\text{T,w-a}}$	δ_{vn}	δ_{va}	δ_{vw}	$\delta_{\text{hs,H}}$	$\delta_{\text{hs,C}}$
EPS HOT	U1 HOT	U2 HOT	EPS COLD	U1 COLD	U2 COLD	
4.250000E 01	8.432349E -01	1.321485E -01	4.250000E 01	9.187337E -01	1.055292E 00	
II-12	II-13	II-14	II-12	II-13	II-14	
ϵ_H	$U_{1,H}$	$U_{2,H}$	ϵ_C	$U_{1,C}$	$U_{2,C}$	

609

FIGURE A-8
(PAGE 2 OF 3)

TYPICAL CASE - INPUT VALUES FROM TABLE II

(TITLE CARD)

HOT CHANNEL (ALL NUMBERS UNDER THIS HEADING, INCLUDING BURNOUT LINE, FROM STEP II-15, HOT CHANNEL CALCULATION)

DEL T BN	V I	DEL T BHS	V BHS	H HS	DEL T FHS	TS HS	QMAX
1.835985E 02	3.891199E 01	2.395043E 02	4.847203E 00	1.937655E 03	1.160973E 03	1.521677E 03	2.249565E 06
I-2	I-9	I-11	I-13	I-14	I-15	I-17	I-15
ΔT_{Bnom}	V_i	ΔT_{Bhs}	V_{hs}	h_{hs}	ΔT_{film} hs	T_s hs	$(Q/A)_{max}$ hs

ZENKEVICH-SUBBOTIN BURNOUT CORRELATION K # 6.380630E-01 (STEP II a-7, SYMBOL K)

DEL T BN	V I	DEL T BHS	V BHS	P HS	T S	T SAT	Q
1.185809E 02	3.844159E 01	1.546888E 02	4.549716E 00	7.352849E 02	6.118823E 02	5.092704E 02	1.435364E 06
I-2	I-9	I-11	I-13	I-14	I-15	I-17	I-15
ΔT_{Bnom}	V_i	ΔT_{Bhs}	V_{hs}	h_{hs}	ΔT_{films}	T_s hs	$(Q/A)_{max}$ hs

COLD CHANNEL (ALL NUMBERS UNDER THIS HEADING, INCLUDING BURNOUT LINE, FROM STEP II-15, COLD CHANNEL CALCULATION)

DEL T BN	V I	DEL T BHS	V BHS	H HS	DEL T FHS	TS HS	QMAX
1.835985E 02	3.891199E 01	2.198226E 02	4.162289E 01	1.720806E 04	1.376335E 02	4.786560E 02	2.368405E 06

ZENKEVICH-SUBBOTIN BURNOUT CORRELATION K # 1.361932E 00

DEL T BN	V I	DEL T BHS	V BHS	P HS	T S	T SAT	Q
2.480106E 02	3.923175E 01	2.969432E 02	4.439656E 01	7.352078E 02	5.939407E 02	5.092586E 02	3.225647E 06

SYMBOLS AND
STEP NUMBERS
IDENTICAL TO
HOT CHANNEL
DATA.

110

AT CONVERGENCE, Q/A # 1.268904E 06 AND K(0) # 9.999973E-01

II-17 II-16
(Q/A)_{new} K

FIGURE A-8
(PAGE 3 OF 3)

TYPICAL CASE -INPUT VALUES FROM TABLE II

24 ITERATIONS

INPUT DATA

1.833000E 00	5.150000E 01	4.850000E 01	2.000000E 01	2.000000E 00	7.350000E 01	1.200000E 02	1.450000E 00
1.150000E 00	9.000000E 02	8.000000E 05	1.000000E 00	1.000000E 00	1.150000E 00	0.	1.050000E 00
1.010000E 00	9.000000E-01	1.000000E 00	7.702000E-01	1.000000E 00	1.100000E 00	1.000000E 00	1.100000E 00
1.010000E 00	1.000000E 00	4.782050E 02	9.123300E-01	7.854000E-04	6.670000E-01	1.640000E-01	4.000000E 01
4.000000E 02	1.000000E 00	-2.000000E 00	3.100000E 01	1.000000E 00	6.000000E 00	1.000000E 01	0.
0.	1.000000E 00	0.	7.600000E 03	1.875000E-01	0.	1.000000E 02	5.298100E-01
2.823000E-02	3.900000E-05	3.500000E-01	1.000000E 00	8.280000E 03	3.124000E-02	5.000000E-01	1.000000E-05
1.100000E 00	1.300000E 00	1.300000E 00	1.118000E 00	8.460000E-01	-0.	-0.	

DATA FOR OXIDE FILM BUILD-UP CALCULATION

TIME INCREMENT	TIME (I)	Q/A (I)	U12 (I)	DPC (I)
1	3.600000E 02	8.000000E 05	1.000000E 00	7.350000E 01

ABOVE DATA LISTING IS IDENTICAL TO BURNOUT OUTPUT, FIG. A-8 PAGE I

NOTE:

1. ALL CALCULATION STEP NUMBERS APPEARING ON THE FOLLOWING 5 PAGES CORRESPOND TO THOSE OF SECTION I "HOT SPOT SUBROUTINE" AND OF SECTION III "HOT SLOT INCIPIENT BOILING CALCULATION PROCEDURE."
2. STEPS ARE LISTED BY SECTION AND NUMBER (EG. III-5 SIGNIFIES SECTION III, STEP # 5).
3. SYMBOLS GIVEN FOR OUTPUT NUMBERS ARE THOSE EMPLOYED IN THE EQUATIONS OF SECTIONS I AND III. FIGURE A-9
4. ALL OUTPUT NUMBERS ARE FROM THE FINAL ITERATION. (PAGE 1 OF 6)

(TITLE CARD)

TYPICAL CASE - INPUT VALUES FROM TABLE II THIS STATEMENT SPECIFIES WHETHER NEXT 2-SHEETS APPLY TO HOT OR COLD CHAN.

THE FOLLOWING OUTPUT IS FOR THE COLD CHANNEL CALCULATION

HOT PLATE - NARROW CHANNEL (ALL NUMBERS UNDER THIS HEADING ARE FROM STEP III-1, NARROW CHANNEL CALCULATION)

DEL T BN	V I	DEL T BHS	V BHS	H HS	DEL T FHS	TS HS	QMAX
2.085967E 02	3.905200E 01	2.085967E 02	4.277864E 01	1.731638E 04	1.524024E 02	4.821990E 02	2.639057E 06
I-2	I-9	I-11	I-13	I-14	I-15	I-17	I-15
$\Delta T_{B \text{ nom}}$	V_i	$\Delta T_{B \text{ hs}}$	V_{hs}	h_{hs}	$\Delta T_{\text{film hs}}$	$T_{\text{s hs}}$	$(Q/A)_{\text{max hs}}$

HOT PLATE - WIDE CHANNEL (ALL NUMBERS UNDER THIS HEADING ARE FROM STEP III-1, WIDE CHANNEL CALCULATIONS)

DEL T BN	V I	DEL T BHS	V BHS	H HS	DEL T FHS	TS HS	QMAX
1.413951E 02	4.492713E 01	1.413951E 02	4.739541E 01	1.665394E 04	1.584644E 02	4.210595E 02	2.639057E 06
(STEP NUMBERS AND SYMBOLS IDENTICAL TO THOSE FOR NARROW CHANNEL)							

FACTORS CAUSING DEFLECTIONS

PRESS. DIFF.	DELTA TF N	DELTA TF A	DELTA TF W	T SIDE PLATE
3.229024E 00	1.793707E 02	1.423097E 02	1.117220E 02	1.917641E 02
III-2	III-3	III-3	III-3	III-5
Δp	ΔT_{fn}	ΔT_{fa}	ΔT_{fw}	$T_{\text{side plate}}$

PLATE DEFLECTIONS

PRESS. DEFL.	FP BUCKL N	FP BUCKL A	FP BUCKL W	HC DEFL H	HC DEFL C	
2.511804E 00	1.993211E 01	1.626013E 01	1.310019E 01	1.043522E 01	-4.828884E 00	
III-7	III-6	III-6	III-6	III-10	III-10	
δ_p	δ_{Tn}	δ_{Ta}	δ_{Tw}	$\delta_{\text{streak,H}}$	$\delta_{\text{streak,C}}$	
TEMP DIFF N	TEMP DIFF W	VOL EXP N	VOL EXP A	VOL EXP W	HS DEFL H	HS DEFL C
2.803170E 00	2.534866E 00	5.940839E-01	5.261657E-01	4.647483E-01	3.619224E 01	3.671980E 00
III-8	III-8	III-9	III-9	III-9	III-11	III-11
$\delta_{T,n-a}$	$\delta_{T,w-a}$	δ_{Vn}	δ_{Va}	δ_{Vw}	$\delta_{\text{hs,H}}$	$\delta_{\text{hs,C}}$
EPS HOT	UI HOT	U2 HOT	EPS COLD	UI COLD	U2 COLD	
4.250000E 01	0.	0.	4.250000E 01	9.227036E-01	1.064004E 00	
III-12	III-13	III-14	III-12	III-13	III-14	
ϵ_H	$U_{1,H}$	$U_{2,H}$	ϵ_C	$U_{1,C}$	$U_{2,C}$	

FIGURE A-9
(PAGE 2 OF 6)

112

TYPICAL CASE - INPUT VALUES FROM TABLE II

(TITLE CARD)

HOT CHANNEL (ALL NUMBERS UNDER THIS HEADING, NOT INCLUDING BURNOUT LINE, ARE FROM III-15)

DEL T BN	V I	DEL T BHS	V BHS	H HS	DEL T FHS	TS HS	QMAX
2.065869E 02	3.904150E 01	2.462823E 02	4.305039E 01	1.773827E 04	1.512146E 02	5.186969E 02	2.682286E 06
I-2 ΔT_{Bmon}	I-9 V_i	I-11 ΔT_{Bhs}	I-13 V_{hs}	I-14 h_{hs}	I-15 $\Delta T_{film\ hs}$	I-17 $T_{s,hs}$	I-15 (Q/A) _{max hs}

BERGLES-R. BURNOUT CORRELATION K # 1.000003E 00 (STEP III-5 SYMBOL K)

DEL T BN	V I	DEL T BHS	V BHS	P HS	T S	T SAT	Q
2.065887E 02	3.904150E 01	2.462845E 02	4.305043E 01	7.351948E 02	5.945447E 02	5.092566E 02	2.682303E 06
III-23 $\Delta T_{Bnom\ ib}$	III-15 (I-9) V_i	III-22 $\Delta T_{Bhs\ ib}$	III-15 V_{hs}	III-16 $P_{hs\ ib}$	III-15 $T_{s,vo}$	III-17 T_{sa+ib}	III-15 (I-15) (Q/A) _{max hs}

COLD CHANNEL

DEL T BN	V I	DEL T BHS	V BHS	H HS	DEL T FHS	TS HS	QMAX
2.065849E 02	3.904150E 01	2.462823E 02	4.305039E 01	1.773827E 04	1.512146E 02	5.186969E 02	2.682286E 06

BERGLES-R. BURNOUT CORRELATION K # 1.000003E 00

DEL T BN	V I	DEL T BHS	V BHS	P HS	T S	T SAT	Q
2.065887E 02	3.904150E 01	2.462845E 02	4.305043E 01	7.351948E 02	5.945447E 02	5.092566E 02	2.682303E 06

AT CONVERGENCE, Q/A # 1.432543E 06 AND K(D) # 1.000008E 00

III-24
(Q/A)_{ib}

III-27
K

THESE LINES
ARE REPEAT
OF THE
ABOVE HOT
CHANNEL
DATA AND MAY
BE IGNORED.

113

FIGURE A-9
(PAGE 3 OF 6)

TYPICAL CASE - INPUT VALUES FROM TABLE II

7 ITERATIONS

INPUT DATA

1.833000E 00	5.150000E 01	4.850000E 01	2.000000E 01	2.000000E 00	7.350000E 01	1.200000E 02	1.450000E 00
1.150000E 00	9.000000E 02	8.000000E 05	1.000000E 00	1.000000E 00	1.150000E 00	0.	1.050000E 00
1.010000E 00	9.000000E-01	1.000000E 00	7.702000E-01	1.000000E 00	1.100000E 00	1.000000E 00	1.100000E 00
1.010000E 00	1.000000E 00	4.782050E 02	9.123300E-01	7.854000E-04	6.670000E-01	1.640000E-01	4.000000E 01
4.000000E 02	1.000000E 00	-2.000000E 00	3.100000E 01	1.000000E 00	6.000000E 00	1.000000E 01	0.
0.	1.000000E 00	0.	7.600000E 03	1.875000E-01	0.	1.000000E 02	5.298100E-01
2.823000E-02	3.900000E-05	3.500000E-01	1.000000E 00	8.280000E 03	3.124000E-02	5.000000E-01	1.000000E-05
1.100000E 00	1.300000E 00	1.300000E 00	1.118000E 00	8.460000E-01	-0.	-0.	

DATA FOR OXIDE FILM BUILD-UP CALCULATION

TIME INCREMENT	TIME (I)	O/A (I)	U12 (I)	DPC (I)
1	3.600000E 02	8.000000E 05	1.000000E 00	7.350000E 01

(THIS PAGE IDENTICAL TO PAGE 1)

FIGURE A-9
(PAGE 4 OF 6)

TYPICAL CASE - INPUT VALUES FROM TABLE II

THE FOLLOWING OUTPUT IS FOR THE HOT CHANNEL CALCULATION

HOT PLATE - NARROW CHANNEL

DEL T BN	V I	DEL T BHS	V BHS	H HS	DEL T FHS	TS HS	QMAX
1.519145E 02	3.870300E 01	1.519145E 02	4.104787E 01	1.608338E 04	1.184308E 02	3.915453E 02	1.904768E 06

HOT PLATE - WIDE CHANNEL

DEL T BN	V I	DEL T BHS	V BHS	H HS	DEL T FHS	TS HS	QMAX
1.028856E 02	4.456373E 01	1.028856E 02	4.617945E 01	1.547390E 04	1.230955E 02	3.471811E 02	1.904768E 06

FACTORS CAUSING DEFLECTIONS

PRESS. DIFF.	DELTA TF N	DELTA TF A	DELTA TF W	T SIDE PLATE
3.336116E 00	1.294627E 02	1.027136E 02	8.063653E 01	1.720990E 02

PLATE DEFLECTIONS

PRESS. DEFL.	FP BUCKL N	FP BUCKL A	FP BUCKL W	HC DEFL H	HC DEFL C
2.117906E 00	1.349875E 01	1.107458E 01	8.984816E 00	8.629787E 00	-5.319447E 00

TEMP DIFF N	TEMP DIFF W	VOL EXP N	VOL EXP A	VOL EXP W	HS DEFL H	HS DEFL C
1.655170E 00	1.497129E 00	4.529248E-01	4.037856E-01	3.593384E-01	2.457332E 01	2.424169E 00

EPS HOT	U1 HOT	U2 HOT	EPS COLD	U1 COLD	U2 COLD
4.250000E 01	8.595144E-01	4.221752E-01	4.250000E 01	9.227036E-01	1.064004E 00

OUTPUT ON THIS PAGE IS IDENTICAL TO THAT OF PAGE 2 EXCEPT IT APPLIES TO THE COLD CHANNEL CALCULATION. FIGURE A-9 (PAGE 5 OF 6)

~~TYPICAL CASE - INPUT VALUES FROM TABLE II~~

~~HOT CHANNEL~~
~~DEL T BN V I DEL T BHS V BHS H HS DEL T FHS TS FS QMAX~~
~~1.504514E 02 3.869244E 01 1.925466E 02 1.523032E 01 1.139503E 04 2.043022E 02 5.180488E 02 2.328031E 06~~

~~BERGLES-R. BURNOUT CORRELATION K # 1.000009E 00~~
~~DEL T BN V I DEL T BHS V BHS P HS T S T SAT Q~~
~~1.504528E 02 3.869244E 01 1.925484E 02 1.523032E 01 7.352333E 02 6.070690E 02 5.092624E 02 2.328031E 06~~

THESE LINES
 ARE A REPEAT
 OF THE COLD
 CHANNEL DATA
 BELOW AND
 MAY BE
 IGNORED.

COLD CHANNEL
 DEL T BN V I DEL T BHS V BHS H HS DEL T FHS TS FS QMAX
 1.504514E 02 3.869244E 01 1.925466E 02 1.523032E 01 1.139503E 04 2.043022E 02 5.180488E 02 2.328031E 06

BERGLES-R. BURNOUT CORRELATION K # 1.000009E 00
 DEL T BN V I DEL T BHS V BHS P HS T S T SAT Q
 1.504528E 02 3.869244E 01 1.925484E 02 1.523032E 01 7.352333E 02 6.070690E 02 5.092624E 02 2.328031E 06

AT CONVERGENCE, Q/A # 1.033952E 06 AND K(I) # 1.000005E 00

OUTPUT ON THIS PAGE IS IDENTICAL TO THAT OF PAGE 3 EXCEPT THAT IT APPLIES TO THE COLD CHANNEL CALCULATIONS AND THE FIRST TWO LINES SHOULD BE OMITTED RATHER THAN THE LAST TWO.

FIGURE A-9
 (PAGE 6 OF 6)

APPENDIX B

HOMOGENEITY INSPECTION SPOT SIZE REQUIREMENTS

I. Introduction

The high heat transfer performance requirements of HFIR make it essential that the heat transfer analysis and fuel element fabrication and inspection techniques consider as many of the potential sources of local hot spots as possible. One of these sources, which must be considered, is that of local fuel segregation. Nondestructive testing techniques are available for measuring the total fuel content of a given area of the fuel plate, but they are not capable of measuring the degree of local segregation within this area. Consequently, in order to insure that HFIR fuel plates will not exceed the anticipated hot spot operating characteristics, it is necessary to specify an inspection spot size sufficiently small to insure that local fuel segregation within this spot will not be a problem. An analysis of the problem has shown that a spot size can be arrived at that will result in a percentage increase in heat flux equal to the percentage increase in fuel content within the spot. This diameter, however, is dependent on the location across the width of the fuel plate because of the variation in thickness of the fuel core. The smallest diameter occurs where the fuel core is the thinnest, and the use of this diameter in other areas results in a higher predicted heat flux than would actually occur. As a matter of convenience in inspection and in order to be on the conservative side a spot diameter corresponding to the minimum thickness portion of the fuel core was specified for use over all portions of the fuel plates for both the inner and outer elements. This inspection spot size was established by the following calculations:

II. Method of Analysis and Results

The model used to examine the effects of segregated fuel is shown in Fig. B1.

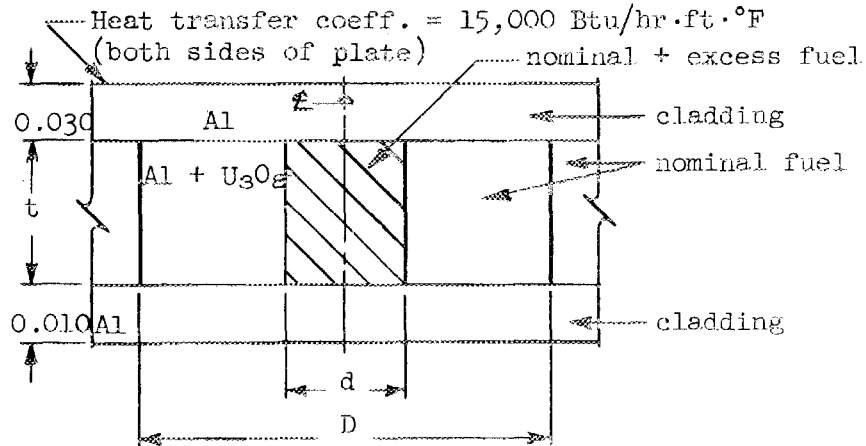


Fig. B1. Fuel Segregation Homogeneity Model

where

D = inspection area diameter,

d = diameter of segregated area within inspection area,

t = thickness of meat.

The value of d can be as small as permitted by the limitations associated with the density of the U_3O_8 particles and their maximum packing fraction (assumed to be 0.74, based on closely packed spherical particles). The largest value of d is D .

A relationship between d and D can be obtained as follows:

$$Wt_a = \frac{d^2}{4} \times t \times \rho_o \times (\text{p.f.}) - \frac{d^2}{4} \rho_n \quad (1)$$

$$Wt_n = \frac{d^2}{4} \rho_n \quad (2)$$

where

Wt_a = weight of U_3O_8 within inspection area in addition to nominal,

Wt_n = weight of nominal U_3O_8 within inspection area,

ρ_o = volumetric density of U_3O_8 ,

$$\frac{\text{g } U_3O_8}{\text{cm}^3 U_3O_8},$$

ρ_n = surface density of nominal fuel, g U_3O_8/cm^2 of fuel plate surface,

(p.f.) = packing fraction of U_3O_8 spheres within volume defined by diameter d and height t .

Dividing Eq. (1) by Eq. (2) gives

$$\frac{Wt_a}{Wt_n} = \frac{d^2}{D^2} \left[\frac{t \rho_o (p.f.) - \rho_n}{\rho_n} \right] = F, \quad (3)$$

where

$$F = \frac{Wt_a}{Wt_n} = \text{fractional increase in fuel over nominal in volume defined by diameter } D \text{ and height } t.$$

Solving for D ,

$$D = \frac{d}{F^{1/2}} \left[\frac{\rho_o}{\rho_n} t (p.f.) - 1 \right]^{1/2} \quad (4)$$

Suppose now that a two-dimensional analysis of the temperature distribution is made for the case indicated in Fig. B1, assuming heat to be transferred symmetrically in the radial and axial directions, and assuming that heat generation sources in the fueled regions to be proportional to the fuel densities. A curve such as that shown in Fig. B2 would be obtained,

ORNL-DWG. 67-8070

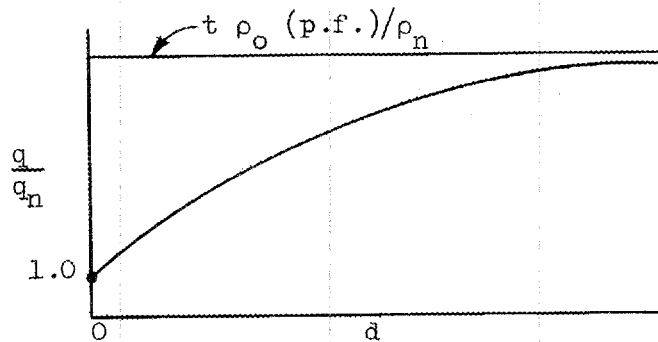


Fig. B2. Effect of Segregation Spot Diameter on Heat Flux Peaking Value

where

$\frac{q}{q_n}$ = ratio of peak heat flux on fuel plate surface to that achieved with only nominal fuel densities.

For $d = 0$, $q = q_n$, and for $d = \infty$,

$$\begin{aligned} \frac{q}{q_n} &= \frac{\text{weight of all fuel in area "d"}}{\text{weight of nominal fuel in area "d"}} \\ &= \frac{\frac{\pi d^2}{4} t \rho_o (\text{p.f.})}{\frac{\pi d^2}{4} \rho_n} = \frac{t \rho_o (\text{p.f.})}{\rho_n} \end{aligned}$$

From Fig. B2 a relationship between d and q/q_n can be obtained for specific values of t and (p.f.). Therefore, Eq. (4) can be rewritten as

$$D = \frac{f(q/q_n)}{F^{1/2}} \left[\frac{\rho_o}{\rho_n} t (\text{p.f.}) - 1 \right]^{1/2} \quad (5)$$

For the HFIR analysis a curve such as that in Fig. B2 was obtained for the minimum value of t (0.010 in.) in the HFIR fuel plates, for the maximum packing fraction (0.74), for the cladding thicknesses shown in Fig. B1, and for an essentially infinite radial extent of nominal fuel surrounding the segregated spot. In addition, the thermal conductivity of the segregated volume was considered to be a function of the packing fraction, although only one packing fraction was considered.

Reducing the packing fraction has the effect of spreading the "additional" fuel within area "D" over a larger area, thus changing the thermal conductivity and changing the value of the peak heat flux. It was assumed in the HFIR analysis that the maximum peak heat flux would occur with the maximum packing fraction. The use of a minimum value of t also results in a maximum peak heat flux.

The calculated q/q_n vs. d curve for the HFIR is shown in Fig. B3. As indicated, the entire curve was not obtained, making it necessary to extrapolate. The extrapolated curve was approximated with the

following equation:

$$\frac{q - q_n}{q_n} = \frac{0.10}{5.814 \times 10^{-7} \text{ in.}^3} \times \frac{\pi d^2}{4} t, \quad (6)$$

where for this particular case

$$t = 0.010 \text{ in.},$$

$$(\text{p.f.}) = 0.74,$$

$$\rho_o = 10 \text{ g/cm}^3,$$

$$\rho_s = 0.0178 \text{ g/cm}^2 \text{ (consistent with 0.010 in.-thick meat in fuel plate of inner element).}$$

From Eq. (5)

$$D = \frac{d}{F^{1/2}} \left[\frac{10 \text{ g/cm}^3}{0.0178 \text{ g/cm}^2} \times 0.01 \text{ in.} \times 2.54 \frac{\text{cm}}{\text{in.}} \times 0.74 - 1 \right]^{1/2} = \frac{d}{F^{1/2}} \times 3.1 \quad (7)$$

From Eq. (6)

$$d = \left[\frac{5.814 \times 10^{-6} \text{ in.}^3}{0.010 \text{ in.}} \times \frac{4}{\pi} \left(\frac{q - q_n}{q_n} \right) \right]^{1/2} = 0.0272 \text{ in.} \left(\frac{q - q_n}{q_n} \right)^{1/2} \quad (8)$$

From Eqs. (7) and (8)

$$D = 0.084 \text{ in.} \left(\frac{q - q_n}{q_n} / F \right)^{1/2} \quad (9)$$

As a matter of convenience $\frac{q - q_n}{q_n}$ was set equal to F , resulting in an inspection spot diameter of 0.084 in. of $\sim 5/64$ in.

As indicated above the inspection spot size is a function of a number of parameters. For instance, if t were increased, the slope of the curve in Fig. B3 would be less, resulting in a larger value of D for given values of q/q_n and F . For a given value of D the peak heat flux would be less, a condition that could be taken advantage of for hot spots away from the narrow portion of the fuel

contour. Another parameter of interest is associated with the possible variations in power density adjacent to the hot spot. These variations are controlled to some extent by fuel distribution specifications and detection techniques. It is possible that some of the unexplored combinations would result in somewhat smaller values of D ; that is, the curve in Fig. B3 would have a steeper slope. Offsetting this effect is the straight line extrapolation of the above curve which tends to give a conservative answer.

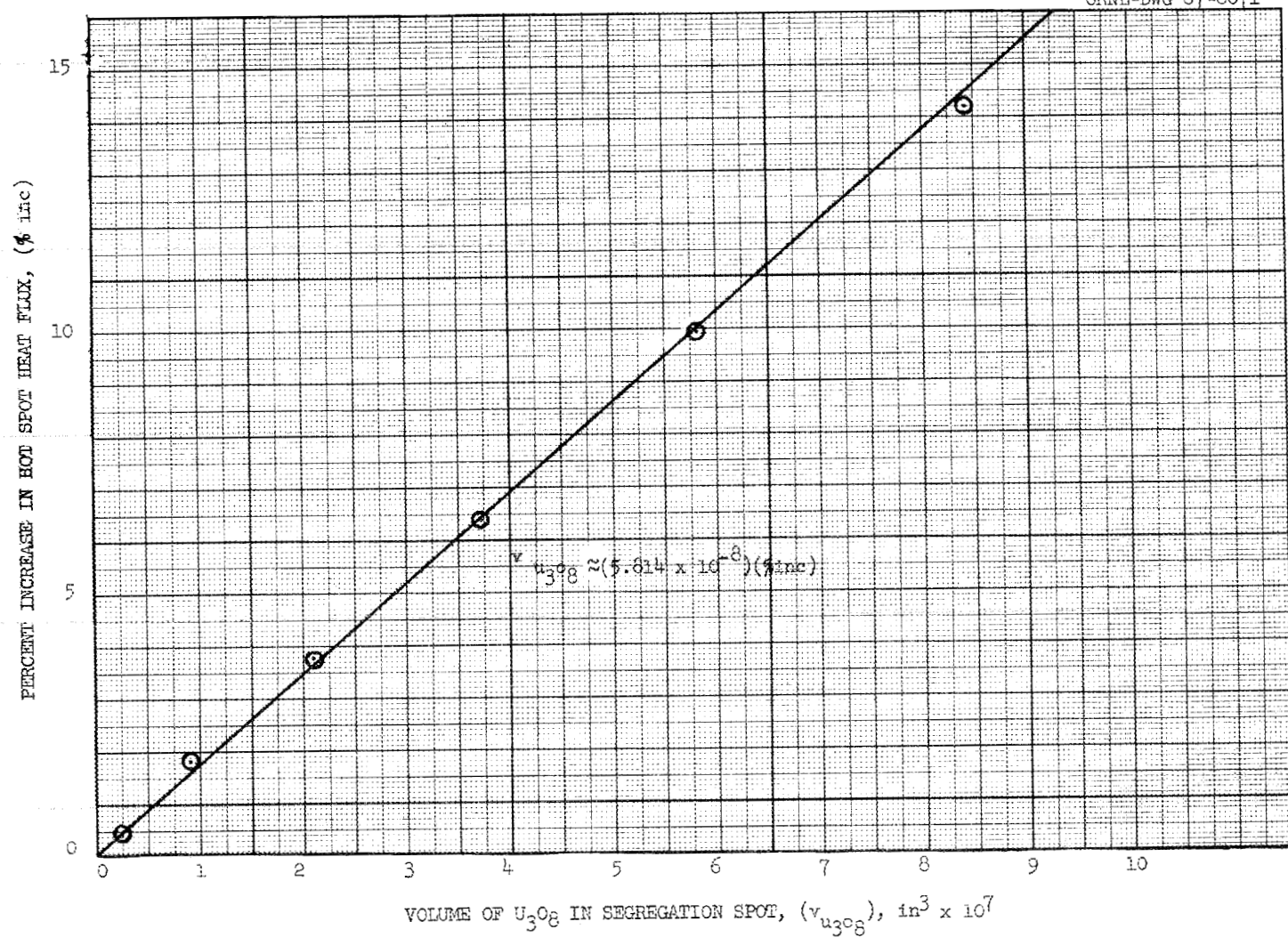


Fig. B-3. Effect of Size of Segregation Spot on Local Heat Flux Heating.

APPENDIX C

INFLUENCE OF FUEL SEGREGATION ON
INCIPIENT BOILING POWER LEVEL

The HFIR fuel element specifications¹ require a NDT inspection for fuel concentration as measured for any 5/64-in.-diam spot (0.0048 in.² area) within the maximum fuel core outline. The data obtained from the scan shall be averaged to provide both local and average fuel concentration deviations resulting from fuel segregation for the Hot Spot Analysis. The influence of both types of deviations on the Incipient Boiling Power Level (IBPL) was investigated with the Hot Spot Code (see Appendix A) using the typical input parameters of Table II except for the following:

$$\begin{aligned} \Delta P \text{ core} &= 73.5, 90, 100 \\ P &= 333, 444, 666, 1000 \\ \Delta P \text{ core (i)} &= 73.5, 90, 100 \\ U_{13} &= 1.10, 1.125, 1.15, 1.175, 1.20 \\ U_{16} = U_{17} &= 1.20, 1.225, 1.25, 1.275, 1.30 \\ \alpha_3 &= 0.0 \\ \alpha_4 &= 1.0 \end{aligned}$$

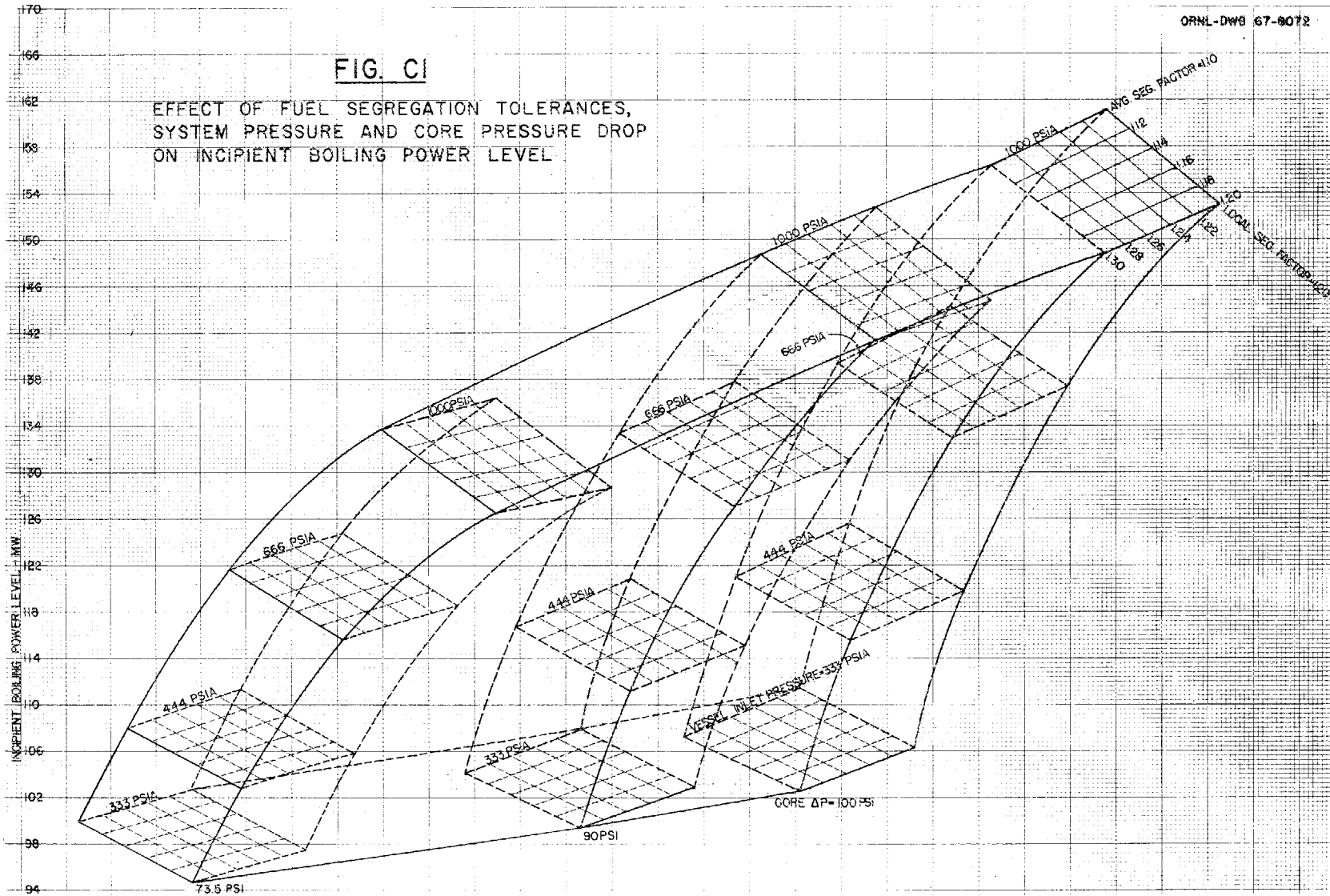
The computational results for the influence of fuel segregation deviations on IBPL are shown in Fig. C1.

The information obtained from this study could be incorporated into the fuel element specifications to gain the flexibility of specifying different combinations of local and average fuel concentration deviations for a particular Incipient Boiling Power Level. The ability to accept various combined tolerances on fuel concentration could increase the fuel plate rejection rate as compared to fixed tolerance bands for each variable.

¹G. M. Adamson, Jr. and J. R. McWherter, Specifications for High Flux Isotope Reactor Fuel Elements, ORNL-TM-902 (Aug. 1964).

FIG. C1

EFFECT OF FUEL SEGREGATION TOLERANCES,
SYSTEM PRESSURE AND CORE PRESSURE DROP
ON INCIPIENT BOILING POWER LEVEL



APPENDIX D

HFIR MODES OF OPERATION

The HFIR has been provided with three general modes of operation which must be investigated for the corresponding maximum operating power levels. The modes can be briefly outlined as follows. Mode 1 (normal operating mode) is for pressurized operation (600 psi) with coolant flows between 2,100 and 15,000 gpm. The steady state power level is restricted to 0-100 Mw for normal full flow and to 0-10 Mw for shutdown coolant flow. Mode 1 also provides for continued operation at reduced power in the event of an electrical power outage. Mode 2 provides for unpressurized operation (vessel head removed) with the flow from three pony-motor-driven pumps (2,100 gpm). The permissible maximum power level under these conditions is 2.5 Mw. Mode 3 permits unpressurized operation at a maximum power level of 100 kw with no forced flow.

Mode 1 has been thoroughly analyzed in the body of this report for the effect of pressure and fuel element flow rate on the incipient boiling power level. The results of the analysis are presented in Figs. 8 and 10. The design criteria require that the safety level trip point for each mode be 1.3 times the corresponding nominal full power level, and that the calculated minimum incipient boiling power level be equal to or greater than the safety level trip point.

Mode 2 operation was also analyzed in the text of the report; the results are shown in Fig. 10. Using a minimum expected inlet pressure of 25 psia, and a minimum expected flow rate of 2,100 gpm to the fuel element, the incipient boiling power level was calculated to be 11.5 Mw. This corresponds to a permissible maximum power level for Mode 2 operation of $11.5 / 1.3 = 8.8$ Mw. The actual operating level selected was set at 2.5 Mw so that asymmetric operation of the control rods could be tolerated, if so desired. During symmetrical operation of the control rods, the level could be increased to 8.8 Mw.

In the calculations for Mode 3 operation heat removal was assumed to take place only by natural convection cooling with no external return flow

passages. The results of a natural convection experimental program,¹ conducted specifically for the HFIR, indicated a nominal critical heat flux of 13,000 Btu/hr·ft² for the case of no external return flow passage, a pressure of 25 psia, a channel width of 0.052 in., and a heated length of 17.5 in. The minimum hot spot channel width at this burnout level is expected to be about 0.033 in., and the effective length in terms of bulk water temperature is significantly less than the 17.5 in. because the hot spot condition is localized. A critical heat flux correlation proposed by Gambill² for the case of no external return flow passage and for hydraulic diameters greater than 0.1 in. indicates that the critical heat flux is proportional to $(D_e)^{1.5}/L_h$, where D_e is the hydraulic diameter and L_h is the heated length of a uniformly heated channel. Gambill also found that for $D_e < 0.1$ in. surface tension effects reduced the critical heat flux below those predicted by the above correlation; however, sufficient data for a correlation that would include this effect and thus cover a range that would include the minimum HFIR channels are not available. It is believed that this can be compensated for by the fact that in the experiments the actual burnout heat flux in some cases was significantly greater than the critical heat flux, for which the above correlation was derived. For a 2-ft long channel (0.087 in. wide) the ratio of heat flux resulting in a 1210°F plate temperature (burnout for aluminum plates) to the critical heat flux was about 5. In the HFIR this ratio would not be so large because of excessive plate buckling and loss of strength at the elevated temperatures; even so, it appears that the ratio is at least large enough to compensate for the surface tension effect associated with the very narrow channel. Using an uncertainty factor of 1.2 in connection with the measured heat flux of 13,000 Btu/hr·ft², which is now interpreted as the burnout heat flux with a surface tension correction, and correcting for the differences

¹W. R. Gambill and R. D. Bundy, Burnout Heat Fluxes for Low Pressure Water in Natural Circulation, ORNL-2036, December 20, 1960.

²W. R. Gambill, Prediction of Critical Heat Flux for Natural Convection of water in Blocked Vertical Channels, ORNL-CF-64-5-39, May 1964.

in channel widths, using the above relationship, gives a hot spot burnout heat flux of $13,000 (0.003/0.052)^{1.5}/1.2 = 5,400 \text{ Btu/hr}\cdot\text{ft}^2$. No correction was made for length because of a lack of sufficient data. This omission and the assumption regarding no external return flow passage constitute a conservative approach.

In order to determine the corresponding core averaged heat flux and thus burnout power level several of the "hot spot" factors in Table 3 were used and are summarized below:

$[q_m/q_a]_c$	1.45
$[q_a]_{hc}/[q_a]_c$	1.15
U5	1.05
U11	1.1
U16	1.3
U18	1.118

The resulting power level was 230 kw, which is considered to be the maximum permissible level trip. The maximum permissible operating power level for Mode 3 should be at least thirty percent less than this and should also be equal to or less than the incipient boiling power level. From ref. 1 it is estimated that the incipient boiling heat flux in the experiment was no more than a factor of seven less than the burnout heat flux. According to Gambill* a decrease in channel width from 0.052 to 0.039 in. (minimum channel width at incipient boiling power level) has a negligible effect on the incipient boiling heat flux. Therefore, for Mode 3 operation the incipient boiling heat flux would be

$$13,000/1.2 \times 7 = 1,500 \text{ Btu/hr}\cdot\text{ft}^2 .$$

The corresponding power level is 65 kw and is the minimum power level at which nucleate boiling would be expected. Actually, it is believed that there is enough external return flow passage to increase both the incipient

*W. R. Gambill, "Review of Draft of Report on HFIR Fuel-Element Steady-State Heat Transfer Analysis," Intra-Laboratory Correspondence to T. E. Cole, February 8, 1965.

boiling and burnout power levels significantly. For this reason the maximum operating power level for Mode 3 has been set at 100 kw instead of 65 kw. The level trip was set at 130 kw as a matter of consistency in maintaining the 1.3 ratio. If through experience with a particular core it is found that a significant amount of boiling does not occur until considerably higher powers are achieved, it will be possible to increase the operating power level and of course the level trip point until the latter reaches a limiting value of 230 kw.

APPENDIX E

FUEL ELEMENT DRAWINGS

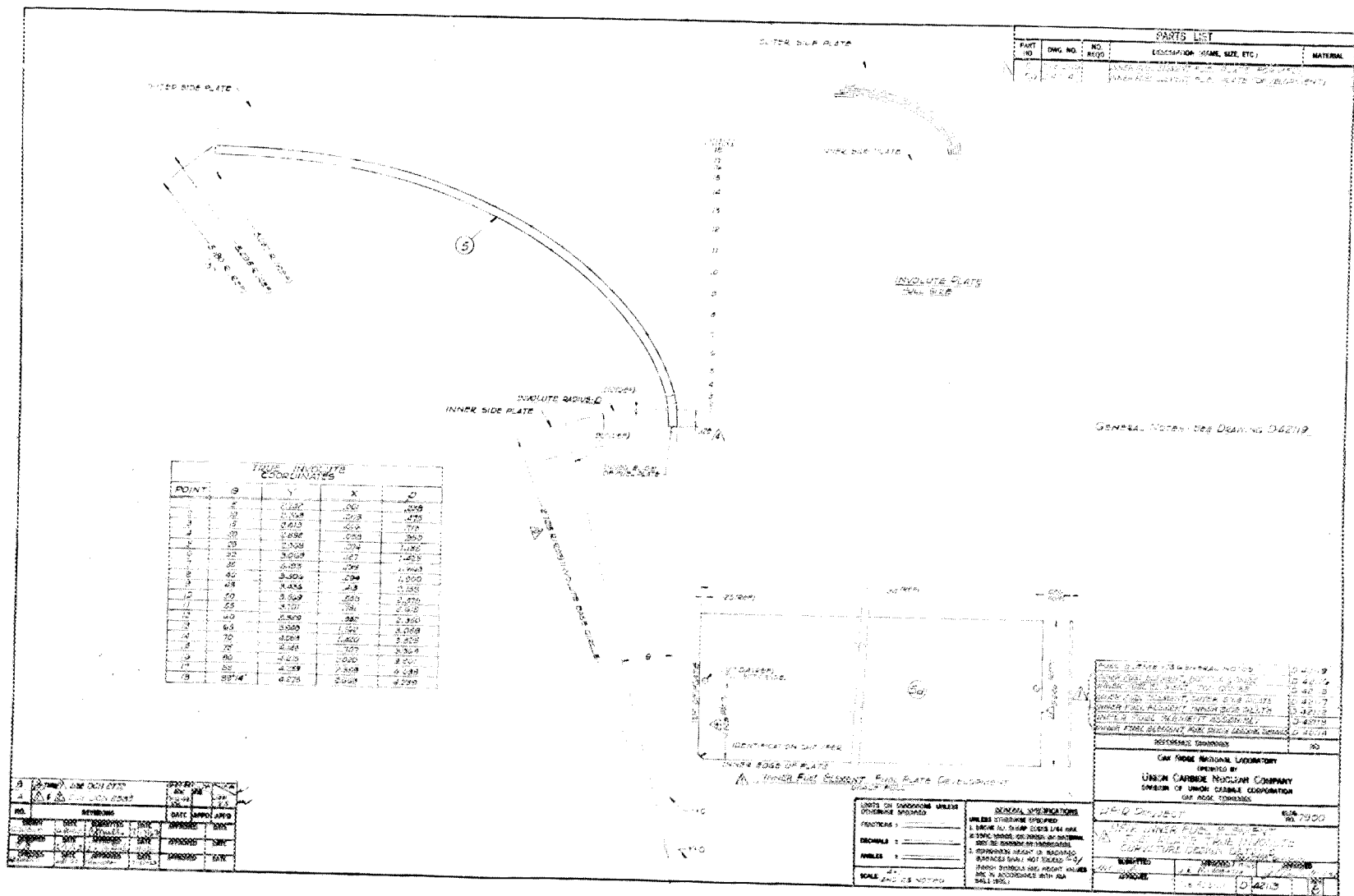


Fig. E-2. HFIR Inner Fuel Element - Fuel Plate True Involute Curvature - Design Details.

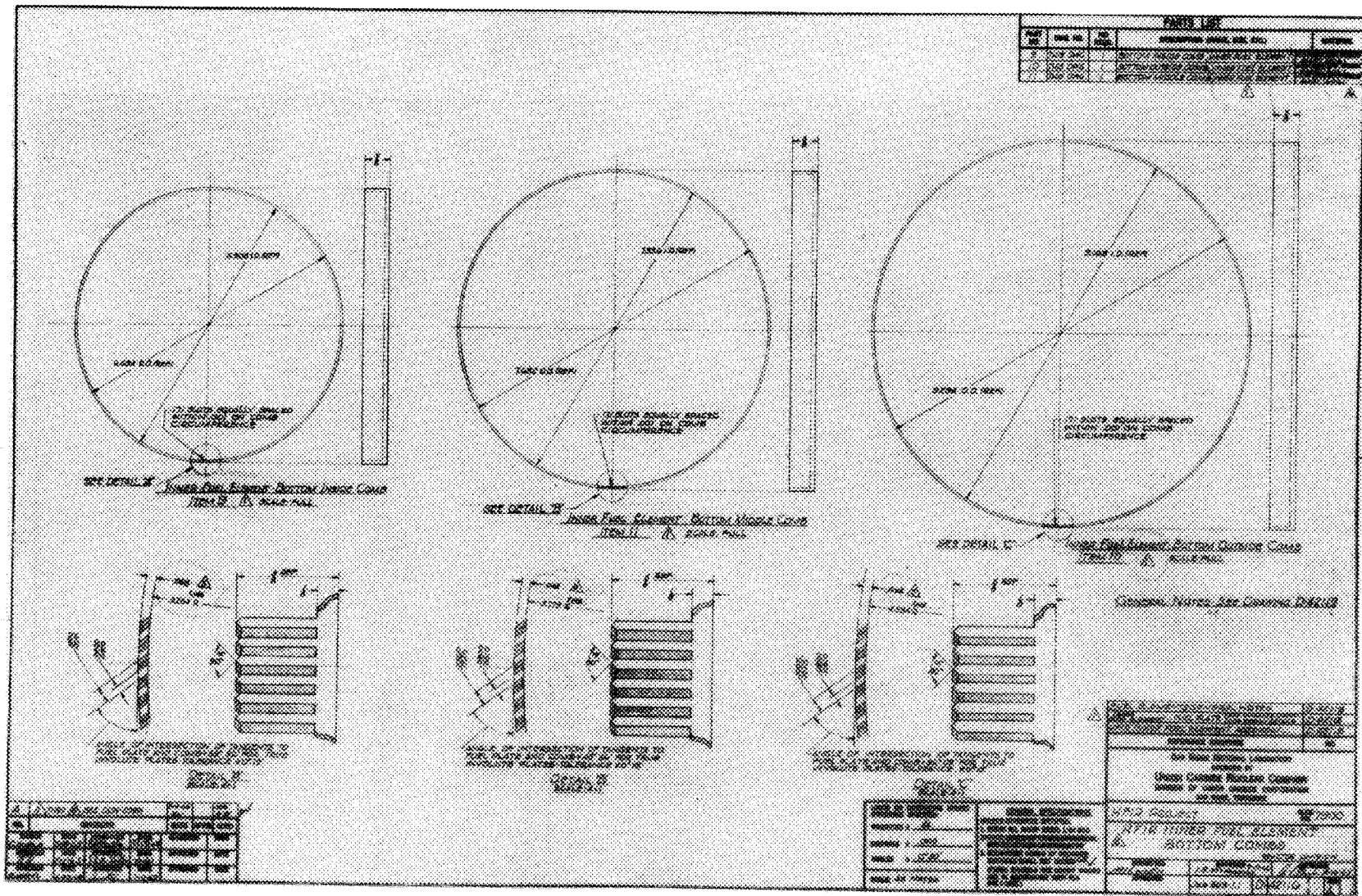


Fig. E-5. HFIR Inner Fuel Element - Bottom Combs.

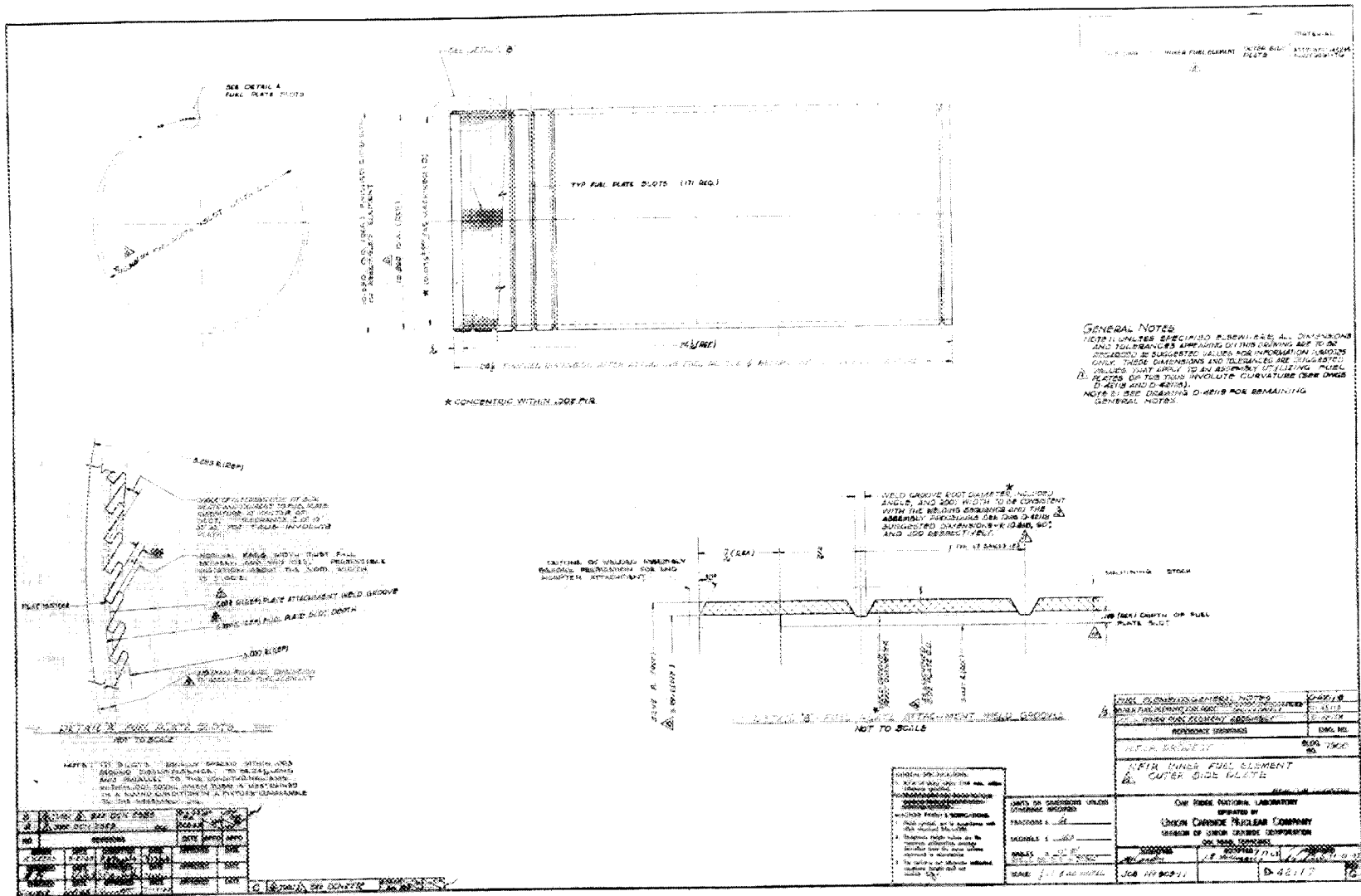


Fig. E-6. HFIR Inner Fuel Element - Outer Side Plate.

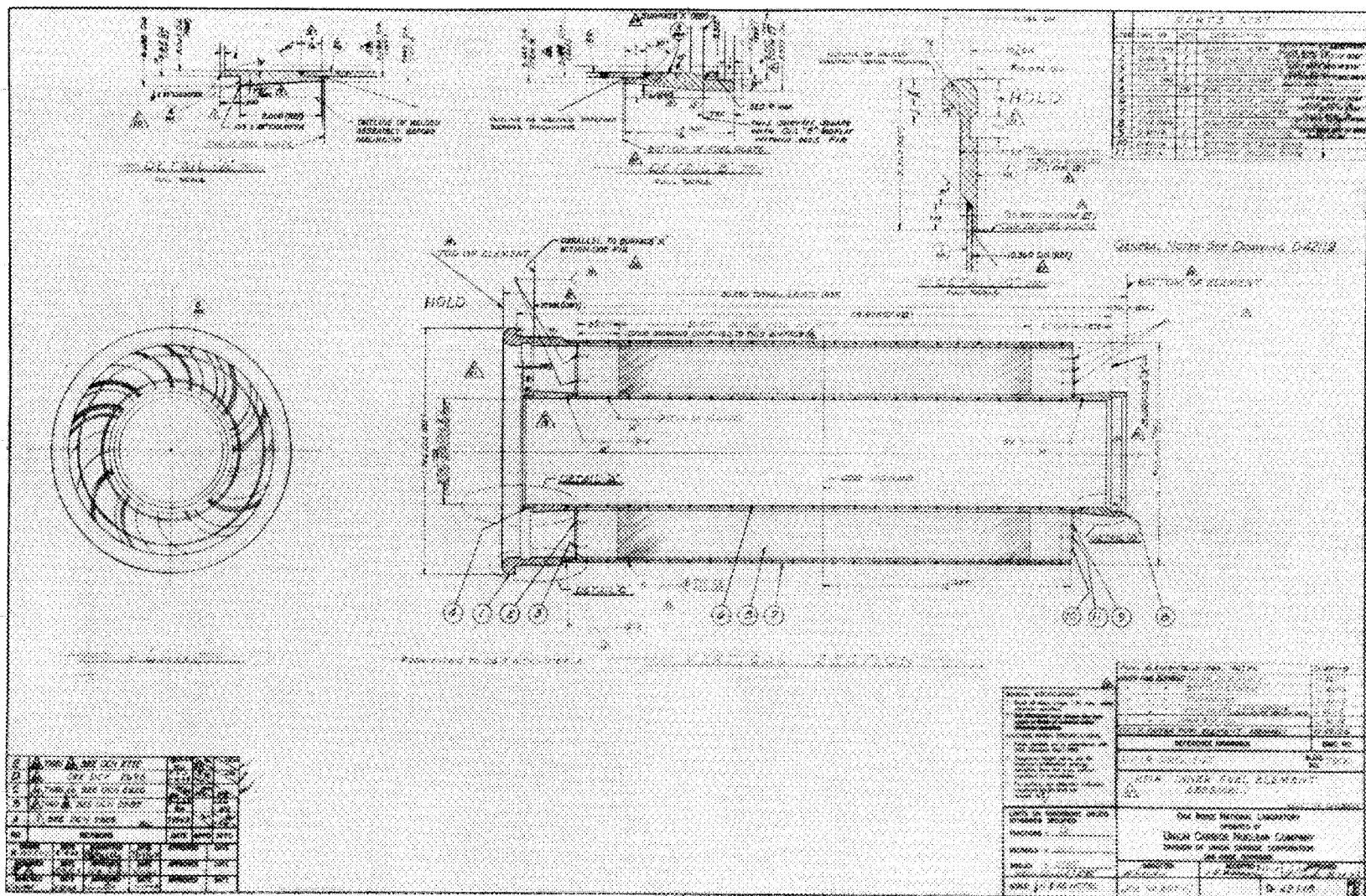


Fig. E-7. HFIR Inner Fuel Element - Assembly.

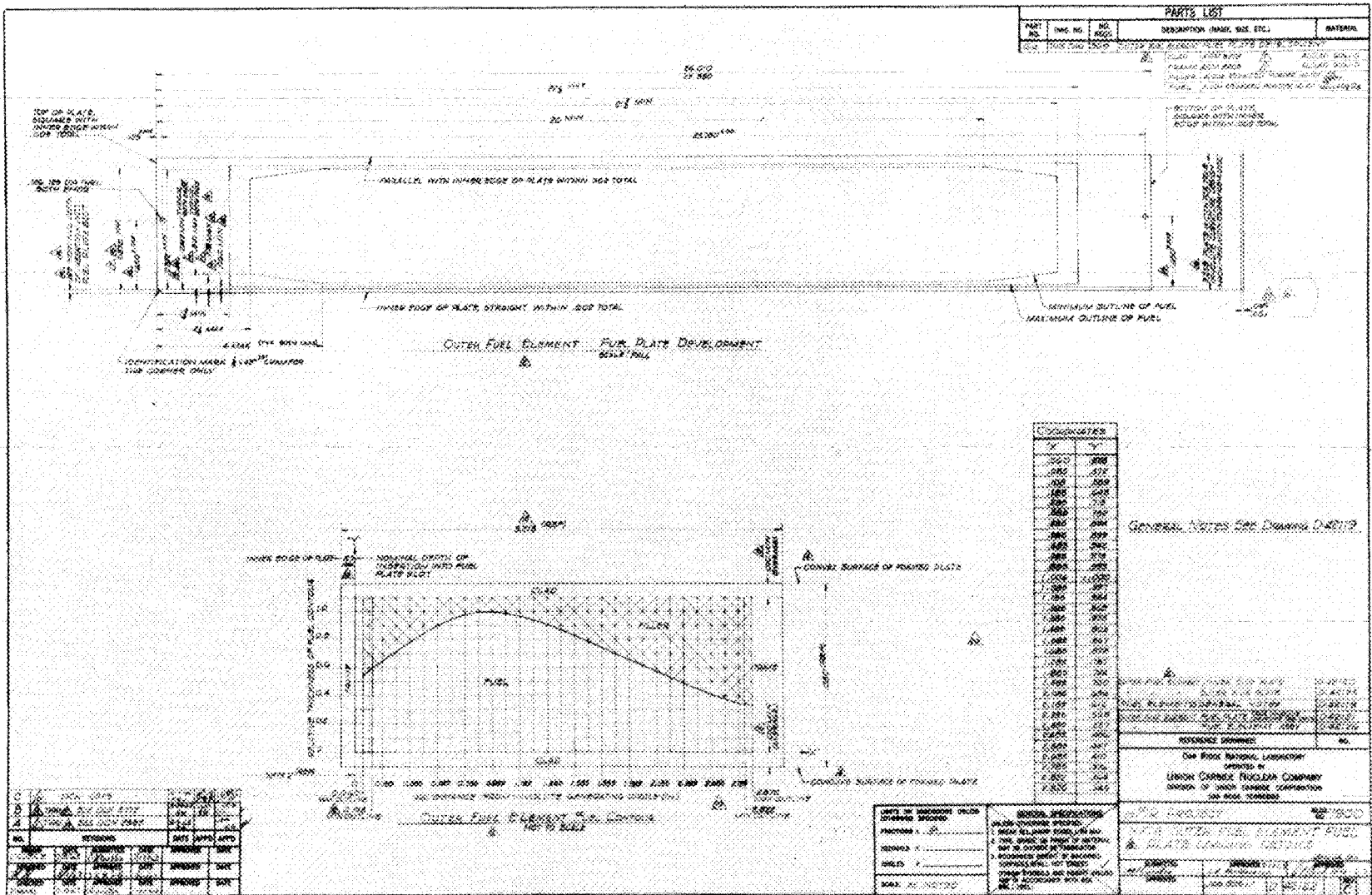


Fig. E-11. HFIR Outer Fuel Element Fuel Plate Loading Details.

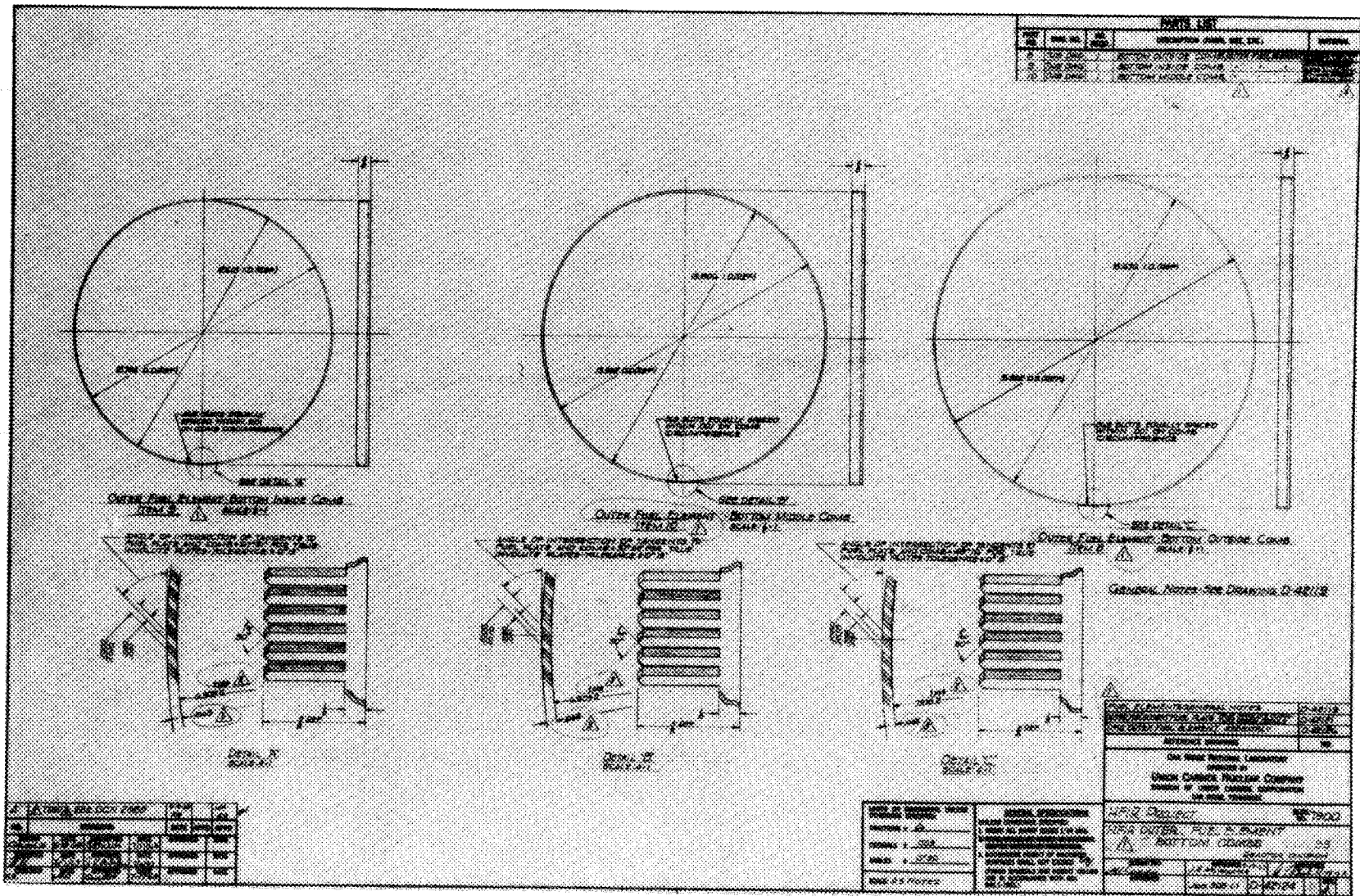


Fig. E-13. HFIR Outer Fuel Element - Bottom Combs.

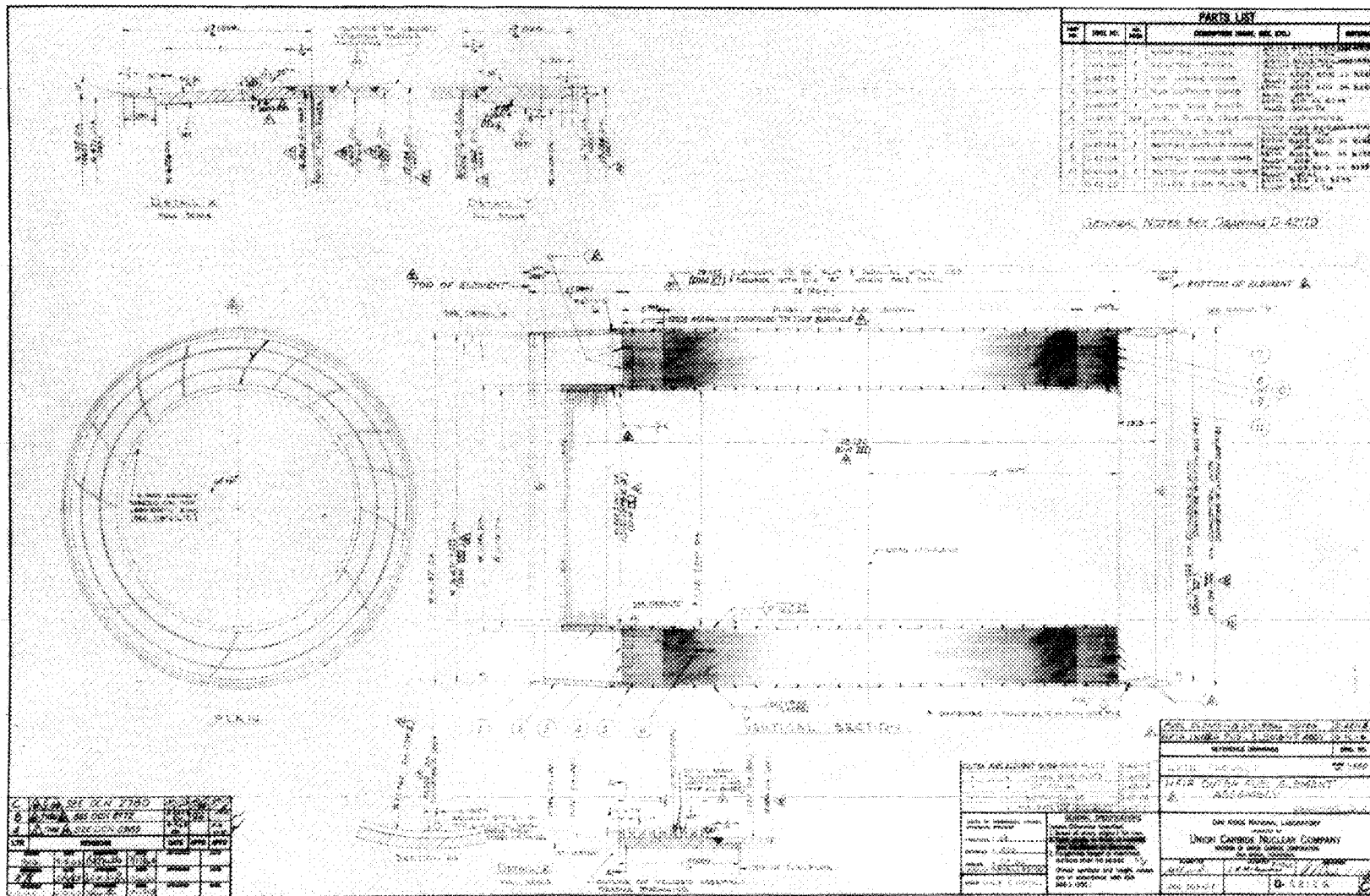


Fig. E-15. HFIR Outer Fuel Element - Assembly.

Internal Distribution

- | | |
|-----------------------|---|
| 1. G. M. Adamson | 31. R. M. Hill, Jr. |
| 2. S. E. Beall | 32. P. R. Kasten |
| 3. M. Bender | 33. J. A. Lane |
| 4. E. S. Bettis | 34. M. I. Lundin |
| 5. F. T. Binford | 35. R. N. Lyon |
| 6. A. L. Boch | 36. H. G. MacPherson |
| 7. E. G. Bohlmann | 37-41. R. V. McCord |
| 8. R. B. Briggs | 42. H. C. McCurdy |
| 9. F. R. Bruce | 43-44. H. A. McLain |
| 10. C. D. Cagle | 45. J. R. McWherter |
| 11. T. G. Chapman | 46. A. J. Miller |
| 12. R. D. Cheverton | 47. L. C. Oakes |
| 13. W. G. Cobb | 48. A. M. Perry |
| 14. T. E. Cole | 49. K. H. Poteet |
| 15. B. L. Corbett | 50. M. W. Rosenthal |
| 16. W. B. Cottrell | 51. A. W. Savolainen |
| 17. J. A. Cox | 52. T. M. Sims |
| 18. E. N. Cramer | 53. M. J. Skinner |
| 19. F. L. Culler | 54. I. Spiewak |
| 20. J. E. Cunningham | 55. R. S. Stone |
| 21. G. J. Dixon | 56. D. B. Trauger |
| 22. B. C. Duggins | 57. A. M. Weinberg |
| 23. E. P. Epler | 58. G. D. Whitman |
| 24. W. K. Ergen | 59. R. Q. Wright (K-25) |
| 25. D. E. Ferguson | 60-61. Central Research Library, CRL |
| 26. A. P. Fraas | 62-63. Y-12 Document Reference Section, DRS |
| 27. W. R. Gambill | 64-78. Laboratory Records Department, LRD |
| 28. J. C. Griess | 79. Laboratory Records Department, LRD-RC |
| 29. L. A. Haack | 80. ORNL Patent Office |
| 30. P. N. Haubenreich | |

External Distribution

81. D. F. Cope, AEC, ORNL
82. M. Shaw, Division of Reactor Development and Technology, AEC, Washington, D.C.
83. L. N. Rib, Division of Compliance, AEC, Washington, D.C.
84. T. R. Jones, Division of Research, AEC, Washington, D.C.
- 85-99. Division of Technical Information Extension, DTIE
100. Laboratory and University Division, AEC, ORO
- 101-102. Reactor Division, AEC, ORO
103. R. R. Rohde, ANL
104. D. H. Shaftman, ANL

105. M. Levenson, ANL
106. B. Kristianson, ANL
107. N. Hilvety, Union Carbide Corporation, Parma Research Center,
Cleveland, Ohio
108. A. L. Babb, University of Washington, Seattle, Washington, 98105